UNIVERSITY ABBES LAGHROUR OF KHENCHELA
FACULTY OF SCIENCE AND TECHNOLOGY
Department of Industrial Engineering
جامـــعة عبـــاس لـــغرور خـنـشـلة
كليـــة العلـــوم والتكنـــولـــوجيـا
قسم الهنـدسة الصنـاعية

Serial number: ……..

Thesis submitted to the Department of industrial Engineering in Candidacy for the Degree of Master in electrotechnics

Option: Electrical Control

By:

- Chakhrit Djamal Eddine
- Sid Oussama

Supervised by :

- Mr.Saidi Abdelakader

THEME

Study of the different MPPT methods for the Photovoltaic system

Thesis defended on 10 July 2021

Board of Examiners:

Chairperson: Mr. Labdani Rafik	ABBES LAGHROUR (Khenchela)
Supervisor: Mr.Saidi Abdelkader	ABBES LAGHROUR (Khenchela)
Member: Dr. Menadi Abdelkrim	ABBES LAGHROUR (Khenchela)

Promotion 2020/2021

ACKNOWLEDGEMENT:

After understanding and completing the exciting task of “Study of the different MPPT techniques for the Photovoltaic system,” we see it is our duty to say Alhamdulilah and to express our sincere gratitude towards our families for the support all over the past 24 years and all the people who have contributed their precious time and effort to help us, without them this work would never have been brought off the ground To all of we wish to convey the heartiest gratitude. We would especially like to thank MR.Saidi Abdelkader, our Project Supervisor, for his guidance, support, motivation, and encouragement throughout the period this work was carried out. His readiness for consultation at all times, his educative comments, concern, and assistance, have been invaluable. We are grateful to all the teachers who have contributed to our training, from the first grade of primary school until today.

Djamal eddine & Oussama

CONTENTS

CONTENTS

CONTENTS

CONTENTS

CONTENTS

Chapter IV : MPPT methods Implemenation

CONTENTS

List of Figures :

Chapitre I

Chapitre II

Chapitre III

Chapitre IV

List of Figures

LIST OF TAIBLES

CHAPTER I

CHAPTER III

CHAPTER IV

List of abbreviations and symbols

I : Cell current [A]

Iph : The photo-current [A]

Ish : The current flowing through the shunt resistor [A]

Irs : Diode saturation current [A]

Vd : Voltage across the diode [V]

Vt : Thermal potential [V]

T : Cell temperature [K]

n : Ideality factor of the diode

γ : Electron charge (1.602 * 10^-19 C)

T : Cell temperature [K]

G : Irradiation [W / m ^ 2]

G_ref : The reference irradiation = 1000 [W / m^2]

T_ref : The reference temperature = 25 ° C = 298 K

I_sc : The short-circuit current of the cell [A].

K_i : Constant representing the variation of the current with the temperature [A / K]

I_pv : Current of the GPV [A]

V_pv : GPV voltage [V]

N_s : Number of cells connected in series per module

N_p : Number of modules connected in parallel.

L : represents the inductance [H].

Id : Diode current (A)

Vd : Diode voltage (V)

Io : Diode saturation current (A)

nI : Diode ideality factor, a number close to 1.0

K : Boltzman constant = 1.3806e-23 J.K-1

List of abbreviations and symbols

Q : Electron charge = 1.6022e-19 C

T : Cell temperature (K)

Ncell : Number of cells connected in series in a module

AC : Alternating current

DC : Direct current

Vo : voltage at the terminals of the load

IL : inductance current

Vi : input voltage

SC : static converter

HC : Hill climbing

P&O : Perturb and Observe

INC : Incremental Conductance

FLC : fuzzy logic control

GA : Genetic algorithms

SMC : sliding mode control

MPPT : Maximum power point tracking

GPV : photovoltaic generator

PPM : maximum power point

Isc : short circuit current

Voc : open circuit voltage

D : duty cycle

PV : Photovoltaic

Vpv : PV voltage

Ipv : PV current

Ppv : PV power

i : iteration

List of abbreviations and symbols

ΔV : variation of the voltage

Eff : efficiency

ΔP : variation of the power

ΔI : variation of the current

dG : variation (increment) of conductance

Err **:** the input variables of the FLC are the error

Δ*Err* **:** the change of error

ΔD : change of the duty cycle

NB : big negative

NS : small negative

ZE : zero

PS : small positive

PB : big positive

COG : center of gravity

S : is the fuzzy MPPT controller output scale factor.

N **:** the number of individuals

A **:** The binary form of the individual;

x : The actual form of the individual;

$d \subset \mathcal{R}$ **:** The search space allowed;

x_{max}, x_{min} : The lower and upper bounds of the variable x;

i_d : The length of the interval d.

f **:** objective function.

F **:** Fitness function (cost), positive non zero.

g **:** Function ensuring the transition from the objective

e (x) : Deviation of the variable to be adjusted, **e (x) =** X_{ref} **- X**

λ_x **:** Positive constant which interprets the bandwidth of the desired control.

List of abbreviations and symbols

r : Relative degree

S (x) = 0 : is a linear differential equation whose unique solution is e (x) = 0.

u_n **:** corresponds to the not linear component.

X : represents the system state vector

U : represents the control vector

ψ : is the macro-variable

Ψ (x,t) : is a user-defined function

T : is a control parameter

PWM : Pulse-Width Modulation

GENERAL INTRODUCTION

General Introduction :

Global electricity consumption observed over the past decades is closely linked to the development of industry, transport and communications[1]. Today, the bulk of electricity production is provided by non-renewable resources, such as coal, natural gas, petroleum and uranium. Their rates of regeneration are extremely slow in the human range. This will lead to a more or less non-zero risk of depleting these resources in the short term[1]. In particular, as demand continues to grow, there is now oversupply leading for example, to sharp fluctuations in the world oil prices.

On the other side, this type of energy consumption is not neutral on the environmental impacts. Where fossil fuels (coal, oil and natural gas) produce environmental pollution problems due to the pollutant gases which are emitted during their combustion[2]. These problems are worldwide known such as acid rain, urban pollution or more important global warming, caused by greenhouse gases (GHG), mainly carbon dioxide (CO2) and methane (CH4). [2]

This finding prompts us to seek more and more innovative solutions that alleviate the energy deficit and limit the negative impact on the environment. Thus, the development of non-polluting sources based on renewable energy is increasingly sought by both energy producers and public authorities. Renewable energies' resources are directly extracted from nature, like sun, wind, water or thermal energy from the Earth, and the energy is generated in a sustainable way. The contribution of the sun is essential because its availability far exceeds any conceivable future energy demands[1]. That is the reason why solar energy has been developed for about the last 40 years and different applications are currently utilized, such as thermal solar energy or photovoltaic (PV) systems. However, similarly the sun is a potential resource and it is completely irregular due to atmospheric changing conditions and hence, the efficiency of this kind of energy ,it can be questioned.[1]

This work will be focused on PV systems and the methods to maximize the power produced and the electricity generated as it will be seen later. PV systems have a non-linear P-V characteristic which shows a maximum power point (MPP), and this operating point can be changed due to atmospheric conditions. Then, the aim of the maximum power point tracking (MPPT) methods will be estimate the MPP and keep the operating point close to it.

There are many different MPPT methods but only the most utilized will be explained, and some of them will be implemented and simulated to support a theory with results.

Therefore the main objective of this work is to make a review of the most known and modern methods; moreover, the implementation of some MPPT methods as a result the features described can be verified.

Thus, for achieving this aim implicitly, other intermediate objectives are defined:

- Understanding the operation of solar photovoltaic systems, as well as their electrical modeling and technologies are used for their manufacture.
- Understand the impact of weather conditions on the operation of PV systems, and thus the need to use Maximum Power Point Tracking (MPPT) methods to maintain power at the required level.
- Making a selection of the most influential MPPT methods and understanding their operation and main features.
- Acquiring an adequate level in the implementation of models in Simulink R. Implementing some of the methods selected, as well as analyzing the results obtained and contrasting the information previously found.
- Obtaining a conclusion about the results obtained through the evaluation of interesting parameters.

Methodology for this project is compound of several stages, which are mentioned below:

In the first chapter, we will briefly describe the most used solar cells and their operating principles, as well as the modeling of a photovoltaic cell (CPV),and the influence of different meteorological parameters (temperature and irradiation). Towards the end of this chapter, we will present the photovoltaic system and mention some advantages of the latter.

In the Second chapter, we will review the types of static converters DC / AC and DC / DC converters (buck, boost and buck boost).

In our study, we need a DC / DC converter of Boost type, which is frequently used in photovoltaic systems to generate the desired voltages and currents.

The Third chapter is devoted to the study of various selected MPPT methods by grouping them according to their principles.The most commonly encountered are: Hill climbing, Perturb and Observe, Incrémental Conductance, fuzzy logic control, Genetic algorithms, sliding mode control and Synergitic control.

The Fourth chapter is about Implementing a simplified model of a PV system which is tested to work. Then, different methods are implemented. Finally,after checking that all methods are operating correctly, main features are analyzed and compared to other algorithms, so that all results and conclusions are obtained.

Reference:

[1] Guney, M. S. (2016). Solar power and application methods. Renewable and Sustainable Energy Reviews, 57, 776-785.

[2] Bose, B. K. (2010). Global warming: Energy, environmental pollution, and the im- pact of power electronics. Industrial Electronics Magazine, IEEE, 4(1), 6-17.

Chapter I

Photovoltaic System

I.1. Introduction:

The photovoltaic effect was discovered in 1839. This conversion is the result of the direct transformation of sunlight into electrical energy. Although the sun is an unlimited source of energy, man has long sought to take advantage of this Source. In our time, humanity is based on solar cells. [1]

In this chapter, we will briefly describe the most used solar cells and their operating principles, as well as the modeling of a photovoltaic cell (CPV), the influence of different metrological parameters (temperature and illumination). Towards the end, we will present the photovoltaic system and cite some advantages and inconvenibles of the latter.

I.2. Solar energy:

The sun is a virtually inexhaustible source of energy that sends radiation to the earth's surface approximately 8,400 times the energy used each year.

This corresponds to an instantaneous power received of 1 peak kilowatt per square meter (KWp / m ^ 2) distributed over the entire spectrum, from ultraviolet to infrared. The deserts of our planet receive in 6 hours more energy from the sun than humanity consumes in a year. Solar energy is produced and used in several ways:

- **Solar thermal energy:** which simply consists of producing heat using dark panels. You can also produce with steam from the heat of the sun and then convert the steam into electricity.
- **Photovoltaic solar energy:** which consists of producing electricity directly from light using solar panels. This form of energy is already exploited in many countries, especially in countries or regions that do not have conventional energy resources such as hydrocarbons or coal. [2]

I.3. Solar radiation:

The sun is one star among many. It has a diameter of 1,390,000 km, about 50 times that of the earth. It is composed of 80% hydrogen, 19% helium and 1% of a mixture of 100 elements, which is practically all the chemical elements known since Langevin and Perrin, based on the theory of relativity of Einstein, put forward the idea about sixty years ago that it is the energy of nuclear fusion that provides the sun with its power, it is now accepted that the sun is a thermonuclear hydrogen-helium bomb transforming 564 million tonnes of hydrogen into 560

million tonnes of helium every second; the reaction taking place in its nucleus at the temperature of about 25 million degrees Celsius. Thus, every second, the sun is lightened by 4 million tons scattered in the form of radiation. [3]

Its light, at a speed of 300,000 km / s, takes about 8 minutes to reach the earth, its spectral distribution of the atmosphere is presented a maximum for a wavelength of about 0.5μm, the black body temperature at the surface of the sun is about 5780 ° K [4]:

Sun diameter Ds = $1.39.10^{9}$ m;

Earth diameter Dt = $1.27.10^{7}$m;

Average distance sun_ earth Lts = $1.5.10^{11}$ m.

I.3.1 Rayonnement direct:

Solar flux in the form of parallel rays coming from the sun's disk without having been dispersed by the atmosphere. [5]

I.3.2 Diffuse radiation:

It is the part of the radiation coming from the sun, having undergone multiple reflections (dispersions), in the atmosphere. [5]

I.3.3 Reflected radiation:

C'est la partie de l'éclairement solaire réfléchi par le sol, ce rayonnement dépend directement de la nature du sol (nuage, sable...).Il se caractérise par un coefficient propre de la nature de lien appelé Albédo(ε) $0< \varepsilon <1$. [5]

I.3.4 Global radiation:

A plane receives from the ground a global radiation which is the result of the superposition of the three compositions direct, diffuse and reflected. [5]

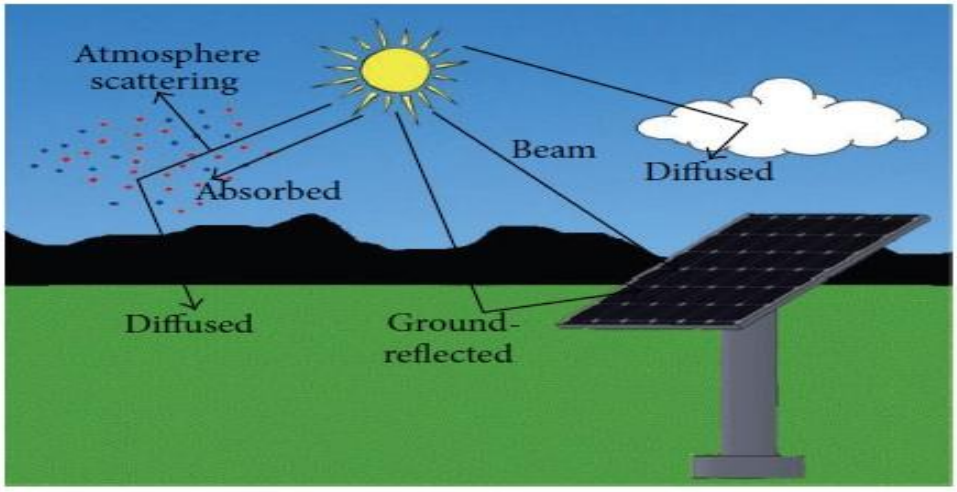

figure I.1. Components of solar radiation on the ground.

I.4. Solar photovoltaic:

The term photovoltaic refers to the physical process of transforming part of solar radiation into electrical energy through photovoltaic cells. [6]

The word photovoltaic comes from the Greek which means:

- **Photo:** light,

- **Volt:** unit of electrical voltage named after the physicist Alessandro Volta.

I.5. History of the photovoltaic cell:

In 1887 "Heinrich Rudolph Hertz" first presented the photoelectric effect in an article in the scientific journal "Annalen der Physik". The photoelectric effect is called the emission of electrons by a material subjected to illumination or electromagnetic radiation of an intensity specific to the materials.

In 1875 "Wiener Von Siemens" exhibited before the Berlin Academy of Sciences an article on the photovoltaic effect in semiconductors. But until the Second World War. the phenomenon is still an anecdotal discovery .

In 1954 American researchers "Gerald Pearson", "Darry Chapin" and "Calvin Fuller" work for Bell Laboratories develop a silicon PV cell.

In 1958 a cell with an efficiency of 9% was developed and the first satellites powered by solar cells were sent into space. [7]

I.6. Thougths on photovoltaics:

I.6.1 Photovoltaic cell:

The photovoltaic cell is the basic element of a solar generator. A PV cell is a sensor made of a semiconductor material (usually silicon-based) that converts absorbed light energy into electric current.

I.6.2 Structure and mode of operation of a cell:

The basic structure of a PV cell is made from two layers of silicon, one P doped (doped with boron) and the other doped N (doped with phosphorus) thus creating a PN junction with a potential barrier. The N zone is covered by a metal grid which serves as a cathode, while a metal plate (back contact) covers the other side of the P zone of the crystal and acts as an anode [8]. When photons are absorbed by the semiconductor, they transmit their energy to the atoms of the PN junction. Thus, the atoms are bombarded by the photons constituting light (Fig. (I.2)), and under the action of this bombardment, the electrons of the valence shells tend to be torn / unhooked from their orbits. This then creates a potential difference between the two layers. This potential difference is measurable between the connections of the positive and negative terminals of the cell, through a load.

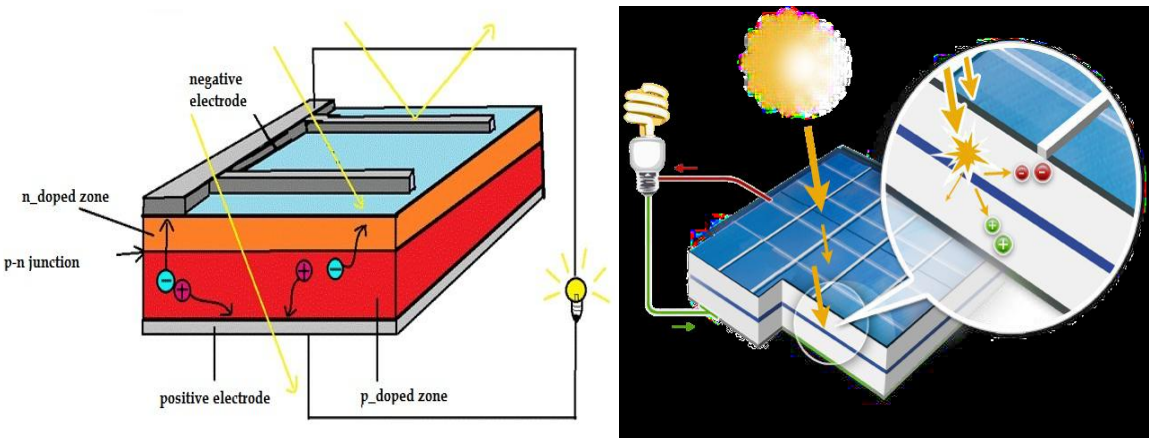

figure I.2. Operating principle of a PV cell. [9]

I.6.3 types of photovoltaic cells:

There are several types of PV cells, but silicon-based technologies make up over 90% of the global photovoltaic market.

There are three categories of PV cells made from silicon:

Monocrystalline cells	Polycrystalline cells	Amorphous cells
each layer is cut from a silicon single crystal. This type of cell has very good efficiency and converting power, but is very expensive.	they are also very efficient cells, but slightly lower than that of monocrystalline cells, which justifies their lower cost.	this type of cells do not have crystal structures. They have the advantage of being integrated on flexible and rigid supports. They are often used in portable devices, calculators, watches, etc.
		

Table I.1. different types of photovoltaic cells.

Recently, a new generation of PV cells has appeared, these are thin film cells in the form of thin films, they have very high energy conversion efficiency and good efficiency. Thin film cells can be built on a flexible substrate.

Monocrystalline and polycrystalline cells are the two most common types of PV cells in the photovoltaic market.

I.7. The influence of temperature and irradiation:

I.7.1 The influence of temperature:

For a solar panel to function, the PV cell must be exposed to sunlight. This causes heating and the temperature acts on the different characteristics of the cell. [10]

The sunshine is set at 1000 W / m2 and the temperature is varied from 25 °C to 75 °C, the paces obtained are presented below:

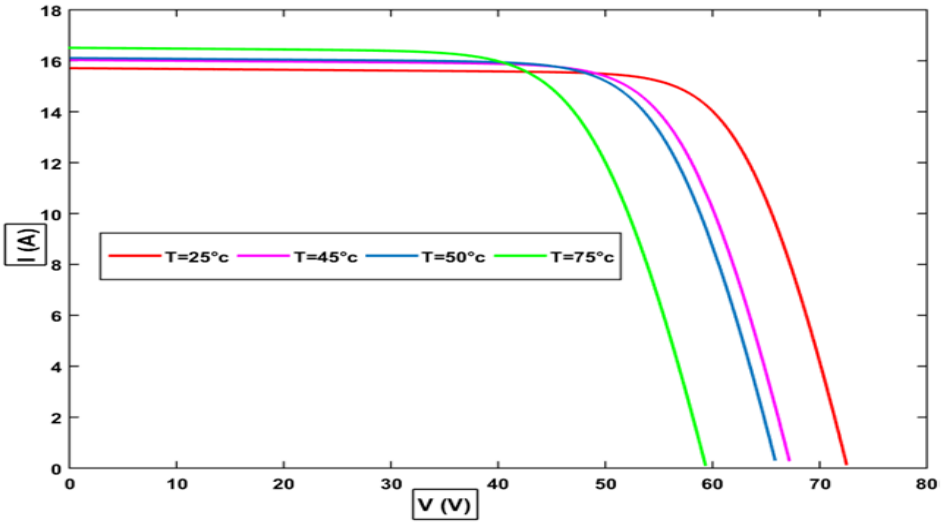

figure I.3. Influence of temperature on PV current.

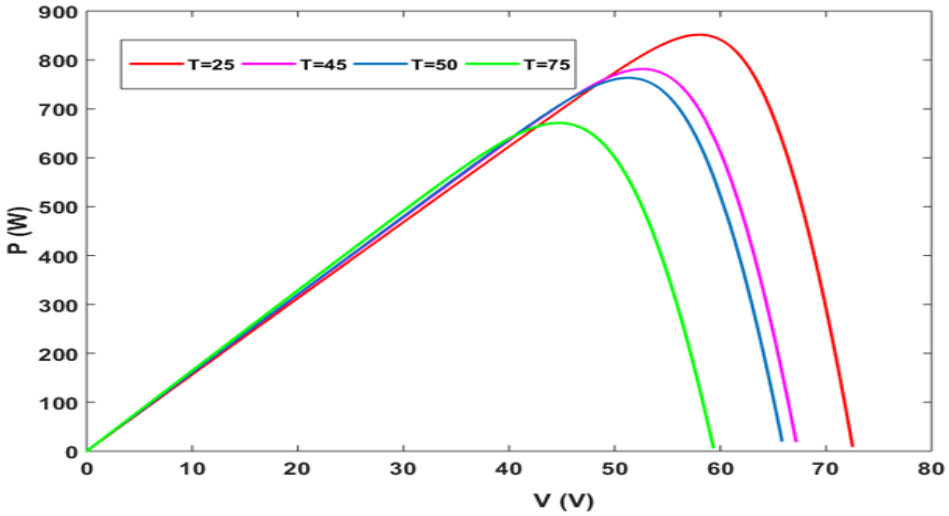

figure I.4. Influence of temperature on power on the GPV.

Note that the increase in temperature mainly leads to a decrease in voltage therefore the power of the GPV decreases. Figure I.5 shows that an increase in temperature 25 ° C to 75 ° C results in a power drop of 25% .

I.7.2 The influence of irradiation:

We apply a temperature T = 25 ° C kept constant and we vary the sunlight (G) from 200 W / m2 up to 1500 W / m2, the results obtained are illustrated by the following figures.

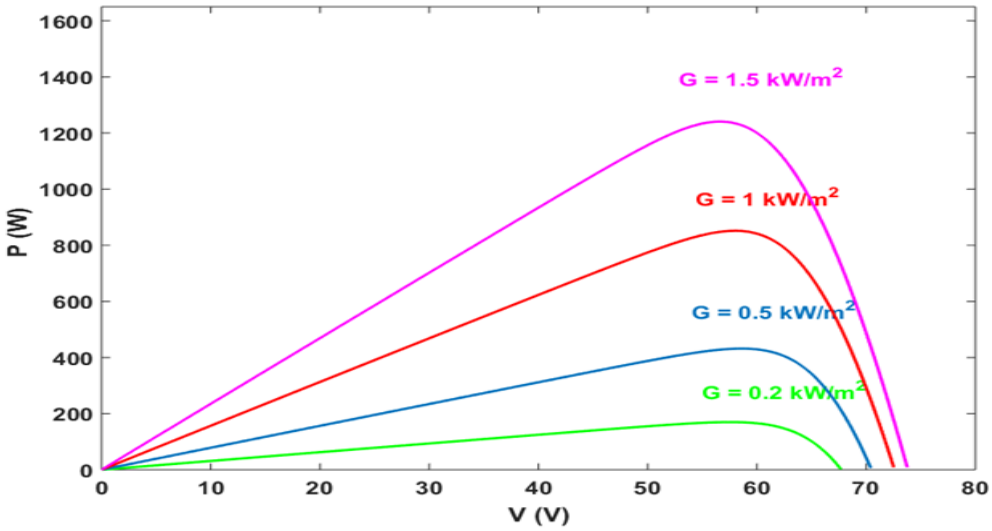

figure I.5. influence of irradiation on power.

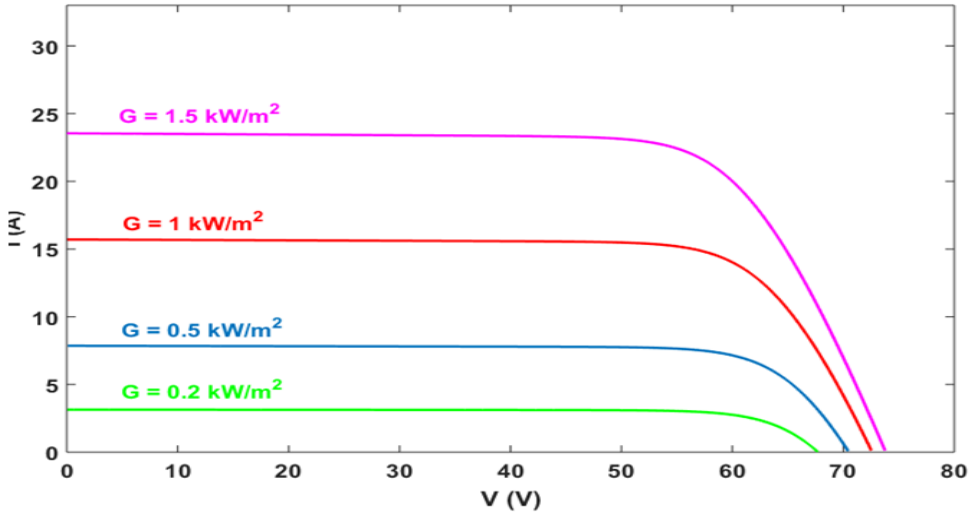

figure I.6. Influence of irradiation on PV current.

The current-voltage characteristic for different values of irradiation is shifted by a distance in proportion to the solar radiation.

An increase in solar irradiance essentially causes an increase in PV current, therefore the power of the PV increases.

I.8. Photovoltaic generator:

The power delivered by an elementary photovoltaic cell of some ten square centimeters is low compared to the needs of domestic or industrial applications.

To produce more power, several cells must be grouped together to create a generator or a photovoltaic module. Indeed, a generator is a set of cells placed in series and / or in parallel producing a continuous and high power. [3]

I.8.1 Serial association:

The voltage of a photovoltaic generator made up of several cells in series is the sum of the voltages flowing through each cell, while the current is the same as that flowing through each cell as shown in figure (I.7).

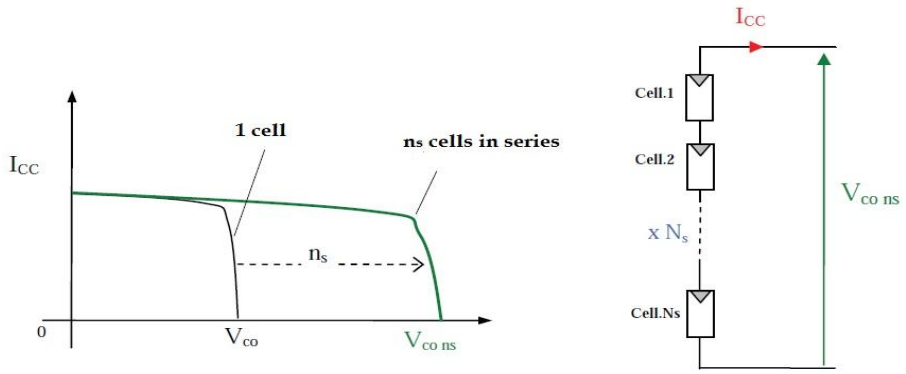

figure I.7. characteristic I (v) resulting from a series grouping. [11]

I.8.2 Parallel association:

The voltage at the output of the generator is the same as that flowing through each cell, while the current is the sum of the currents flowing through each cell constituting this generator. Figure (I.8).

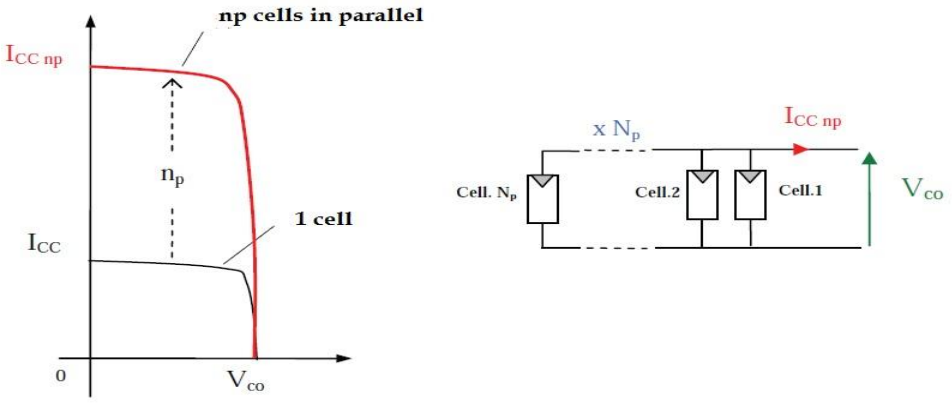

figure I.8. characteristic P(v) resulting from parallel grouping. [11]

I.8.3 Series-parallel association:

In the series grouping, the voltages of the cells add up which increases the total voltage of the PV generator. On the other hand, cells connected in parallel increase the current at the output of the generator. The figure below shows another association structure of photovoltaic cells.

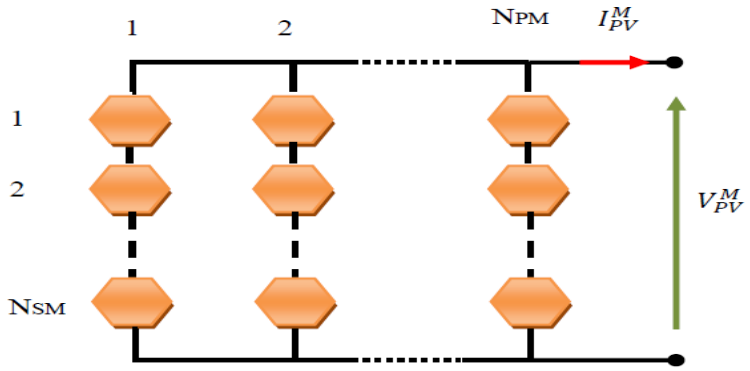

figure I.9. PV panel made up of NSM cells in series and NPM cells in parallel. [12]

Since power is the product of voltage and current, therefore this product will be optimal for maximum voltage and current which are the results of series grouping and parallel grouping respectively.

I.8.4 Photovoltaic parameters:

There are several parameters that characterize a solar cell. These parameters are called photovoltaic parameters which are deduced from the characteristic I (V) shown in figure (I.10). [13]

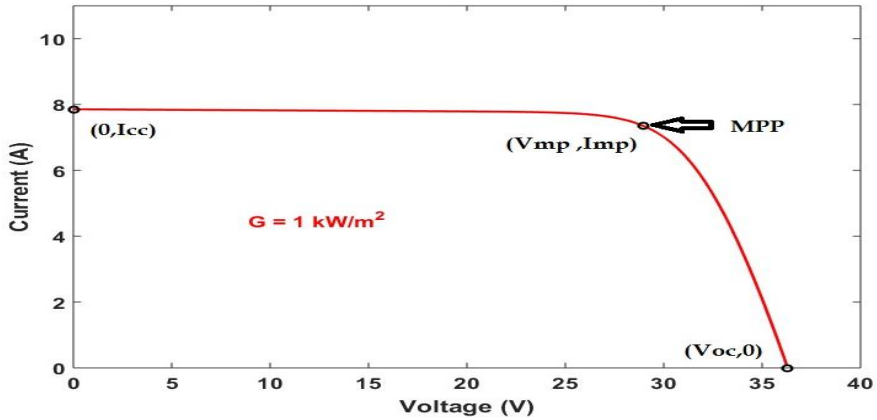

figure I.10. Characteristic I (V) of a photovoltaic cell.

- **Short-circuit current (Isc):** this is the current delivered by a module photovoltaic in absence of voltage (short circuit),
- **Open circuit voltage (Voc):** this is the voltage across the open circuit photovoltaic module,
- **Efficiency (η):** this is the ratio between the power supplied by the cell and the incident power,

- **Maximum power (peak Pc):** this is the maximum electrical power that a photovoltaic module can provide under standard meteorological conditions of temperature and sunshine (T = 25 ° C and E = 1000 W / m2).
- **Form factor (FF):** It represents the ratio between the optimum power and the maximum power that a cell can deliver.

I.8.5 Protection of a photovoltaic generator :

In order to extend the lifespan of a photovoltaic installation intended for the production of electrical energy over years, its electrical protection must be ensured while avoiding destructive breakdowns linked to the association of cells and their operation. To do this, two types of protection are used [14]:

- **Anti-reverse diode:** protects installations when several modules are connected in parallel to prevent the flow of negative currents,
- **By-pass diode:** provides protection when connecting several photovoltaic modules in series, and allows, in the event that an element of the chain is defective, to isolate it and thus ensure the continuity of operation of the chain.

Figure (I.11) shows the diagram of a photovoltaic module with the insertion of the two protections mentioned.

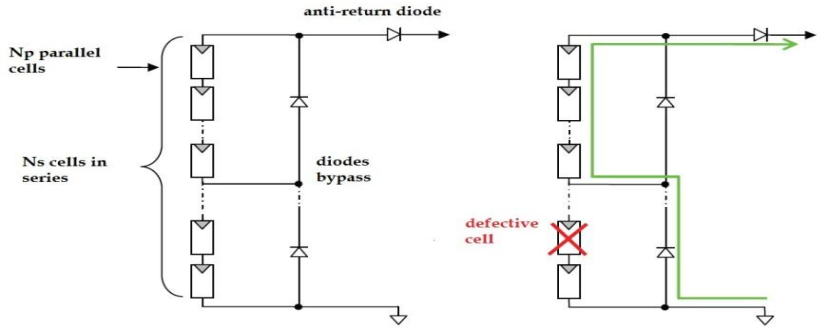

figure I.11. Architecture of a photovoltaic module with the two protection diodes. [14]

I.9. Modeling of the photovoltaic generator:

The PV cell is a photodiode, it can be represented by a simple circuit (Figure I.12), it is the ideal model.

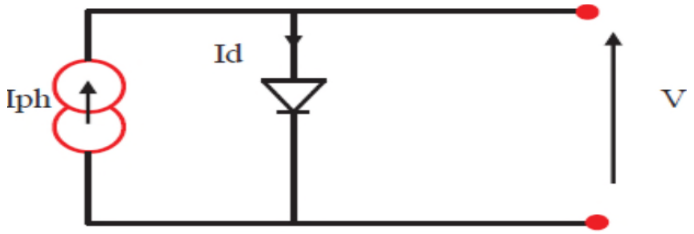

figure I.12. Equivalent diagram of an ideal PV cell.

Taking into account the connection resistances and the leakage currents and starting from the ideal model, we can represent a CPV by the diagram in Figure I.13, also called the 5 parameter model.

There are more complex models (with 2 or 3 diodes) but we limit ourselves in our study to this model which is also used in most research work.

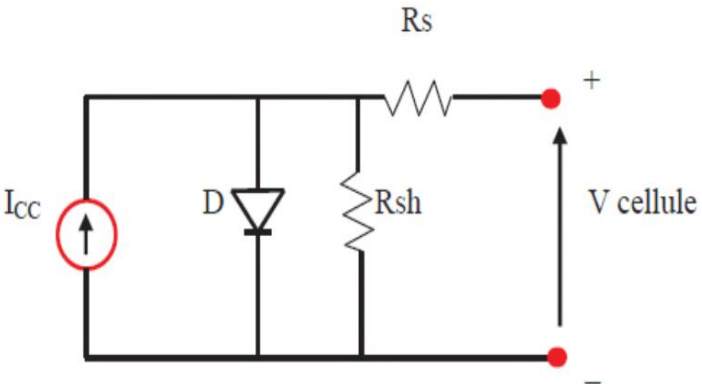

figure I.13. Equivalent circuit of the 5 parameter model.

The resistance Rs represents the cant contact and connection resistances, Rsh characterizes the leakage currents.

According to the law of the knot:

$$I = I_{ph} - I_d - I_{sh} \quad \text{(I-1)}$$

With:

$$I_d = I_{rs}\left[e^{-\frac{V_d}{V_t}} - 1\right] \quad \text{(I-2)}$$

$$V = V_d - R_s I \quad \text{(I-3)}$$

$$I_{sh} = \frac{V_d}{R_{sh}} \quad \text{(I-4)}$$

Which give:

$$I = I_{ph} - I_{rs}\left[e^{-\frac{V+R_s I}{V_t}} - 1\right] - \frac{V+R_s I}{R_{sh}} \quad \text{(I-5)}$$

$$V_t = \frac{nKT}{q} \tag{I-6}$$

The photo-current, generated by the cell, can be expressed as a function of sunlight with the following equation:

$$I_{ph} = [I_{sc} + K_i(T - T_{ref})]\frac{G}{G_{ref}} \tag{I-7}$$

In general, we can put the equivalent electrical circuit of a solar cell in a block diagram (under Simulink) including all the previous parameters, which makes it possible to trace the characteristics of the cell. [15]

PV modules are usually wired in series-parallel to increase the voltage and amperage at the generator output. These are interconnected to form a unit producing high continuous power compatible with the usual electrical equipment.

The expression of the total current can be expressed by:

$$I_{pv} = \left[I_{ph} - I_{rs}\left[e^{\frac{\frac{V_{pv}}{N_s} + R_s \cdot \frac{I_{pv}}{N_p}}{n\,V_t}} - 1\right] - \frac{\frac{V_{pv}}{N_s} + R_s \cdot \frac{I_{pv}}{N_p}}{R_{sh}}\right] \tag{I-8}$$

I.10. The specific advantages of photovoltaics:

Compared to other renewable sources, photovoltaics offers particular advantages:

- It is usable practically everywhere, the sunlight being available all over the world.
- Production equipment can almost always be installed close to the point of consumption, thus avoiding line losses.
- It is completely modular and the size of the installations can be easily adjusted according to needs or means.
- No movement, no direct or indirect pollution (atmospheric or liquid factors, cleaning products, risk of physical accident, ...) no waste, no disturbance for the local environment, it is purely clean, ecological energy.
- Maintenance and repairs are reduced to almost nothing for the photovoltaic part and little choice for the associated electronics.

I.11. Conclusion:

In this chapter we have made general descriptions about photovoltaic energy. All the necessary elements have been introduced in order to allow a good understanding of the functioning of PV systems.

This chapter allowed us to explore the principle of photovoltaic conversion. Both technological and electrical aspects were discussed in order to better understand the entire photovoltaic conversion mechanism.

Reference:

[1] R. Merahi, Modélisation d'un diapositif MPPT pour l'étude de l'augmentation de la puissance produite par les générateurs photovoltaïques, Université de Annaba, 2010.

[2] S.Belakehal, "Conception & Commande des Machines à Aimants Permanents Dédiées aux Energies Renouvelables", thèse de Doctorat, université de Constantine, 2010

[3] R.P. Mukund, « Wind and solar Power Systems », Ph.D, P.e U.S merchant Marine Academy,Kings Point, New York, CRC Press LLC 1999.

[4] F.Hananou et AI.Rouabah. Modélisation et simulation d'un système photovoltaïque .Mémoire de Master Académique, Université KASDI MERBAH OUARGLA, 2014.

[5] M.N.Mechalikh et CH.E.Hamada. Modélisation et simulation d'un système Photovoltaïque en fonctionnement autonome et connecté au réseau. Mémoire de Master Académique, Université KASDI MERBAH OUARGLA, 2013.

[6] Helali Kamelia, « Modélisation d'une cellule photovoltaïque : Etude comparative », Mémoire de Magistère, UMMTO, 2012.

[7] N.Benhaddouche .La commande d'un système photovoltaïque d'un satellite .Mémoire de Master, Université Abou-Baker Bel kaïd-Tlemcen, 2014.

[8] TRAHI Fatiha. «Prédiction de l'irradiation solaire globale pour la région de Tizi- Ouzou par les réseaux de neurones artificiels. Application pour le dimensionnement d'une installation photovoltaïque pour l'alimentation du laboratoire de recherche lampa.» mémoire de magister en électronique Université Mouloud Mammeri de Tizi- Ouzou 2011.

[9] A. AZIZ, « Propriétés Electriques des Composants Electroniques Minéraux et Organiques, Conception et Modélisation d'une Chaîne Photovoltaïque Pour une Meilleure Exploitation de l'Energie Solaire », Thèse de Doctorat, Université Paul Sabatier, Toulouse III, France, 2006.

[10] Singh, P., Singh, S. N., Lal, M., & Husain, M. (2008). Temperature dependence of I–V characteristics and performance parameters of silicon solar cell. Solar Energy Materials and Solar Cells, 92(12), 1611-1616.

[11] S. ABBOUDA, « Contribution à la commande des systèmes photovoltaïques », thèse de doctorat, Université de Reims Champagne-Ardenne et université de Sfax, 2015.

[12] C. R. Sullivan and M. J. Powers, « High-efficiency maximum power point tracker for photovoltaic arrays in a solar-powered race vehicle », The 1993 IEEE 24th Annual Power Electronics Specialists Conference, PESC Record, pp 574-580, Seattle, WA, USA, 1993.

[13] Hua, C., Lin, J., & Shen, C. (1998). Implementation of a DSP-controlled photovoltaic system with peak power tracking. IEEE Transactions on Industrial Electronics, 45(1), 99-107.

[14] Missoume Mohammed, « Contribution de l'énergie photovoltaïque dans la performance énergétique de l'habitat à haute qualité énergétique en Algérie », Mémoire de Magistère, Université de Chlef, 2011.

[15] Vincheh, M. R., Kargar, A., & Markadeh, G. A. (2014). A hybrid control method for maximum power point tracking (MPPT) in photovoltaic systems. Arabian Journal for Science and Engineering, 39(6), 4715-4725.

Chapter II

The static converters

II.1. Introduction:

New technology electronic devices must meet certain criteria such as high quality, reliability, size, weight and reduced cost [1]. Linear power regulators, whose operating principle is based on a current or voltage divider, can provide a very high quality output voltage [1,2]. However, this type of regulator remains inefficient because their main area of application is at low power levels. [3]

Switching regulators called DC/DC converters use electronic switches, based on semiconductors such as: the thyristor, power transistor or IGBT, etc..., because they generate a low loss of power when switching over 'one state to another ' [4]. These converters provide high energy conversion efficiencies and can operate at high frequencies. The dynamic characteristics of DC/DC converters improve with increasing operating frequencies. The high operating frequencies therefore allow for a faster dynamic response to rapid changes in load current or input voltage . [3]

There are several types of static converters on the market, in this chapter we will review the following converters:

II.2. DC / AC converters:

A converter (DC / AC) is a static converter which allows the transformation of energy of the continuous type, into an alternating energy. The form of the voltage of the output of the inverter must be closer to a sinusoid (l sinusoidal shape), is that the harmonic rate is very low, and it depends mainly on the control technique used.

Converters (DC/AC) are distinguished mainly by the nature of the DC stage and by the number of phases of the AC source. If the DC stage is seen as a source of current, the associated DC-AC converters are current inverters. If the DC stage is seen as a voltage source, the associated DC-AC converters are voltage inverters.

Most often, two or three phases are used. These converters (DC / AC) are direct converters, they are composed only of semiconductor switches, and the nature of the DC source dictates the nature of the AC source. [5]

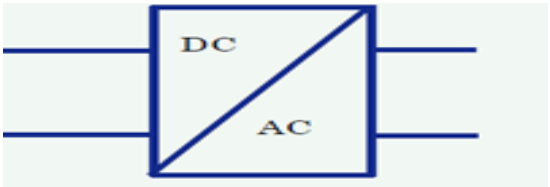

Figure II.1. Single-phase and three-phase DC-AC converter symbol.

II.2.1 Description:

The main function of an off-grid solar inverter is to convert a direct voltage such as that of a battery into an alternating voltage similar to that of the 230V household electrical network. Starting from a battery park in 12V, 24V or 48V we obtain a sinusoidal alternating output voltage, 230Vac in single phase.

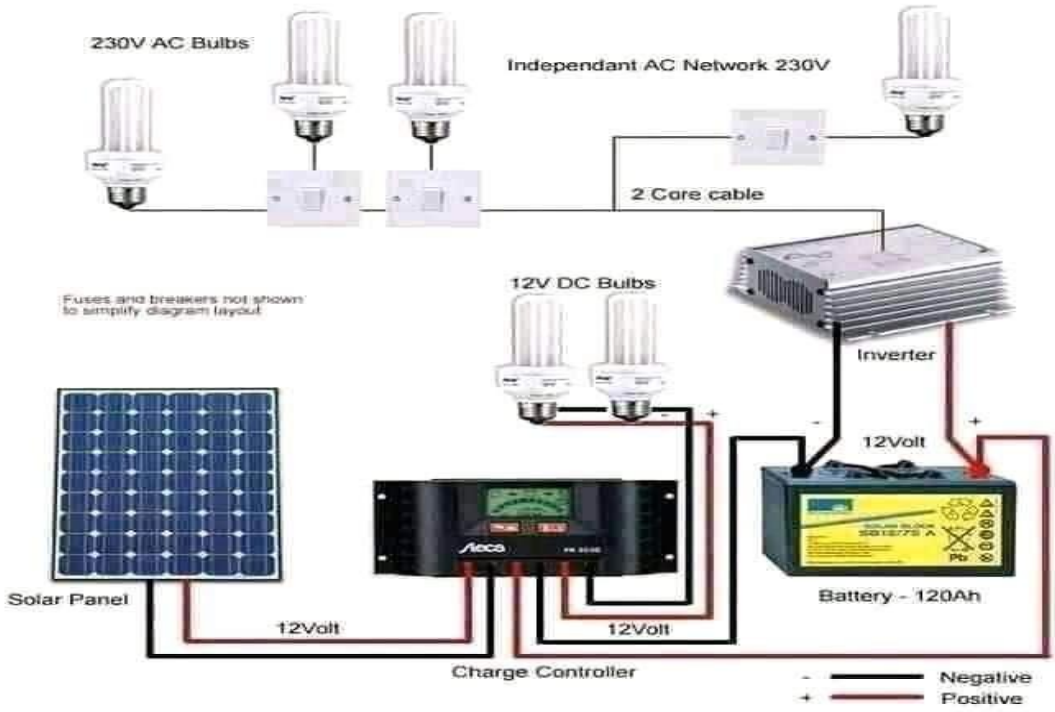

Figure II.2. Structure of a singl-phase inverter.

II.2.2 Principle of operation:

The creation of a sinusoid from a direct voltage is obtained thanks to voltage pulses of well-determined width, this technology uses PWM (Pulse width Modulation).

In practice, the inverter is made up of a set of active components (electronic switches) and passive components (transformer).

The inverter must tolerate a wide input voltage range (-10% to + 30%) due to variations in nominal battery voltage under different operating conditions.

II.2.3 Use of the solar inverter:

a) Nominal power:

The nominal power of an inverter is generally expressed in Volt / Ampere (VA), apparent power, or in Watt (W). This is the power that the converter can deliver in constant speed at a given temperature (often 25 ° C).

b) Overload capacity:

More commonly referred to as "peak / peak power", this function is the ability of the inverter to withstand a higher inrush current than its rated current over a short period of time. It is on average twice the nominal power.

c) Output signal:

The quality of the sine wave is important because it directly influences the power supply of sensitive receivers such as electronic cards and PC power supplies for example. This sinusoidal output voltage is defined by the rate of harmonics, it must be less than 5%.

d) Efficiency:

Like all energy converters, the inverter has an efficiency expressed in%, it is the ratio between the energy absorbed and the energy returned with a given power factor (Cos Phi).

This yield is variable depending on the model but it also depends on:

- The nominal power of the inverter
- DC input voltage
- The technology used
- The presence or absence of a transformer

e) Consumption:

The inverter consumes energy whether there is a load connected or whether it is on standby. When it is empty, that is to say that no receiver is powered, its consumption varies between 0.5 and 1% of its nominal power depending on the models. Or about ~ 10W for a 1000W inverter, which is not negligible on a stand-alone site.

To reduce this consumption, there are "stand-by" modes. The inverter sends pulses at regular intervals, every 2 seconds for example, to detect the presence of a consumer. When a load is connected, starting a fridge for example, the inverter detects the passage of current at the moment of the voltage pulse and starts up.

f) Protections:

The inverters incorporate several basic safeguards:

- Overload protection
- Short circuit protection
- Temperature protection
- Protection against too high or too low voltage (usually configurable)

II.3. Modeling of the DC / DC static converter:

II.3.1 Definition:

A chopper is a DC-DC converter that generates a variable DC voltage source from another DC voltage source Figure II.3. It consumes less power, which is why choppers have very good performance.

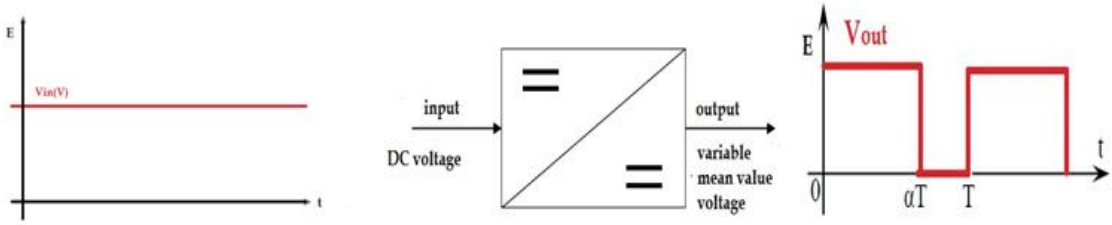

Figure II.3. Basic principle of a chopper.

Depending on the position of the switch and the chopper, different types of voltage converters can be made as shown in the diagram below [6]:

- "Boost " voltage booster or in particular called a booster chopper.
- "Buck" voltage step-down or step-down chopper.
- "Buck-Boost" voltage step-down / step-up device.

II.3.2 Buck converter:

The mathematical model of the Buck chopper is obtained by applying Kirchhoff's laws to the basic diagram of the chopper, shown in figure II.4 and with respect to the operating speed and the condition of switch S.

The scheme of the buck converter is given by the figure II.4: [7,8]

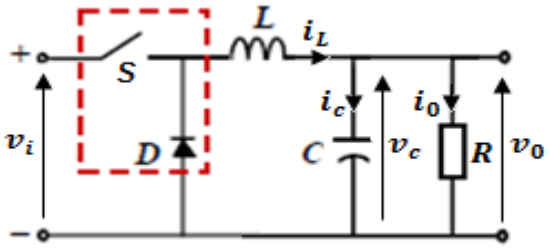

Figure II.4. Block diagram of the Buck Converter.

II.3.2.1 The state equations for buck mode:

During a period of time T, two switching modes can be expressed, Mode DT, i.e. (S1-ON & S2-OFF) and Mode (1- D) T i.e. (S1-OFF & S2-ON) Figure II.5: [9,10]

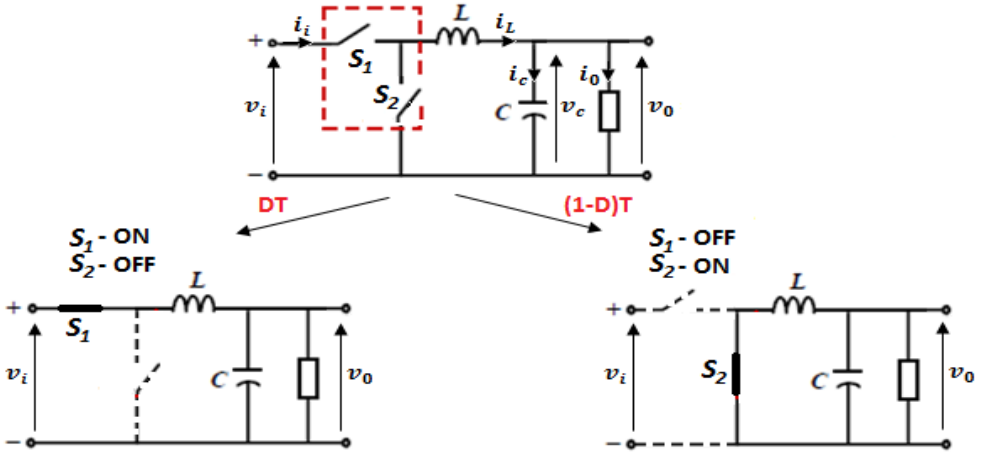

Figure II.5. Switching cycle for Buck converter.

Then the equations of state become :

Mode DT (S1-ON & S2-oFF):

$$\begin{cases} L\dfrac{di_L}{dt} = v_i - v_c \\ C\dfrac{dv_c}{dt} = i_L - \dfrac{v_c}{R} \end{cases} \quad \text{(II. 1)}$$

Mode (1- D)T (S1-OFF & S2-ON):

$$\begin{cases} L\dfrac{di_L}{dt} = 0 - v_c \\ C\dfrac{dv_c}{dt} = i_L - \dfrac{v_c}{R} \end{cases} \quad \text{(II. 2)}$$

The state equation from (II.1) is:

$$\begin{bmatrix} \dot{i}_L \\ \dot{v}_C \end{bmatrix} = \begin{bmatrix} 0 & -\dfrac{1}{L} \\ \dfrac{1}{C} & -\dfrac{1}{RC} \end{bmatrix} \begin{bmatrix} i_L \\ v_C \end{bmatrix} + \begin{bmatrix} \dfrac{1}{L} \\ 0 \end{bmatrix} [v_i]$$

The equation of state from (II.2):

$$\begin{bmatrix} \dot{i}_L \\ \dot{v}_C \end{bmatrix} = \begin{bmatrix} 0 & -\dfrac{1}{L} \\ \dfrac{1}{C} & -\dfrac{1}{RC} \end{bmatrix} \begin{bmatrix} i_L \\ v_C \end{bmatrix} + \begin{bmatrix} 0 \\ 0 \end{bmatrix} [v_i]$$

Basically, equations (II.1), and (II.2) we can express the control equations for the two switching sequences :

$$\begin{cases} \dfrac{di_L}{dt} = u\dfrac{1}{L}v_i - \dfrac{1}{L}v_c \\ \dfrac{dv_c}{dt} = \dfrac{1}{C}i_L - \dfrac{1}{RC}v_c \end{cases} \Rightarrow \begin{cases} \dot{x}_1 = u\dfrac{1}{L}v_i - \dfrac{1}{L}x_2 \\ \dot{x}_2 = \dfrac{1}{C}x_1 - \dfrac{1}{RC}x_2 \end{cases} \Rightarrow \begin{bmatrix} \dot{x}_1 \\ \dot{x}_2 \end{bmatrix} = \begin{bmatrix} 0 & -\dfrac{1}{L} \\ \dfrac{1}{C} & -\dfrac{1}{RC} \end{bmatrix} \begin{bmatrix} x_1 \\ x_2 \end{bmatrix} + \begin{bmatrix} \dfrac{d}{L} \\ 0 \end{bmatrix} [v_i] \quad \text{(II. 3)}$$

The characteristic equation for the inductance current is:

$$\frac{dI}{dt} = \frac{V_i - V_o}{\mathrm{L}} \quad \text{(II.4)}$$

The switching process described by the position of the switch, in the first time (D.T), the inductance discharges. In the second time (D -1) T, the inductance releases with a decrease in current IL.

$$\frac{dI}{dt} = \frac{V_i}{\mathrm{L}} \quad \text{(II.5)}$$

The characteristics of the currents and the voltage representing the operation of the step-down chopper are given by the following Figures:

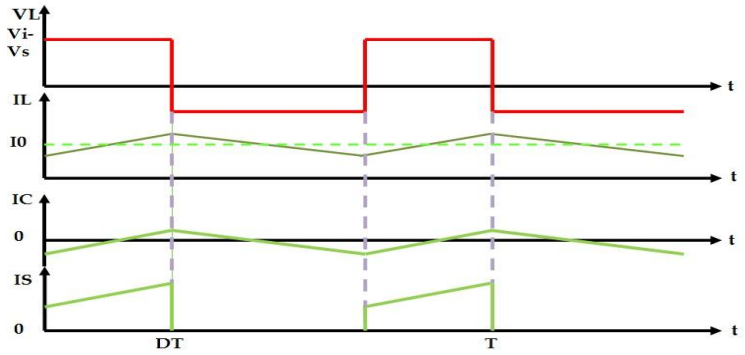

Figure II.6. Characteristic of voltage-current.

II.3.3 Boost:

The mathematical model of the Boost chopper is presented in Figure II.7. [10]

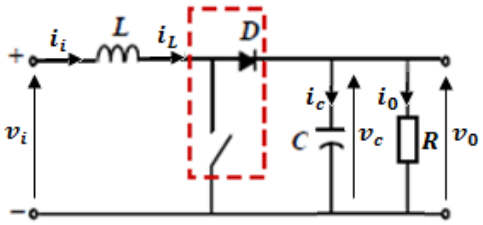

Figure II.7.Boost principle diagram.

II.3.3.1 Equations of state for Boost mode:

The mathematical model of the Boost chopper is presented in Figure II.8. The operation of this converter is made according to two switching modes. [9]

During a period of time T, two switching modes can be expressed, Mode DT, i.e. (S1-ON & S2-OFF) and Mode (1- D) T i.e. (S1-OFF & S2-ON) : [9,10]

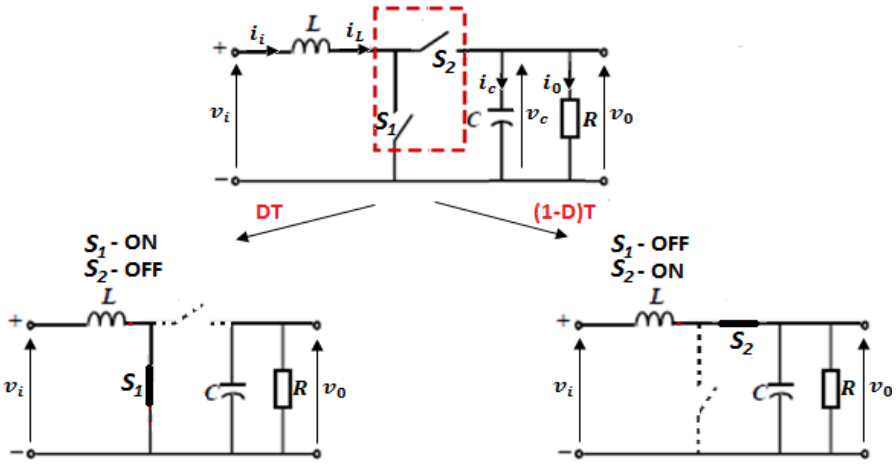

FigureII.8. Switching cycle for Boost converter.

In the same way as in Buck converters, we obtain the following two formulas:

$$\begin{cases} \dfrac{di_L}{dt} = \dfrac{1}{L}v_i - (1-u)\dfrac{1}{L}v_c \\ \dfrac{dv_c}{dt} = (1-u)\dfrac{1}{C}i_L - \dfrac{1}{RC}v_c \end{cases} \Rightarrow \begin{cases} \dot{x}_1 = \dfrac{1}{L}v_i - (1-u)\dfrac{1}{L}x_2 \\ \dot{x}_2 = (1-u)\dfrac{1}{C}x_1 - \dfrac{1}{RC}x_2 \end{cases} \quad \text{(II. 6)}$$

In this case, the equation of the voltage at the terminals of the load describing the operation in continuous conduction is given as follows:

$$V_o = \frac{1}{1-D} Vi \qquad \text{(II.7)}$$

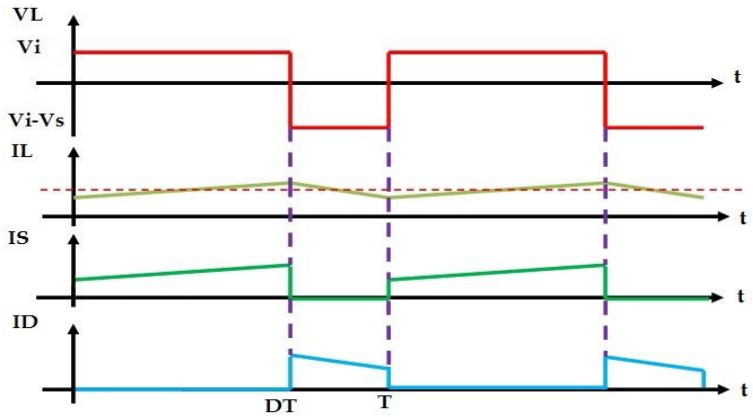

Figure II.9. Characteristic of the voltage and current of the BOOST converter.

II.3.4 Buck-boost:

The presentation of the operation of this type of converter by mathematical equations must be carried out taking into account the state of the switch S in Figure II.10. [9]

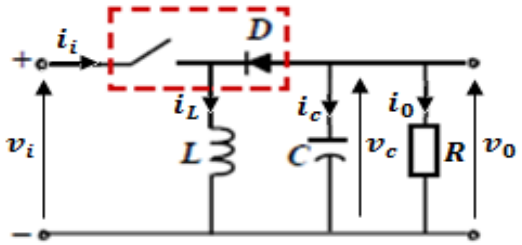

Figure II.10. diagram of the Buck-boost.

II.3.4.1Equations of state for buck-boost mode:

The mathematical model of the buck-boost chopper is presented in Figure II.11. The operation of this converter is made according to two switching modes. [10]

When the switch is on, then Ton = D * T. As a result, the energy stored in the inductance increases.

When S is blocked, then Toff = (1-D) * T and the energy accumulated in the inductance transfers to the capacitance and the load. [9]

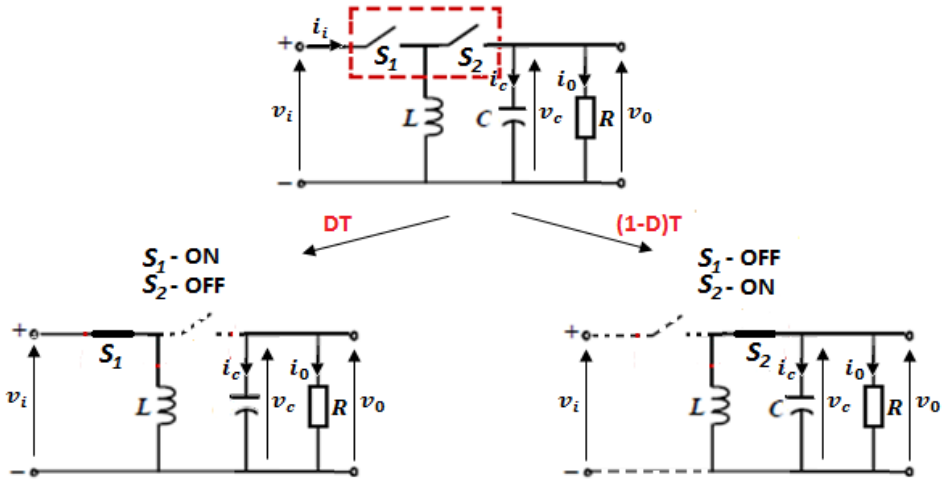

Figure II.11.switching cycle for buck-boost converter.

In the same way as in Buck converters

$$\begin{cases} L\frac{di_L}{dt} = u.v_i + (1-u)v_c \\ C\frac{dv_c}{dt} = -(1-u)i_L - \frac{v_c}{R} \end{cases} \Rightarrow \begin{bmatrix} \dot{i_L} \\ \dot{v_C} \end{bmatrix} = \begin{bmatrix} 0 & -\frac{(1-d)}{L} \\ \frac{(1-d)}{C} & -\frac{1}{RC} \end{bmatrix} \begin{bmatrix} i_L \\ v_C \end{bmatrix} + \begin{bmatrix} \frac{d}{L} \\ 0 \end{bmatrix} [v_i] \quad \text{(II. 8)}$$

In this case, the equation of the voltage at the terminals of the load describing the operation in continuous conduction is given as follows:

$$V_o = \frac{\mathrm{D}}{1-\mathrm{D}} V_i \quad \text{(II.9)}$$

The characteristics of the charging current and voltage are given in the Figure below:

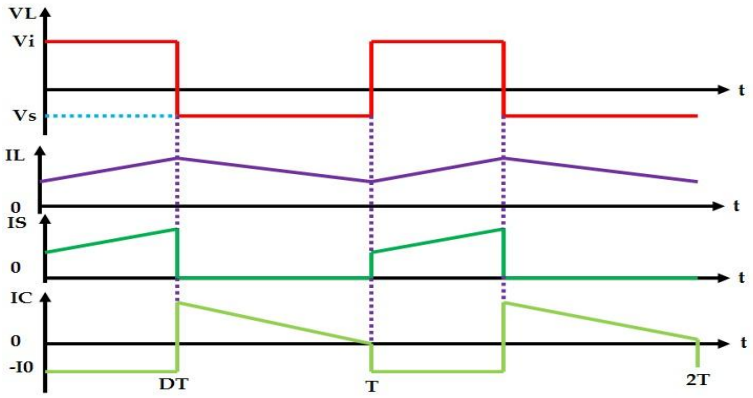

Figure II.12. Characteristic of the voltage and current of the Buck-BOOST converter.

II.4. Conclusion:

Currently, the systems rely on a reliable power supply in terms of the high quality delivered, efficiency and weight reduction. For this, the linear power supply has been replaced by the switching power supply or the DC / DC converter. In this chapter, we have mentioned some converters used in the field of PV energy (DC / DC; DC / AC static converter).

References:

[1] Babaei E, Esmaeel M, Mahmoodieh S. Electrical Power and Energy Systems Systematical method of designing the elements of the Cuk converter. Int J Electr Power Energy Syst 2014;55:351–61. https://doi.org/10.1016/j.ijepes.2013.09.024.

[2] Enrique JM, Dura E. Theoretical assessment of the maximum power point tracking efficiency of photovoltaic facilities with different converter topologies 2007;81:31–8. https://doi.org/10.1016/j.solener.2006.06.006.

[3] Rashid MH. POWER ELECTRONICS. Academic Press Series in Engineering; 2001.

[4] Mazouz N, Midoun A. Electrical Power and Energy Systems Control of a DC / DC converter by fuzzy controller for a solar pumping system. Int J Electr Power Energy Syst 2011;33:1623–30. https://doi.org/10.1016/j.ijepes.2011.06.016.

[5] M. Yousef, «Etude de raccordement d'un système photovoltaïque au réseau électrique», Mémoire de Master, Université Kasdi Merbah Ouargla, 2015.

[6] A.Luque, S. Hegedus: Handbook of Photovoltaic Science and Engineering Ltd, 2003.

[7] Hamza SAHRAOUI , Larbi CHRIFI-ALAOUI , Said DRID , Pascal BUSSY, " Second Order Sliding Mode Control of DC-DC Converter used in the Photovoltaic System According an Adaptive MPPT ", INTERNATIONAL JOURNAL of RENEWABLE ENERGY RESEARCH, Vol.6, No.2, 2016.

[8] Ali Jaafar, ''Contribution à la modélisation, l'analyse et l'optimisation de lois de commande pour convertisseurs DC-DC de puissance'', THÈSE DE DOCTORAT, Soutenue le 14 novembre 2011

[9] Asma MERDASSI, ''Outil d'aide à la modélisation moyenne de convertisseurs statiques pour la simulation de systèmes mécatroniques'', Institut National Polytechnique de Grenoble - INPG, 2009.

[10] André C., Gabriel A, Bruno J, René Z, '' Ingénierie de la commande des systèmes'', Ellipses Edition Marketing S.A., 2001, ISBN 2-7298-0498-6.

Chapter III

Maximum power point tracking (mppt) methods review

III.1. Introduction:

There are specific control laws to operate the equipment to the maximum of its characteristics, without knowing these points in advance, without knowing when they are modified or without knowing when they are modified, which is the reason for this change. In terms of energy, this translates to the maximum power point. This type of command is commonly referred to in the literature as "Maximum Power Point Tracking" (MPPT). The principle of these controls is to seek the maximum power point (PPM) while ensuring a perfect match between the generator and its load in order to deliver maximum power.

This chapter is devoted to the study of various selected MPPT methods by grouping them according to their principle.The most commonly encountered are:

- Hill climbing
- Perturb and Observe
- Incrémental Conductance
- fuzzy logic control
- Genetic algorithms
- sliding mode control
- Synergistic control

III.2. Historical:

Maximum power point tracking (MPPT) is an essential part in photovoltaic systems. Several techniques have been developed since 1968, when the first control law of this type was published, adapted to a renewable energy source such as PV. These techniques differ from each other in their complexity, number of sensors required, speed of convergence, cost, efficiency and field of application.

III.3. First types of MPPT command:

BOEHRINGER applied the first MPPT command to PV in 1968 [1]. It is a simple algorithm that can be implemented digitally (FigureIII.1). It is intended for space applications which had much less temperature and illumination variation constraints than terrestrial applications.

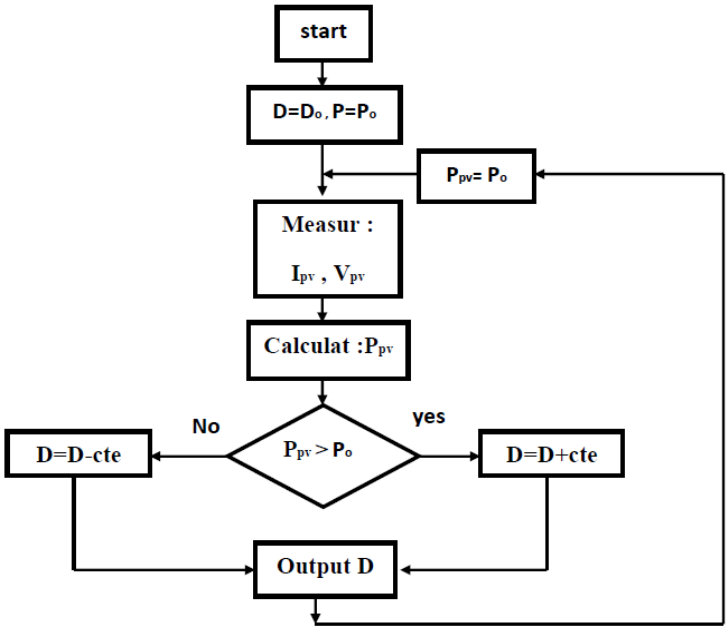

Figure III.1. Flowchart of the first MPPT command. [1]

III.4. Principle of the mppt control:

By definition, an MPPT control, associated with an intermediate adaptation stage, makes it possible to operate a GPV in such a way as to constantly produce the maximum of its power. Thus, whatever the weather conditions (temperature and irradiation), the converter control places the system at the maximum operating point (VPPM and IPPM). The photovoltaic conversion chain will be optimized through a static converter (CS) controlled by an MPPT [2]. It can be represented by the diagram in Figure III.2

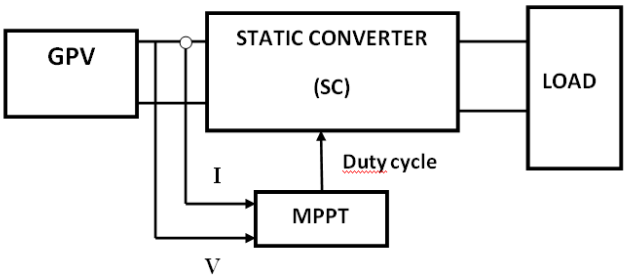

Figure III.2. Solar energy conversion chain.

The MPPT control varies the duty cycle of the static converter (CS), using an appropriate electrical signal, to get the maximum power that the GPV can deliver. The MPPT algorithm can be more or less complicated to find the MPP. In general, it is based on the variation of the duty cycle of the CS according to the evolution of the input parameters of the latter (I and V and consequently of the power of the GPV) until it is placed on the MPP. [3]

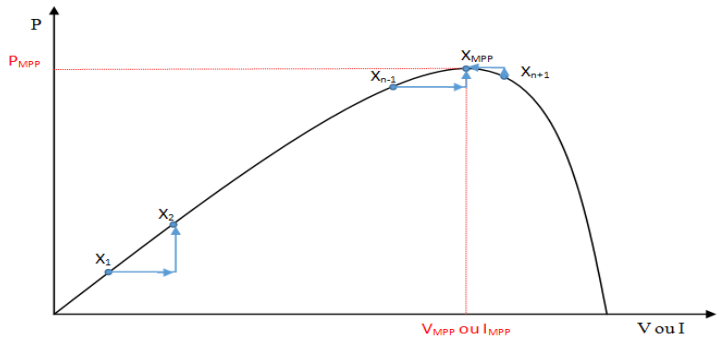

Figure III.3. Principle of MPPT control.

III.5. State of the art on mppt techniques in photovoltaic applications:

The operating power of solar panels is easy to calculate. It is equal to the product current voltage. However, the determination of the reference power is more difficult since the latter is a function of the meteorological parameters (temperature and illumination). This variable reference, characterized by a non-linear function, makes operation at maximum power more difficult to achieve. So an order for the continuation of the PPM is needed. This command, called the MPPT algorithm, can be more or less complicated. It is generally based on adjusting the duty cycle of the static converter until it sits on the PPM. Different MPPT methods have been published in the literature in order to obtain optimal operation. Many researchers are interested in recalling and comparing the different MPPT techniques that exist in the literature [4,5,6]. BHATNAGAR cites more than thirty MPPT techniques in his article [7]. ESRAM and CHAPMAN compare several MPPT algorithms according to their dependencies on solar panel parameters and their implementation complexities. We can classify these methods according to PASTOR by [8]:

_The type of electronic implementation: analog, digital or mixed;

_ The input parameters of the command: MPPT commands operating from the input or output parameters of the CS;

_The type of research or control.

III.6. Classification of mppt commands:

We can broadly classify MPPT commands according to the type of electronic implementation: analog, digital, or mixed. However, it is more interesting to classify them according to the type of search they perform and according to the input parameters of the MPPT command. [9]

III.6.1 Classification of mppt commands according to input parameters:

a) Mppt commands operating from the cs input parameters:

There are a number of MPPT commands which search for the PPM according to the evolution of the power supplied by the GPV. Like the hill climbing method, Perturb & Observe and the conductance increment algorithms which use the value of the power supplied by the GPV for the application of an adequate control action for the follow-up of the PPM or the commands which are based on proportionality relations between the optimal parameters characterizing the maximum power point (VOPT and IOPT) and the characteristic parameters of the PV module (VOC and ISC). In particular, the MPPTs inspired by neural networks. In these orders, either one uses large computer memory systems having stored all the possible cases, or the orders are once again more approximate. All these commands have the advantages of their precision and speed of reaction [9].

b) Mppt controls operating from converter output parameters:

In the literature, there are also algorithms based on the output parameters of the CS. For example MPPT commands based on maximizing the output current which are mainly used when the load is a battery.

In all systems using the output parameters, an approximation of Pmax is made through the efficiency of the converter. In short, the better the conversion stage, the more valid this approximation is. On the other hand, in general, all systems with a single sensor are inherently not precise. Most of these systems were originally designed for space [9].

III.6.2 Classification of mppt commands by search type:

a) Mppt indirect:

This type of MPPT command uses the link between the measured variables (Isc or Voc), which can be easily determined, and the approximate position of the MPP. It also counts the commands based on an estimate of the operating point of the GPV made from a parametric model defined in advance. There are also commands that establish an optimal voltage tracking by taking into account only the variations in the temperature of the cells given by a sensor. These commands have the advantage of being simple to perform. Rather, they are intended for inexpensive and imprecise systems that need to operate in geographic areas where there is little climate change. [9-10]

b) Mppt direct:

This type of MPPT control determines the optimum operating point (MPP) from the currents, voltages or powers measured in the system. It can therefore react to unpredictable changes in the operation of the GPV. Usually, these procedures are based on a search algorithm, with which the maximum of the power curve is determined without interruption of operation. For this, the operating point voltage is incremented at regular intervals. If the output power is larger, then the seek direction is maintained for the next step, otherwise it will be reversed. The actual operating point then oscillates around the MPP. This basic principle can be preserved by other algorithms against misinterpretation. These errors can occur, for example, due to poor search direction, resulting from an increase in power which is due to a rapid increase in the radiation level. The determination of the value of the power of the PV generator, essential for the search for the MPP, requires the measurement of the voltage and the current of the generator, as well as the multiplication of these two variables. Other algorithms are based on the introduction of sinusoidal variations in small signal on the switching frequency of the converter to compare the AC component and the DC component of the voltage of the GPV and thus to place the operating point of the GPV closest possible from MPP. The advantage of these types of commands is their precision and speed of reaction. [10-9]

III.7. Mppt algorithms:

III.7.1 Hill climbing:

III.7.1.1 Definition:

hill climbing is an optimization technique through which a "local optimal" solution to a computational problem can be found. This is an iterative method and belongs to the local search family.

III.7.1.2 working principle:

The “Hill Climbing” control technique consists in giving a disturbance on the duty cycle which results in a displacement of the operating point along the power-duty cycle characteristic of the photovoltaic generator. Theoretically, research should stop when the maximum power point is reached. [11]

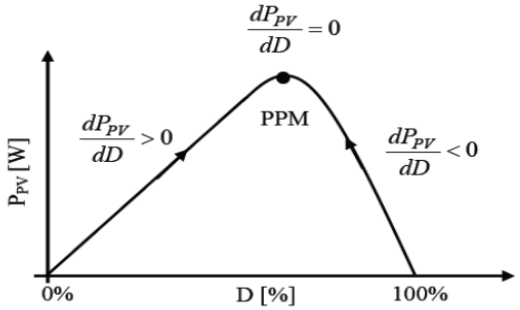

Figure III.4.Relationship between power and duty cycle.[12]

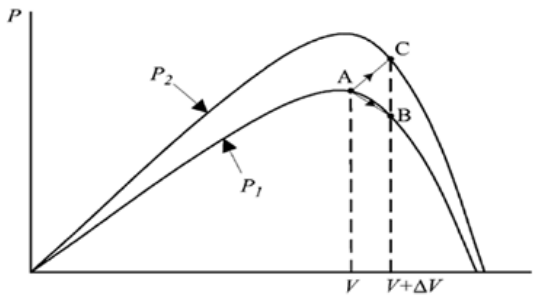

Figure III.5.Divergence from MPP .[13]

More clearly, its working principle consists on periodically measuring PV voltage (Vpv) and current (Ipv), for calculating present PV power (Ppv) and then, a perturbation in the duty ratio (D) of the DC/DC converter is applied, so that its direction makes the operation point approach the MPP [14,15]. The modi cation of duty cycle directly a ects Ipv value, which consequently changes the Vpv [16]. The perturbation direction depends on the comparison of current and just earlier measurement of Ppv, and it has axed step-size. [15]

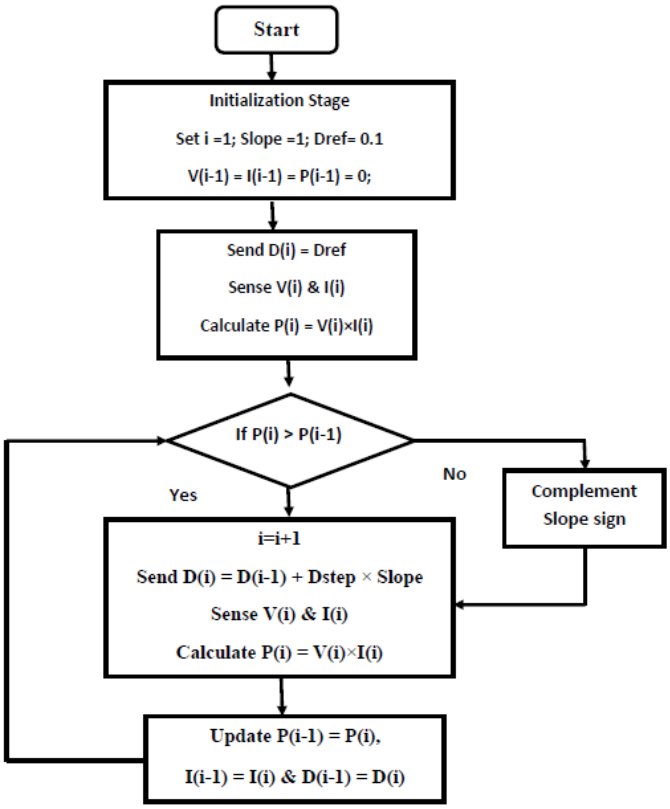

Figure III.6. Flow chart of conventional HC MPPT Algorithm. [12]

In HC, at each iteration i, the algorithm starts sensing the voltage, V(i) and current, I(i) of PV array and the corresponding power, P(i)= V(i)×I(i) is then calculated. Next, the duty cycle (D) of the converter is perturbed by an increment of duty cycle step size (D_{step}), and the resulting change of power, dP = P(i+1) - P(i) is obtained. If the dP is positive, then perturbation is in the right direction, and more perturbation is applied in the same direction to reach the MPP. The perturbation direction is reversed if dP is negative, an indication that the tracking is moved away from the MPP. The flowchart of the HC algorithm is shown in FigureIII. 6. [12]

III.7.1.3 The goal of employing hill climbing:

The goal of employing MPPT is to extract maximum power from PV Array at any varying atmospheric conditions especially solar irradiance changes. To do so, MPPT algorithm perturbs the duty cycle of the DC-DC converter to match the resistance of load as seen by the source (Rin) to the internal optimal resistance of PV Array (RMPP). In this work, the conventional Hill Climbing algorithm as discussed in [17, 18-19] has been applied to track the MPP when subjected to sudden changes in solar irradiance. Practically, it can replace the expensive MPPT controller with lower cost controller while maintaining similar optimum results.

III.7.1.4 Advantages and disadvantages of hill climbing technique:

finaly This technique is mainly characterized by its easy implementation [24] and simple calculations [24]. Hence, together with P&O method, it is a widely applied technique among all the MPPT algorithms. [21,20]

Nevertheless, HC algorithm presents some disadvantages. Because of fast changing of environmental conditions, such as broken clouds, deviations from the MPP can appear [6]. This is produced since the characteristic curve of the PV array changes. According to [21], this change can become a problem, if the variation of power caused by di erent intensity of irradiance, is larger than the one produced by the perturbation.

III.7.2 Perturb And Observe (P&O):

III.7.2.1 Définition:

The P&O method is generally the most used because of its simplicity and ease of implementation. As its name suggests, this method is based on the disturbance (an increase or decrease) of the voltage Vref, or of the current Iref, and the observation of the consequence of this disturbance on the measured power (P = VI) [22]. However, the ideal variable that characterizes the MPP is that which varies little during climate change. The variation in radiation affects the current more than the photovoltaic voltage. On the other hand, the variation of the temperature modifies more the tension of the GPV. However, the temperature dynamics are slow and vary over a small range. Therefore, it is better to check the voltage of the GPV. [23]

III.7.2.2 working principle:

Its working principle is based on the disturbance of the operating point (by increasing or decreasing the operating voltage) and the observation of its effect on the power (P). If the power increases ($\Delta P > 0$), we are therefore in the right direction, we continue the disturbance in the same direction otherwise ($\Delta P < 0$), so we move away from the PPM, we reverse the disturbance. Figure III.8 illustrates its principle of operation. [24,25]

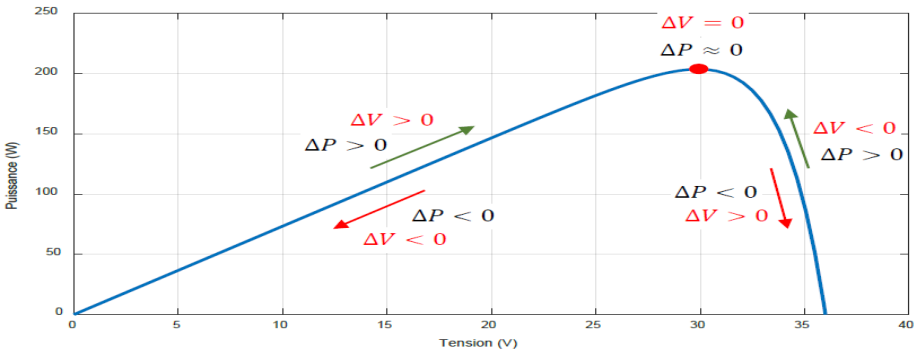

Figure III.7. Principle of MPPT with the P&O method. [26]

More clearly the operation principle is based on periodical perturbation on the terminal voltage of the PV module and comparison between the current power value of the PV output and the power at the previous perturbation. The operating point is continuously moving in the same direction if the PV module power rises with increasing operating voltage; otherwise, the operating point direction will be reversed. [27]

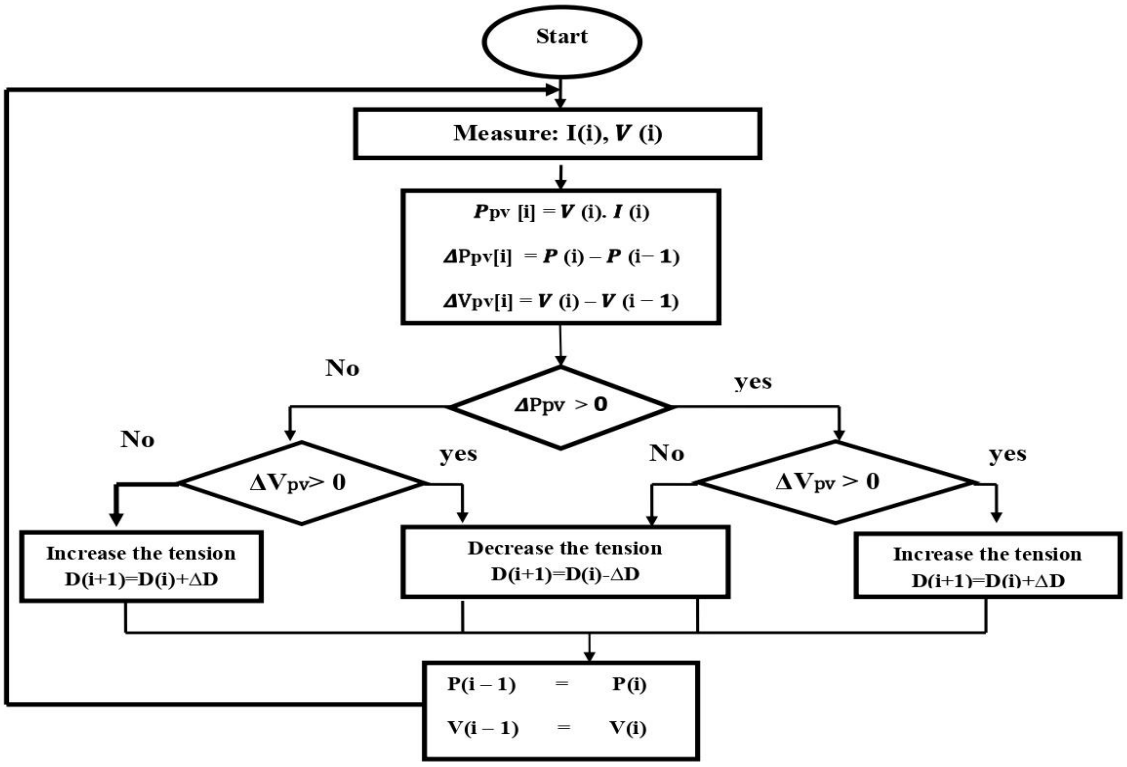

Figure III.8. Flowchart of the P&O method.[26]

The flowchart of this method is given in Figure II.18. We recover the current and the PV voltage then we calculate the new power P (t) and the variation of the voltage (Δv), if the power has increased (ΔP> 0) we are therefore in the right direction, we continue thus d " increase V (if Δv> 0) or continue to decrease it (if Δv <0), otherwise (ΔP <0) it is necessary to invert (increase V if Δv <0 and decrease if ΔV> 0). [26]

III.7.2.3 The goal of employing perturb and observe:

The goal of employing the P&O method is to modify the operating voltage or current of the PV panel until you obtain maximum power from it and to get a steady performance and high energy utilization efficiency .

III.7.2.4 Advantages and disadvantages of perturb and observe technique:

the P&O algorithm offers a steady performance and high energy utilization efficiency, when its step size and perturbation frequency are chosen appropriately. [26]

This method has a drawback during a rapid change of light, in which case the power of the search point will be disturbed by the sunshine and not by the disturbance of the algorithm. This can cause the algorithm to diverge, thus taking time to return to the correct direction and longer to reach the PPM. [26]

Figure III. 9 illustrates this problem. Suppose we are at point A going to the right in the right direction of search ($\Delta V > 0$), if we assume that the sunshine does not change (or changes slowly) the next power measured at point B and higher ($\Delta P > 0$) so we increase V which brings us closer to the PPM. But if a sudden change in light (decrease in our example) occurs we go to point C and the power in this case is lower ($\Delta V > 0$ and $\Delta P < 0$) so the voltage will be reduced and consequently we move away of the PPM . [26]

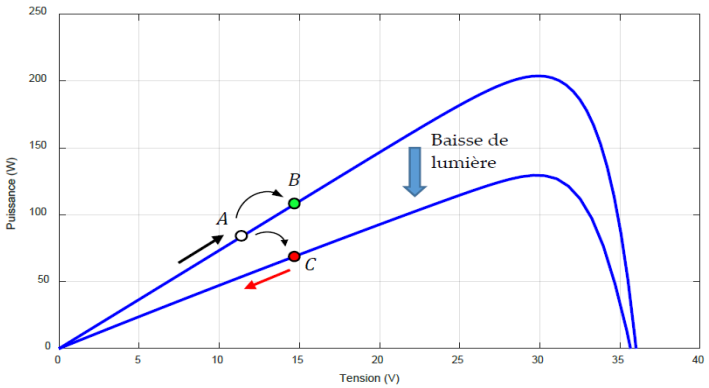

Figure III.9. Rapid temperature change in the case of MPPT with P&O. [26]

The problem in this case is that we monitor the variation of the power in the P-V curve to know if we are to the left or to the right of the PPM, this problem is solved with the method the Incremental Conductance "Incremental Conductance" (IC) and this by monitoring the slope of this curve (take into account the variation of the current) which really gives the position of the search point in relation to the PPM. We notice that even with an abrupt change of light the slope of the curve remains of the same sign which keeps the search in the same direction, this method will be detailed in the following paragraph.

III.7.3 Incremental Conductance:

III.7.3.1 Definition:

The Incremental Conductance method is generally the most used because of its simplicity and ease of implementation .This technique is based on the variation of the conductance of the GPV and its influence on the position of the operating point. [28,29]

III.7.3.2 working principle:

the conductance of the photovoltaic module is defined by the ratio between the current and the voltage of the GPV as shown below. [30,31]

$$G = \frac{I_{pv}}{V_{pv}} \quad \text{(III.1)}$$

So an elementary variation (increment) of conductance can be defined by:

$$dG = \frac{dI_{pv}}{dV_{pv}} \quad \text{(III.2)}$$

On the other hand, the evolution of the power of the GPV relative to the voltage gives the position of the operating point relative to the PPM. When the power derivative is zero, it means that we are on the PPM, if it is positive the operating point is to the left of the maximum, when it is negative, it is to the right. Figure III.10 makes it possible to write the following conditions:

- If $\frac{dP_{pv}}{dV_{pv}} > 0$ the operating point is to the left of the PPM
- If $\frac{dP_{pv}}{dV_{pv}} < 0$ the operating point is on the right of the PPM
- If $\frac{dP_{pv}}{dV_{pv}} = 0$ the operating point is on the PPM

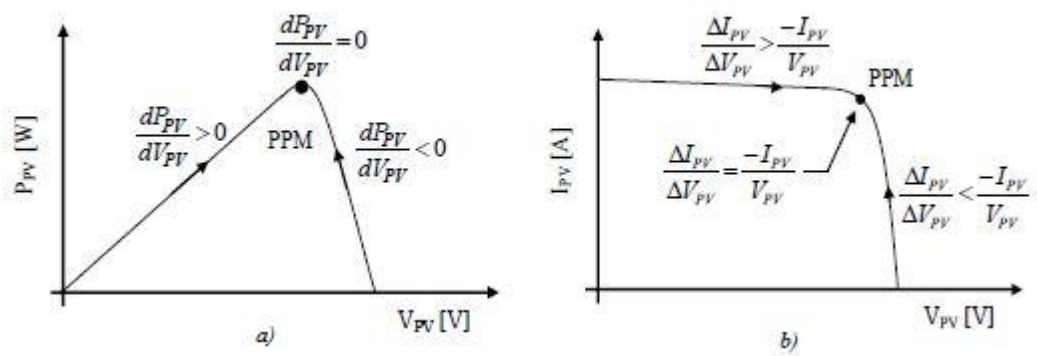

Figure III.10. Positioning of the operating point according to the sign of the derivative of the conductance G. [31]

The link between the conductance given by equation (III.1) and the derivative of the power $\frac{dP_{pv}}{dV_{pv}}$ Can be described by the following equation:

$$\frac{dP_{pv}}{dV_{pv}} = I_{pv} + V_{pv}\frac{dI_{pv}}{dV_{pv}} \cong I_{pv} + V_{pv}\frac{\Delta I_{pv}}{\Delta V_{pv}} \quad \text{(III.3)}$$

From where, one can then write new conditions on the variation of conductance.

- If $\frac{\Delta \boldsymbol{I_{pv}}}{\Delta \boldsymbol{V_{pv}}} > -\frac{\boldsymbol{I_{pv}}}{\boldsymbol{V_{pv}}}$ the operating point is to the left of the PPM.
- If $\frac{\Delta \boldsymbol{I_{pv}}}{\Delta \boldsymbol{V_{pv}}} < -\frac{\boldsymbol{I_{pv}}}{\boldsymbol{V_{pv}}}$ the operating point is on the right of the PPM.
- If $\frac{\Delta \boldsymbol{I_{pv}}}{\Delta \boldsymbol{V_{pv}}} = -\frac{\boldsymbol{I_{pv}}}{\boldsymbol{V_{pv}}}$ the operating point is on the PPM.

The maximum power can then be tracked by making comparisons at each moment of the value of the conductance $\frac{\boldsymbol{I_{pv}}}{\boldsymbol{V_{pv}}}$ with that of the conductance increment $\frac{\Delta \boldsymbol{I_{pv}}}{\Delta \boldsymbol{V_{pv}}}$, as illustrated by the algorithm in Figure III.11. Vr corresponds to the reference voltage and forces the GPV to operate at that value. If we are at the PPM, then the voltage Vr corresponds well to the optimal voltage Vppm Once the PPM is reached, the operating point can be maintained in this position until a variation in $\boldsymbol{\Delta I_{pv}}$ This then indicates a change in climatic conditions, therefore a new PPM to look for. For this, the algorithm increments or decrements the value of Vr until reaching the PPM. [31]

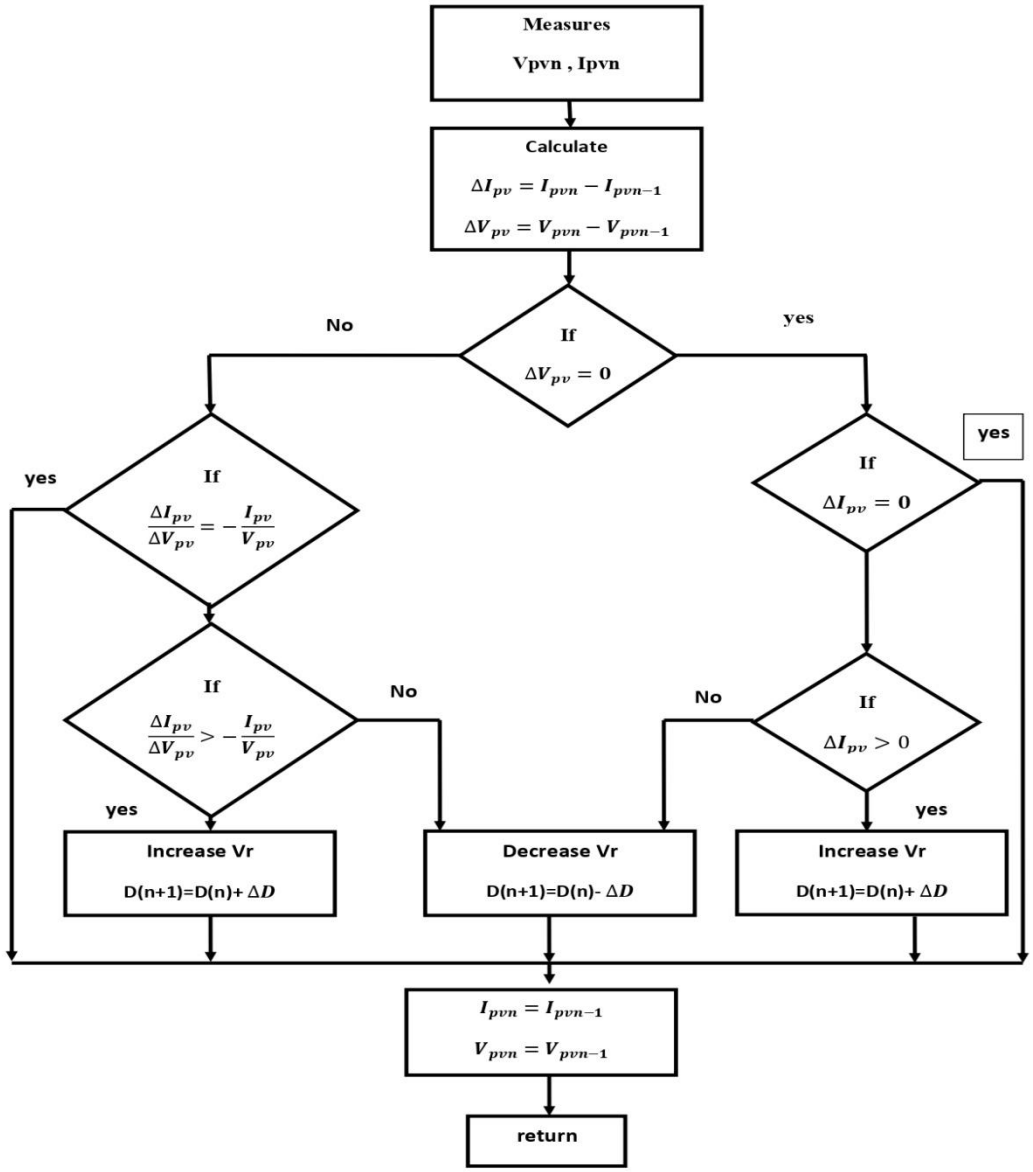

Figure III.11. Algorithm of an MPPT command based on the method Conductance increment. [31]

III.7.3.3 The goal of employing Incremental Conductance:

The goal of employing the Incremental Conductance method is that we monitor the variation of the power in the P-V curve to know if we are to the left or to the right of the PPM until you obtain maximum power from it and to get a steady performance and high energy utilization efficiency.

III.7.3.4 Advantages and disadvantages of Incremental Conductance:

The main advantage of this algorithm is that it is suitable for unstable climatic conditions because, theoretically, it is possible to find an MPP and stop there if the disturbance ceases. In this case, the voltage variation is zero; the appearance of a current variation makes it possible to adjust the value of the reference voltage to reach a new MPP. [30]

In practice, the system presents an oscillation like the P&O command around the PPM, because of the noise at the levels of the acquisitions of the input parameters Vpv, Ipv and of the difficulty for the system to properly analyze whether the relation (III-3) is well filled or not. So, in reality, this condition never being obtained, the system is still looking for it. Compared to the P&O command, the execution time of the algorithm is longer because the latter is more complex. As a result, the time interval between two voltage and current samples is increased causing a delay in the detection of climatic variations. [31]

III.8. application of artificial intelligence techniques:

III.8.1. fuzzy logic control:

III.8.1.1. Definition:

Fuzzy logic is a form of logic that deals with approximate reasoning rather than fixed and exact. Unlike traditional logic which typically defines two-valued logic as true or false, fuzzy logic can have varying values. The variables of fuzzy logic can have a true or false value which varies to different degrees and be expressed by linguistic variables. In these cases, fuzzy logic control could provide both fast process speed and the necessary precision. [32]

III.8.1.2.working principle:

The fuzzy controller consists of three functional blocks namely fuzzification, rules of inference and defuzzification [33,34] (Figure III.12). In the proposed system, the input variables of the FLC are the error (Err) and the change of error (ΔErr) while the output of the FLC is the change of the duty cycle ΔD [35]. The FLC fuzzy controller block is shown in Figure III.13.

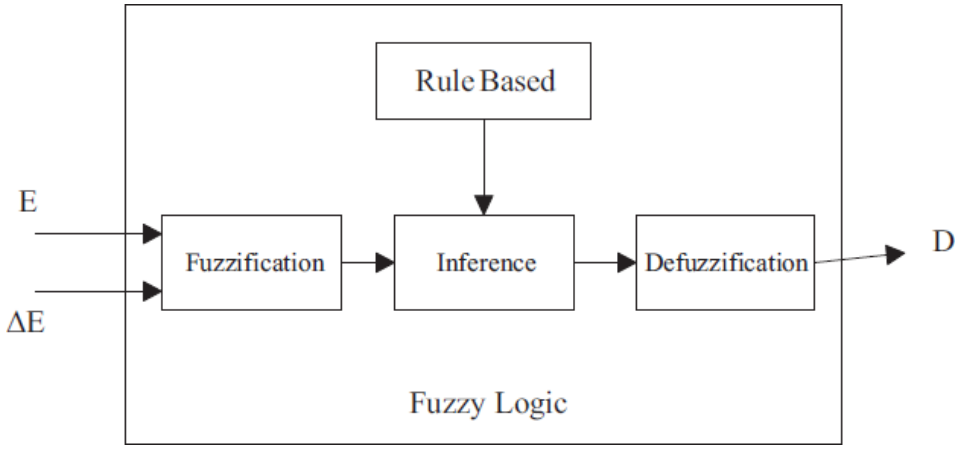

Figure III.12.Fuzzy Logic Based MPPT Flowchart. [36]

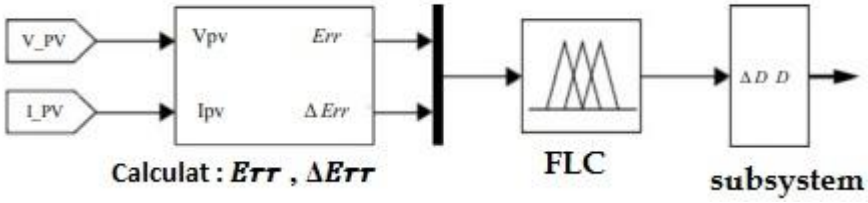

Figure III.13.The controller block based on fuzzy logic. [36]

The two inputs (the error and the variation of the error) are determined from the power and the output voltage of the PV and they are expressed by [32]:

$$\mathrm{Err} = \frac{\mathrm{P(k)-P(k-1)}}{\mathrm{V(k)-V(k-1)}} \quad \text{(III.4)}$$

With

$$\mathrm{P(K)} = \mathrm{Vpv(K)} \,.\, \mathrm{Ipv(K)} \quad \text{(III.5)}$$

And

$$\Delta Err = \mathrm{Err(k)} - \mathrm{Err(k\text{-}1)} \quad \text{(III.6)}$$

In the fuzzification process, the input variables Err and ΔErr and the output variable ΔD are converted into linguistic variables by assigning membership function values [40,28]

In order to be able to process linguistic variables numerically, they must be subjected to a mathematical definition based on membership functions which show the degree of verification of these variables to the different subsets [37]. The membership functions Err, ΔErr and ΔD are shown in Figure III.14 There are several types of membership functions: triangular, Gaussian, trapezoidal, etc...[38]. The membership functions are most often

represented by the triangular and trapezoidal functions, therefore by line segments, and are then said to be piecewise linear, so they are widely used because they are simple and include points making it possible to define the areas where the notion is true or false, which simplifies the collection of expertise. [37]

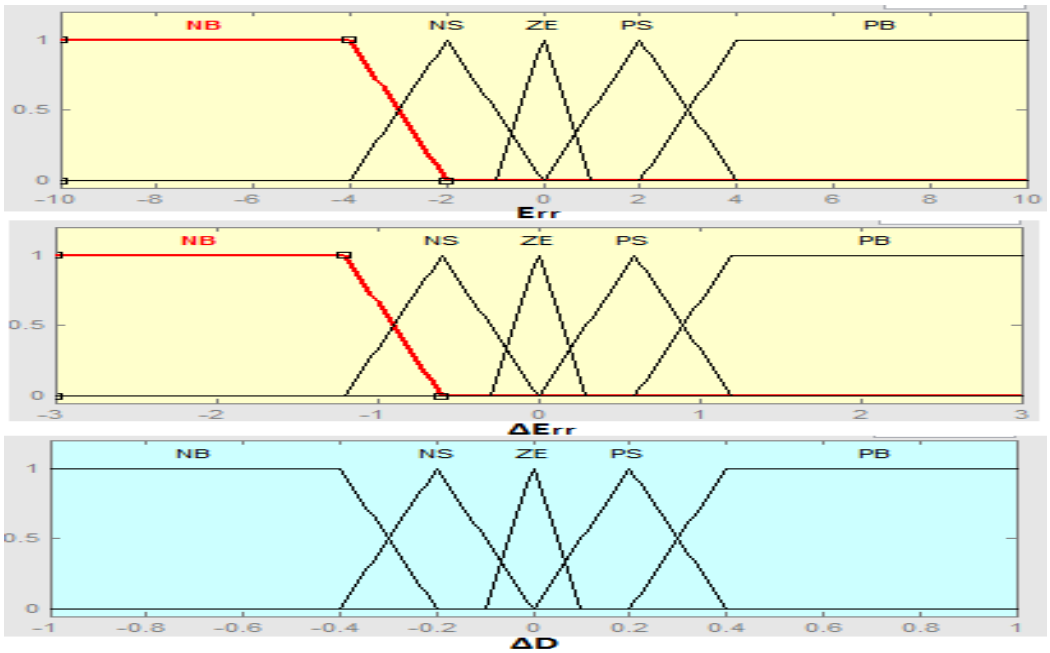

Figure III.14. the membership functions of inputs Err, ΔErr and output ΔD.

ΔE_{rr} / E_{rr}	PB	PS	ZE	NS	NB
PB	PB	PB	PB	PB	ZE
PS	PB	PB	PS	ZE	PS
ZE	PB	PS	ZE	NS	NB
NS	NS	ZE	NS	NB	NB
NB	ZE	NB	NB	NB	NB

Table. III.1. Fuzzy rules for input and output variables.

After the fuzzification step, begins the inference step where we establish the fuzzy rules that lead to the command based on the values of the error and its variation. Fuzzy rules link the output variable to the input variables in order to draw fuzzy conclusions or inferences. A fuzzy rule has a premise like "If the error is negative small AND the variation of the error is negative large" and a fuzzy deduction like "Then the variation of the duty cycle is positive large" [38]. In our case the two input variables are each defined by 5 fuzzy sets, we end up with 25 fuzzy rules. Table III.1 shows the different fuzzy rules of input and output variables used in the fuzzy controller.

The error Err (k) represents the slope of the curve P (V). The closer the operating point is to the MPP, the more Err (k) is canceled.

The variation in error ΔErr (k) is used to determine the magnitude of the duty cycle to increase or decrease [40]. To understand how the fuzzy logic MPPT algorithm works, the P (V) curve is divided into three regions (Figure III.15).

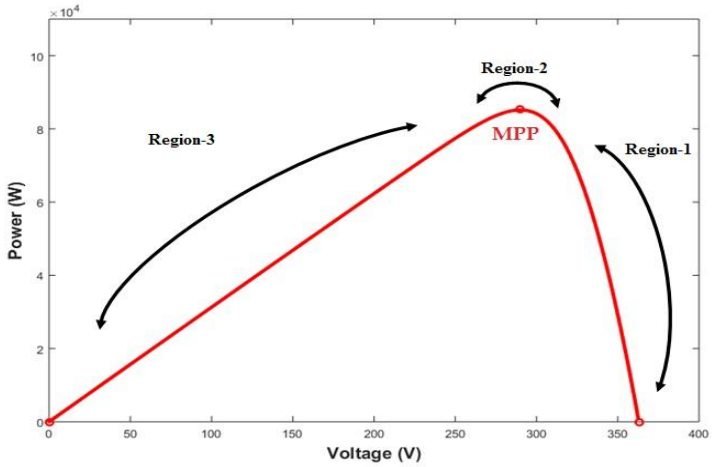

Figure III.15. curve of the PV module indicating different regions for the set of fuzzy rules.

Region-1

- The slope of the PV curve, i.e. Err (k) is negative in this region. This indicates that the operating point of the PV module is to the right of the MPP and the duty cycle should be decreased in order to follow the MPP.
- In order for the operating point to approach the MPP from the right side, Err (k) must be NS (small negative) and ΔErr (k) must be positive. So at this time, the output is set to ZE (zero) in order to prevent the system from wobbling.

Region-2

- In this region Err (k) is ZE (zero) which indicates that the operating point is close to the MPP. Therefore, the principle should be to maintain the same duty cycle under these conditions.
- If ΔErr (k) is NB (big negative), the operating point approaches the MPP from the left side. In order to prevent the operating point from moving to the right side of the MPP, the control rule must be PS (positive small) to suppress the magnitude change of the duty cycle in the opposite direction.

Region-3

- When Err (k) is positive, the operating point is located on the left side of the MPP. The duty cycle should therefore be increased. The ΔErr (k) is used to determine the magnitude of the increased duty cycle.
- When ΔErr (k) is negative at this point, the operating point approaches the MPP from the left side. At this point, the controller should adjust the output to ZE (zero) in order to avoid a large increase in duty cycle and system oscillations around the operating point.

After having established the inference rules giving the operation, it is necessary to indicate to the computer the procedure (mathematical algorithm) that it must follow in order to determine the shape of the membership function of the output variable, as a function of the value presents pre-established input variables and inference rules [41]. There are several inference methods among them, there is the "MAX-MIN" method.

In the "MAX-MIN" inference method, called "Mamdani implication", the operator "AND" is carried out by the formation of the minimum, the operator "OR" is obtained by the formation of the maximum, and the operator "THEN" it is carried out by the formation of the minimum. The "OR" operator that binds the different rules is achieved by the formation of the maximum. [37]

The output of FLC is the change in duty cycle. The defuzzification process converts the linguistic value of the output to an actual value. Many defuzzification techniques are proposed in the literature. The most commonly used method is the center of gravity (COG) or centroid method [39]. In this method, the defuzzifier determines the center of gravity (centroid) and uses this value as the output of FLC. The center of gravity is given by [40]:

$$\Delta \mathrm{d} = \frac{\sum_{\mathrm{i}=1}^{\mathrm{n}} \mathrm{Wi}.\Delta \mathrm{di}}{\sum_{\mathrm{i}=1}^{\mathrm{n}} \mathrm{Wi}} \quad \text{(III.7)}$$

Where, Δd is a net value, wi is the weighting factor and Δdi is a value corresponding to the membership function of Δd.

The output of FLC is the change in duty cycle (Δd), expressed as:

$$(k)=d(k-1)+s.\Delta d \quad \text{(III.8)}$$

III.8.1.3 The goal of employing fuzzy logic:

Fuzzy logic theory is one of the few theories that has set itself the goal of copying human performance.

The idea consists in examining how man makes for himself a model of everything that surrounds him and how he uses this model to endow himself with strategies with which he manages to master and control. enslave his environment.

III.8.1.4. Advantages and disadvantages of fuzzy logic:

The fast convergence time and the high tracking accuracy are the principal advantages of MPPT controllers based on AI techniques.

Fuzzy Logic has no need for an accurate mathematical model. Moreover, it can provide a high performance in controlling non–linear systems of arbitrary complexity by integrating the human experience into the control design process. [41]

Although the fuzzy MPPT command occupies a respectable place in relation to a lot of MPPT methods proposed in the literature, the design of a fuzzy MPPT command presents some difficulties related to the optimal choice of the parameters of the membership functions of the fuzzy controller associated with the MPPT command.

III.8.2 Genetic algorithms:

III.8.2.1 Definition:

Genetic algorithms are optimization algorithms based on techniques derived from genetics and natural evolution mechanisms: selections, crosses, mutations, etc. They belong to the class of evolutionary algorithms [42]. We can say that the genetic algorithm is a programming method which relies on the principle of evolution to carry out the search for an adequate solution to a problem.

III.8.2.2 working principle:

It is a global optimization method applicable to linear and non-linear systems, based on the mechanisms of natural selection and genetics.

Their operation is quite simple, we start from a population of individuals (chromosomes), representing initial solutions, randomly generated, by applying the operations of genetics on this population (the parents) we manage to generate a new population (descendants)) and the most suitable individuals (closer solutions) will be taken to form the next population, and so on until the optimal solution is obtained.

III.8.2.2.1 Steps of a genetic algorithm:

The steps of a simple GA are shown in Figure III.16, they are inspired by the theory of natural reproduction. The general idea is to apply the genetic transformations on a population of individuals to ultimately arrive at a more suitable (optimal) individual. [43]

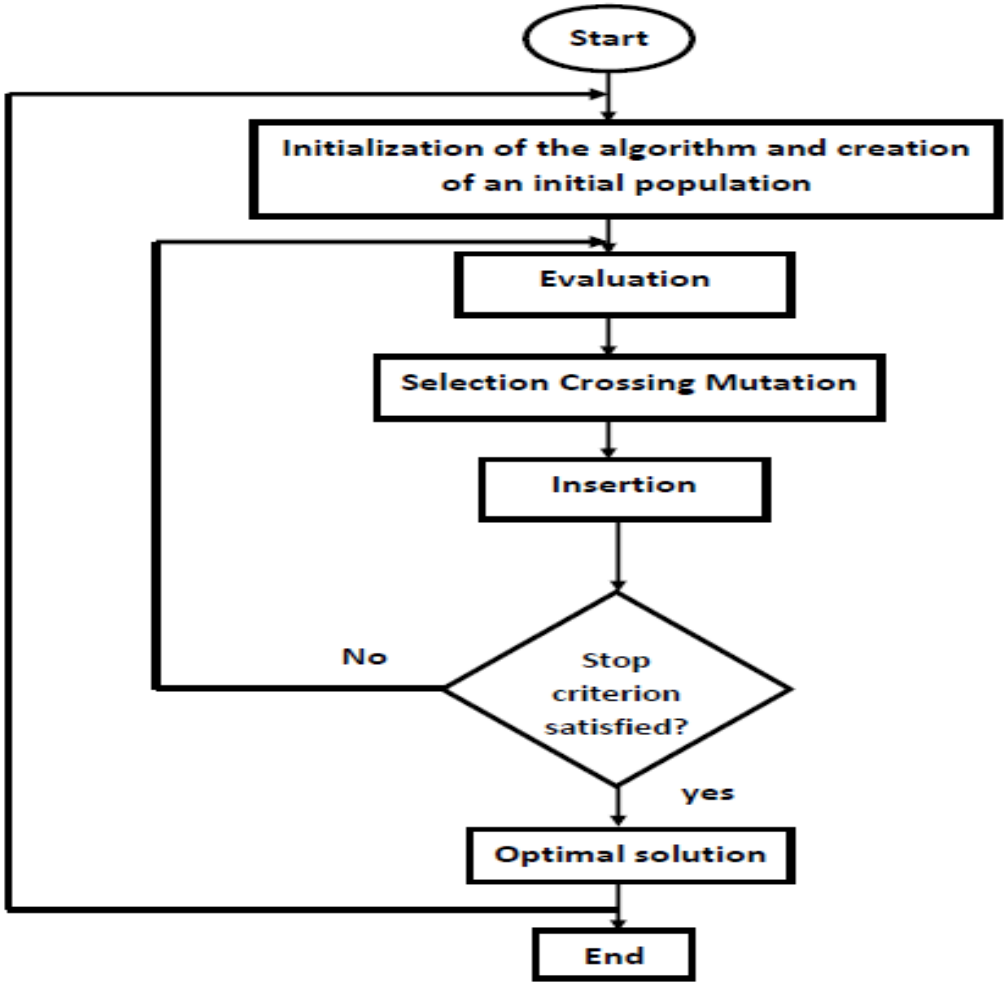

Figure III.16. Steps of a Simple Genetic Algorithm. [43]

The steps of a Genetic Algorithm are therefore as follows:

- **Initialization:** An initial population of N chromosomes is drawn randomly.
- **Evaluation:** Each chromosome is decoded and evaluated.
- **Selection:** Creation of a new population by using an appropriate selection method.
- **Reproduction:** Possibility of crossing and mutation within the new population.
- Insertion of the new population of descendants where the least adapted individuals will disappear.

a) Initialization:

- **Creation of the initial population:**

The procedure is quite simple. It consists of a random selection of "N" individuals in the allowed search space (the population). These individuals are generally coded, there are three main types of coding: binary, gray or real. You can easily switch from one coding to another.

In binary coding, which is the most used, a binary string representing the individual (thus constituted by 0s and 1s) is generated in a random manner with equiprobability, the number of bits SS is called the length of the individual . Obviously, the precision depends on the length of the chromosome. [44]

The population therefore forms a matrix (Figure III.17), in which the number of rows represents the number of individuals "N" and the number of columns is the number of bits "S" of each individual (precision).

An individual can contain two or more variables, in this case the length of this individual is therefore the sum of the precisions of each variable.

$$\text{Population} = \overbrace{\begin{bmatrix} \cdots \\ \vdots \quad \ddots \quad \vdots \\ \cdots \end{bmatrix}}^{\text{Number of bits S}} \Big\} \text{Number of individuals N}$$

Figure III.17. Representation of the population.

- **Decoding / Encoding**:

We present here the simplest coding which is the binary coding, we call Phenotype the real value of the individual (after decoding), and Genotype the binary representation of an individual, We use a binary vector "A" (chromosome), to represent the real values of the variable " $\boldsymbol{x}$ ". The number of bits is the length of the chromosome, noted: [44]

$$S = i\ (A) \tag{III.9}$$

Are:

$$d = [x_{max}, x_{min}] \tag{III.10}$$

$$i_d = x_{max} - x_{min} \tag{III.11}$$

With :

One must then divide this interval d in n_i equal sub-intervals in order to respect the precision, with:

$$n_i = i_d . 10^{prec} \quad \text{(III.12)}$$

*p*rec: represents the precision (digit after the decimal point) with which we are looking for x.

With S the natural number (number of bits) such that:

$$n_i < 2^s \quad \text{(III.13)}$$

Or simply :

$$s = \frac{ln(n_i)}{ln(2)} \quad \text{(III.14)}$$

The transformation of a binary string $A = a_0 a_1 \ldots . a_{s-1}$ into a real number x can then be carried out in two steps [50]:

1. Converting binary string A from base 2 to base 10:

$$x' = \sum_{i=0}^{s-1} a_i \, 2^i \quad \text{(III.15)}$$

2. Finding the corresponding real number x:

$$x = x_{min} + x' \frac{i_d}{2^s - 1} \quad \text{(III.16)}$$

Or simply:

$$x = x_{min} + \frac{i_d}{2^s - 1} \sum_{i=0}^{s-1} a_i \, 2^i \quad \text{(III.17)}$$

b) Evaluation:

Assessment is a very important operation, it ensures the survival of an optimal individual, this is done through a function called "Fitness". [44]

- **Fitness function:**

Also called quality function (or cost function); it gives, in positive numerical value (usually real), the quality of an individual. It is according to this numerical value that the chance of selection of this individual is calculated.

As AGs are an optimization technique, they seek the maximum quality, therefore the optimization of the quality function. [44]

- **"Objective" function:**

It gives the performance of an individual, this function can be negative, zero, or minimal when the individual is optimal.

The AGs seek the maximum quality of the function characterizing the system. The "objective" function therefore sometimes requires a transfer into a positive function that one seeks to maximize (fitness function). [44]

This transformation is ensured by a function g:

$$(x) = g(f(x)) \quad \text{(III.18)}$$

c) Selection:

This operation is perhaps the most important since it allows individuals in a population to survive (reproduce) or die. Generally, an individual's probability of survival will be directly related to their relative effectiveness in the population. [44]

There are several methods for reproduction. Perhaps the most well-known and used method is Goldberg's biased roulette wheel [43]. According to this method (Figure III.18), each chromosome will be duplicated in a new population in proportion to its adaptation value. In a way, as many draws with discounts are made as there are elements in the population.

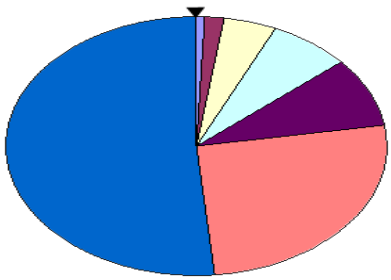

Figure III.18. Diagram of an example of a lottery wheel.

Thus, the fitness of a particular chromosome being $F\ (xi)$ (xi is the phenotype value of the chain), the probability with which it will be reintroduced into the new population of size N is:

$$P_s = \frac{\mathrm{F}(x_i)}{\sum_{\mathrm{j}=1}^{\mathrm{N}} \mathrm{F}(x_j)} \quad \text{(III.19)}$$

Individuals with great fitness are therefore more likely to be selected. This is called proportional selection.

The major disadvantage of this method is that an individual who is not the best can still dominate the selection. It can also cause a loss of diversity through the domination of a super

individual. Another drawback is its poor performance towards the end when all people are alike. H. David [45] sums up all these drawbacks very well.

There are other methods, the best known being that of the "tournament selection": we draw two individuals randomly from the population and we reproduce the best of the two in the new population. This procedure is repeated until the new population is complete. This method can work well, but it has the downside of killing good people. [44]

The selection phase does not create new individuals in the population. This is the role of the crossing and mutation operators.

d) Insertion:

The population resulting from the genetic operations will be inserted into the old population in such a way as to keep the individuals with the highest fitness function. [44]

e) Stop criterion:

The previous genetic operations will be carried out as many times as necessary and each time we obtain a new population with more and more adapted individuals.

The stop criterion can be chosen in several ways, either by the test of the cost function, or by the number of generations, or by the test for changes in the population.

If the number of generations is fixed, you get a fixed execution time, but the program may not stop at the desired precision. If you know the maximum value of the fitness function, the program will stop once it reaches this value, you will obtain the desired precision but this may require an uncontrolled calculation time. [44]

III.8.2.2.2 Application of GA to MPPT:

In the developed algorithm the individuals represent the current and tension of the PV generator (GPV) and the number of bits gives the precision. To code the current in binary, we must set its maximum value which is in our case the short-circuit current and Open circuit tension , we can therefore write:

$$power\ (p) = \begin{bmatrix} I_1 \\ . \\ . \\ . \\ I_N \end{bmatrix} . \begin{bmatrix} V_1 \\ . \\ . \\ . \\ \mathrm{V}_N \end{bmatrix} \qquad \text{with :} \quad \begin{cases} I_{max} = I_{sc} = \overbrace{111\ldots11}^{\text{S bits}} \\ V_{max} = V_{oc} = 111 \ldots 11 \end{cases} \qquad \text{(III.20)}$$

The GA goal is to solve the optimization problems of our photovoltaic system and find the optimal solution (current and voltage) whatever the climatic conditions of temperature and lighting as follows:

$$fitness = \begin{cases} \frac{P(V,I)}{P_{max}}; if\ P_{max} < P \\ 0\ ; \qquad\qquad if\ No \end{cases} \tag{III.21}$$

Power is the objective function or fitness of our problem which is a function of current and voltage. The maximization problem is subject to the following equality and inequality constraints:

$$V < Vmax \text{ and } P < Pmax$$

Figure III.19 The flowchart of the genetic algorithm for the optimization of the MPPT-AG photovoltaic system is shown.

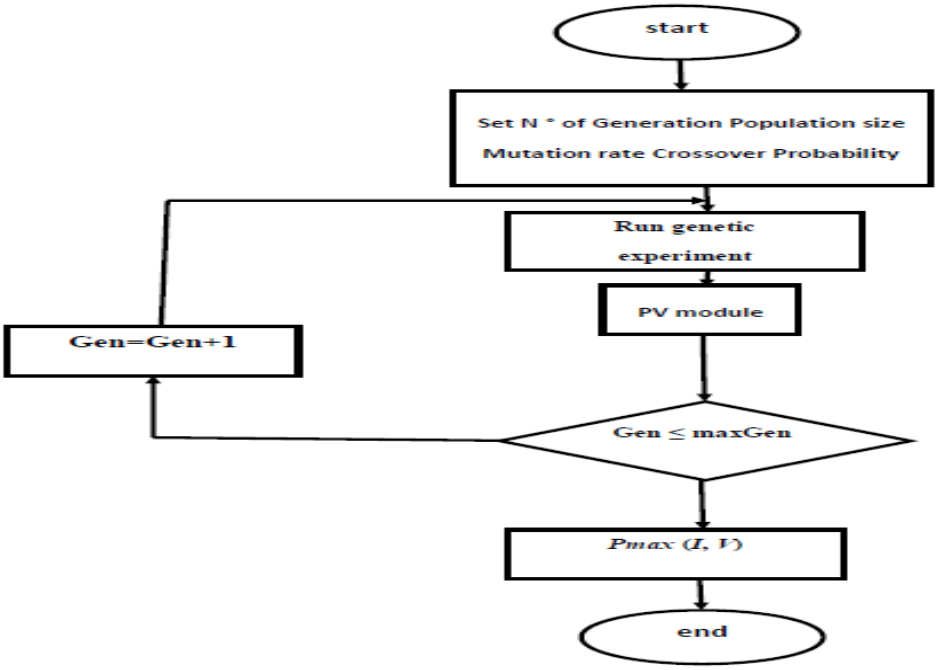

Figure III.19. Flowchart of the MPPT-AG genetic algorithm. [44]

III.8.2.3 The goal of employing genetic algorithm:

This type of optimization includes economic goals, used the genetic algorithm (GA) in order to achieve the optimal system configurations for the minimization of a “goal” “cost” function.

III.8.2.4 Advantages and disadvantages of genetic algorithm:

Among the advantages is in the genetic algorithm are instantaneously calculates the maximum power point PPM of a photovoltaic module in order to maximize the power profit with the constraints of the instantaneous change of the climatic conditions. We can say that these techniques based on the method metaheuristic (MPPT-AG) is the best technique used to track optimal PPM power when compared to other MPPTs.

In addition, it is possible to stop such an algorithm at any time, it always offers a solution, which is not necessarily the best, but which is not too bad either. Finally, genetic algorithms avoid a trap very often encountered in optimization algorithms: they do not stop in the extrema local, that is, they are constantly trying to find better solutions, even if they seem to have achieved them. As a result, genetic algorithms are very robust, but they suffer from not being predictable, and therefore their efficiency is not cannot be calculated in advance.

III.9. Control by sliding and Synergetic mode:

III.9.1 sliding mode control:

III.9.1.1 Definition:

Sliding Mode Control (SMC) is a not-linear type control that was introduced for the control of variable structure systems (such as static converters) and it is based on the concept of changing the structure of the controller. with the state of the system in order to obtain a desired response.

III.9.1.2 Principle of sliding mode control:

The sliding mode controller is based on the assumption of a zero hysteresis on the sliding surface S (x, t) = 0 and therefore on a variable and theoretically infinite switching frequency. It is clear that, from a practical point of view, it is not possible to verify this hypothesis. Due to the technological limitations of using high switching frequencies, it is preferable to limit this frequency.

The idea is to divide the state space by a decision border called: “sliding surface”. This surface delimits two subspaces corresponding to two possible states of the control device (Figure III.20). Stabilization on the sliding surface is obtained by switching each time the decision boundary is crossed.

This control principle is therefore essentially based on the use of a discontinuous control in order to maintain the evolution of the system on a carefully chosen sliding surface. The

synthesis must therefore aim to make the sliding surface attractive (condition of attractiveness) from any point of the state space. Once the surface has been reached, it is necessary to ensure the sliding along this surface (sliding condition) and the stability of the system (stability condition). In other words, it is necessary to find the condition for which the dynamics of the system slide on the surface towards the desired point of equilibrium (Figure III.20). On the surface, the dynamics of the system are independent of that of the initial process, which implies that this type of control falls within the realm of robust controls. These notions of stability are demonstrated by taking into account the principle of stability according to the criterion of LYAPUNOV (theorem 1).

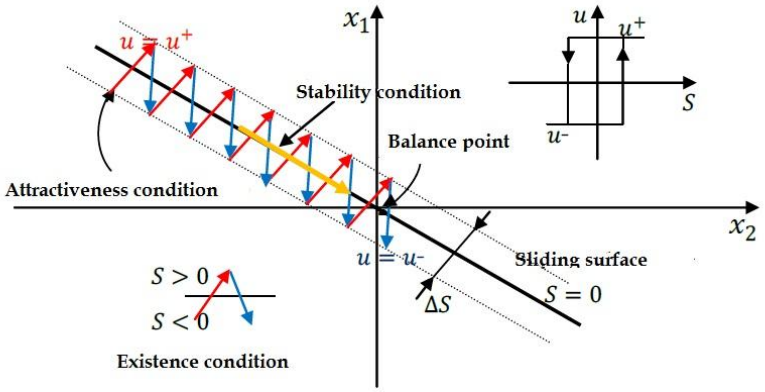

Figure III.20. Principle of sliding mode control.

For each switch, the control is performed by a hysteresis comparator. The direction of the hysteresis must be chosen so that the change of state brings the trajectory back to inside the fork. Thus, we may have to choose:

$$u = \begin{cases} 1 \ if \ s(x) > +\frac{1}{2}\Delta s \\ 0 \ if \ s(x) < -\frac{1}{2}\Delta s \end{cases} \quad \text{(III.22)}$$

Theorem 1:

Let V (x) be a function differentiable from R^n in R^n called the function of LYAPUNOV, which satisfies the following conditions [46]:

$$\begin{cases} V(0) = 0 \\ V(x) > 0 \ \ \forall x \neq 0 \\ \dot{V}(x) \leq 0 \ \forall x \neq 0 \end{cases} \quad \text{(III.23)}$$

If these three conditions are satisfied, x = 0 is a point of stable equilibrium. If the last condition becomes $\dot{V}(x) < 0$ for x ≠0, the point x= 0 is asymptotically stable.

In the case of the command by sliding mode, this function of LYAPUNOV is deduced using a pseudo-output which is the surface of sliding S (x, t) = 0.

III.9.1.2.1 Choice of sliding surface:

The surface S (x) represents the desired dynamic behavior of the system. SLOTINE proposes a form of general equation to determine the sliding surface which ensures the convergence of a variable towards its desired value [47]:

$$S(x) = \left(\frac{d}{dt} + \lambda_x\right)^{r-1} e(x) \quad \text{(III.24)}$$

III.9.1.2.2 Existence condition of the sliding:

The condition of existence of the sliding regime S (x, t) = 0 results in [48, 49]:

$$\lim_{s\to 0} S.\dot{S} < 0 \quad \text{(III.25)}$$

These conditions are deduced from Theorem (1) by applying the criterion of stability of LYAPUNOV in a neighborhood of the sliding surface and by taking $V(x) = \frac{S^2}{2}$ as a candidate function of LYAPUNOV. In this case, the derivative of the function of LYAPUNOV V is equal to S. $\dot{S}$.

The LYAPUNOV conditions stated in Theorem 1 are verified if S and $\dot{S}$ are of opposite signs. Note that these latter conditions become sufficient conditions to ensure the attractiveness of the surface if they are valid over the entire state space and not only in a region close to the sliding surface.

III.9.1.2.3 the command law:

The zig-zag curve between $U^-$and U^+ shown in Figure III.20 is the actual (practical) state path of the system. It surrounds the line S = 0 which is the ideal (theoretical) or reference state trajectory. It is possible to subdivide the displacement of the real trajectory into two components; a high frequency component and a low frequency component. The high frequency component is a discontinuous path that alternates between U^- and U^+, while the low frequency component forms a continuous path that moves along the sliding surface. Ignoring the often filtered fast switching component, the state path will then be determined by the slow switching component. This is called the equivalent command, which can be interpreted as the average value taken by the command quantity when switching rapidly

between U^- and U^+ as shown schematically in Figure III.21 The equivalent command makes the switching surface time invariant $\dot{S} = 0$. [50]

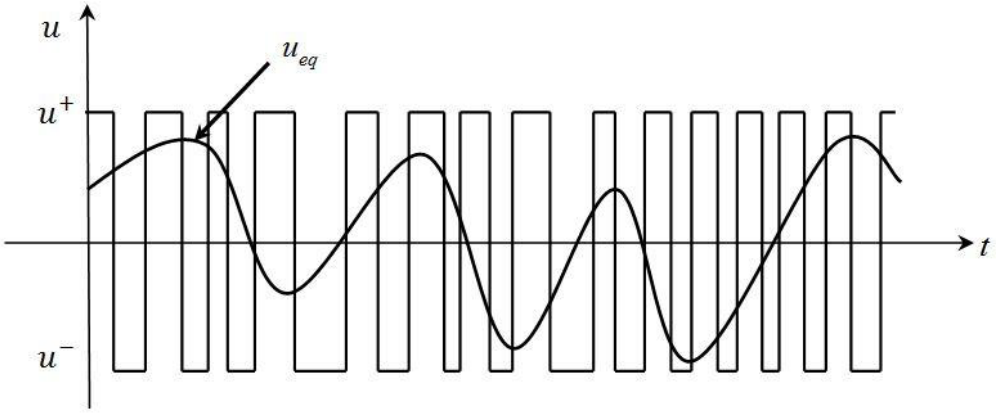

Figure III.21. Equivalent command as average switching value between U^- and U^+.

Let us consider as an example the system governed by the following differential equation:

$$\dot{X} = f'(x,t) + g(x,t)u \tag{III.26}$$

Let us assume that the slip regime exists on the switching surface S (x, t) = 0, its derivative is given by:

$$\dot{s} = \frac{ds(x,t)}{dt} = \frac{1}{dt}\left(\frac{\partial s}{\partial x}dx + \frac{\partial s}{\partial x}dt\right) = \frac{ds}{dx}\dot{X} + \frac{ds}{dt} \tag{III.27}$$

Let ∇S be the gradient of S, then:

$$\dot{S} = \nabla S.\dot{x} + \frac{\partial s}{\partial t} = \nabla S.f(x,t) + \nabla S.g(x,t).u + \frac{\partial s}{\partial t} \tag{III.28}$$

In slip mode and in permanent mode, the derivative of the surface is zero (because its antiderivative is equal to zero). This condition makes it possible to determine the equivalent command to maintain the state trajectory on this surface. It is therefore necessary to solve:

$$\nabla S.f(x,t) + \nabla S.g(x,t).u_{eq} + \frac{\partial s}{\partial t} = 0 \tag{III.29}$$

Thus, we get:

$$u_{eq} = [\nabla S.g(x,t)]^{-1}.\left[\nabla S.f(x,t) + \frac{\partial s}{\partial t}\right] \tag{III.30}$$

Or, we can express it this way:

$$u_{eq} = -\frac{\langle \nabla S(t), f(x.t)\rangle}{\langle \nabla S(t), g(x.t)\rangle} \tag{III.31}$$

Or $\langle .,. \rangle$ denotes the dot product.

It is then possible to express the dynamics of the system on the sliding surface by:

$$\dot{X} = f(x,t) - g(x,t).[\nabla S.g(x,t)]^{-1}.\left[\nabla S.f(x,t) + \frac{\partial s(x)}{\partial t}\right] \quad \text{(III.32)}$$

The command by sliding mode consists of two terms, a discontinuous command according to the sign of the sliding surface $\boldsymbol{u_n}$ and a command known as equivalent $\boldsymbol{u_{eq}}$characterizing the dynamics of the system on the sliding surface.

$$u = u_{eq} + u_n \quad \text{(III.33)}$$

$\boldsymbol{u_n}$ corresponds to the not linear component. It is determined to guarantee the attractiveness of the variable to be controlled towards the sliding surface and to satisfy the condition of convergence.

$$S(x).\dot{S(x)} < 0 \quad \text{(III.34)}$$

From (III.26), (III.27), and (III.33) we can write:

$$\dot{s}(x) = \frac{\partial s}{\partial t}\left(f(x,t) + g(x,t)u_{eq}\right) + \frac{\partial s}{\partial t}(g(x,t)u_n) + \frac{\partial s}{\partial t} \quad \text{(III.35)}$$

Using the slip mode condition, expression (III.35) becomes:

$$\dot{S}(x) = \frac{\partial s}{\partial t}(g(x,t)u_n) \quad \text{(III.36)}$$

The problem comes down to finding $\boldsymbol{u_n}$ such that:

$$S(x).\dot{S}(x) = S(x).\frac{\partial s}{\partial t}(g(x,t)u_n) \quad \text{(III.37)}$$

The simplest solution verifying this condition is given by the sign function "sign" illustrated in figure III.22:

$$u_n = K.sing(S(x)) \quad \text{(III.38)}$$

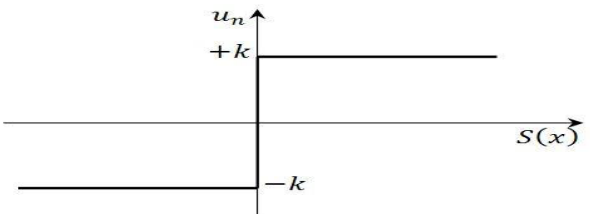

Figure III.22. Representation of the sign function.

By replacing expression (III.38) in (III.37), we obtain:

$$S(x).\dot{S}(x) = S(x)\frac{\partial s}{\partial t}g(x,t)Ksing\big(s(t)\big) < 0 \qquad \text{(III.39)}$$

Where the factor $\frac{\partial s}{\partial t}g(x,t)$ is always negative for the class of system we are considering. The gain k is chosen to be positive to satisfy condition (III.39). The choice of this gain is very influential because, if it is very small the response time will be very long and, if it is chosen very large, we will have strong oscillations at the level of the controller. These oscillations can excite neglected dynamics (chattering phenomenon), or even deteriorate the controller. [48]

III.9.1.3 The goal of employing sliding mode control:

The goal of sliding mode control can be summed up in two essential points:

- Synthesize a surface S (x, t) such that all the trajectories of the system obey a desired behavior of tracking, regulation and stability;
- Determine a control (commutation) law u (x, t) which is capable of attracting all state trajectories towards the sliding surface and maintaining them on this surface.

III.9.1.4 Advantages and disadvantages of sliding mode control:

The sliding mode control is characterized by the discontinuity of the control when passing through a switching surface called: sliding surface. The main advantage of the variable structure control with the sliding mode is the robustness against changing parameters or disturbances. In addition, the sliding mode control is relatively easy to implement compared to other types of non-linear controls. These properties make this control law suitable for many industrial applications, such as in the automotive or aeronautic fields. [42]

On the other hand, there are disadvantages of the command by sliding mode, which are:

- A phenomenon of chattering or chattering caused by the discontinuous part of this command
- The system is subjected at all times to a high frequency control in order to ensure its convergence to the desired state and this is not desirable.

III.9.2 Synergistic control:

III.9.2.1 Definition:

Synergistic control is a control technique quite similar to sliding mode control in the sense that the considered system is forced to evolve with a dynamic pre-chosen by the designer. It differs from it in the fact that the command is always continuous and uses a macrovariable which can be a function of two or more system state variables.

III.9.2.2 Principle of synergistic control:

Synergistic control theory was first introduced generally by Russian researchers in recent years [51]. Recently this theory has been successfully applied in the field of power electronics controls. Its application to a step-up converter has been presented in [52], and some practical aspects concerning simulation and hardware have been discussed in. [53,54]

This new approach does not require linearization of the model and explicitly employs a nonlinear model for the synthesis of the command.

III.9.2.2.1 Synergetic control procedure:

Consider the nonlinear dynamic system SISO of dimension n which can be described by the following nonlinear equation: [55]

$$\frac{dx(t)}{dt} = f(x, d, t) \tag{III.40}$$

Where x represents the system state vector and u represents the control vector. The synthesis of the synergistic controller begins with the definition of a macro-variable by the designer, to achieve the specifications and take charge of any control constraints, which is given as follows: [55]

$$\psi = \Psi(x,t) \tag{III.41}$$

Where ψ is the macro-variable and $\Psi(x,t)$ is a user-defined function, usually a function of state variables and time. The objective of the synergistic control is to force the system to evolve on the domain previously chosen by the designer: [55]

$$\psi = 0 \tag{III.42}$$

The characteristics of the macro-variable can be chosen by the designer, according to the parameters such as the objective of the command, the response time, limitations of the command, etc…. The macro-variable can be a simple linear combination of the variables state, and it is fo rced to evolve in a desired way expressed by a constraint chosen by the designer as shown as an example by the following equation: [55]

$$T\dot{\psi} + \psi = 0, \qquad T > 0 \tag{III.43}$$

Where T is a control parameter which indicates the rate of convergence of the closed loop system towards the indicated domain. [55]

Taking into account the chain of differentiation which is given by:

$$\frac{d\psi(\mathrm{x,t})}{dt} = \frac{d\psi}{dt}\frac{d\mathrm{x}}{dt} \tag{III.44}$$

The substitution of (III.40) and (III.41) in (III.43) allows to write:

$$T\frac{d\psi(\mathrm{x,t})}{dt} f(x,d,t) + \psi(\mathrm{x,t}) = 0 \tag{III.45}$$

By solving (III.45) for d, the control law can be found as:

$$d = g(x, \psi(\mathrm{x,t}), \mathrm{T}, \mathrm{t}) \tag{III.46}$$

From (III.46), it can be seen that the control depends not only on the state variables of the system, but also on the chosen macro-variable and time constant T. In other words, the designer can choose the characteristics of the controller by choosing an appropriate macro-variable and a specific time constant T. By synthesizing the controller, each domain presents a new constraint on the space domain state and reduce the order of the system by one degree, while moving in the direction of overall stability. In the synthesis of the synergistic controller shown above, it is clear that the synergistic controller acts on the nonlinear system and linearization or simplification of the model is not necessary as when applying traditional control theory. [55]

By the appropriate choice of macro-variables, the designer can obtain the following interesting characteristics for the final system [55]:

- Overall stability
- Insensitivity to parameters

- Noise suppression.

It is interesting to note that the law of synergistic control guarantees the overall stability on the chosen domain. This means that once the hypersurface is reached the system is not supposed to leave it, even with rather large variations in the parameters. This property of disturbance invariance is shared by the sliding mode control technique when sliding the trajectories on the sliding surface. An example application is given in the following section to illustrate the simulation of the implementation of synergistic control.

III.9.2.2.2 MPPT system modeling:

Consider a boost type converter connected to a PV module with a resistive load as illustrated in Figure III.23. [56]

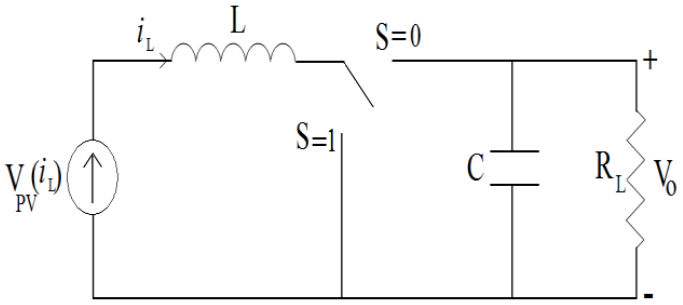

Figure III.23. MPPT system schematics.

According to the position of switch S, the system can be written in two sets of state equations. If the switch is in position S = 0, the differential equations can be written as: [56]

$$\frac{di_{L1}}{dt} = \frac{V_{pv}(i_L)}{L} - \frac{V_o}{L} \quad \text{(III.47.a)}$$

$$\frac{dV_{o1}}{dt} = \frac{i_L}{C} - \frac{V_o}{CR_L} \quad \text{(III.47.b)}$$

If the switch is in position S = 1, the differential equations can be expressed as:

$$\frac{di_{L2}}{dt} = \frac{V_{pv}(i_L)}{L} \quad \text{(III.48.a)}$$

$$\frac{dV_{o2}}{dt} = -\frac{V_o}{CR_L} \quad \text{(III.48.b)}$$

By using the state space averaging method [56], Eqs.(III.47) and (III.48) can be combined into one set of state equation to represent the dynamic of the system. Based on the idea of

Pulse-Width Modulation (PWM), the ratio of the switch in position 1 in a period is defined as duty ratio. Two distinct equation sets are weighted by the duty ratio and superimposed: [56]

$$\frac{dx}{dt} = (1-d)\frac{dx_1}{dt} + d.\frac{dx_1}{dt} \quad \text{(III.49)}$$

where $X_1 = [i_{L1}\ V_{01}]^T$, $X_2 = [i_{L2}\ V_{02}]^T$, and d∈[0 1] is the duty ratio. Hence the dynamic equation of the system can be described by: [56]

$$\frac{di_L}{dt} = -(1-d)\frac{V_o}{L} + \frac{V_{pv}}{L} \quad \text{(III.50.a)}$$

$$\frac{dV_o}{dt} = (1-d)\frac{i_L}{C} + \frac{V_o}{CR_L} \quad \text{(III.50.b)}$$

where *C* is the capacity, L is the inductance, R_L is the resistive load, d∈[0 1] is the duty ratio, which is also the control input. V_o is the output voltage and i_L is the inductor current. Note that the equivalent series resistance (ESR) of the inductor and wiring resistance are neglected in this case, so i_L is assumed to be equal to the PV current (I_{PV}). Eq. III.50 can be written in general form of the nonlinear time invariant system. [56]

$$\frac{dX}{dt} = f(x) + g(x).d \quad \text{(III.51)}$$

III.9.2.2.3 Design of synergetic MPPT controller:

In this study, we introduce the concept of the synergetic control for the MPPT system.

By selecting the manifold as $\frac{\partial P_{pv}}{\partial I_{pv}} = 0$, it is guaranteed that the system state will hit the manifold and produce maximum power output persistently. [57]

$$\frac{\partial P_{pv}}{\partial I_{pv}} = \frac{\partial I^2_{pv}.R_{pv}}{\partial I_{pv}} = I_{pv}\left(2R_{pv} + I_{pv}\frac{\partial R_{pv}}{\partial I_{pv}}\right) = 0 \quad \text{(III.52)}$$

Where $R=V_{PV}/I_{PV}$ is the equivalent load connect to the PV, and I_{PV} the PV current which is equal to i_L in this case. [57]

The solution of (III.52) is:

$$2R_{pv} + I_{pv}\frac{\partial R_{pv}}{\partial I_{pv}} = 0$$

Hence, the manifold is defined as:

$$\psi = 2R_{pv} + i_L\frac{\partial R_{pv}}{\partial i_L} \quad \text{(III.53)}$$

Then the desired dynamic evolution of the macro-variable can be expressed as:

$$T\dot{\psi} + \psi = 0, \qquad T > 0 \quad \text{(III.54)}$$

Where

$$\frac{d\psi(x,t)}{dt} = \frac{d\psi}{dt}\frac{dx}{dt} \tag{III.55}$$

The substitution of Ψ' from Eq. (III.55) into the functional equation (III.54) yields:

$$T_s\left\{\left(\frac{d\psi}{dx_1}\right)(f(x) + g(x).d(x))\right\} + \psi = 0$$

$$\left(\frac{d\psi}{dX}\right)\left(\frac{V_{pv}-V_o}{L} + \frac{V_o}{L}d(t)\right) = -\frac{\psi}{T_s} \tag{III.56}$$

$$d(t) = 1 - \left(\frac{\psi L}{V_o T_s \frac{d\psi}{dX}}\right) - \frac{V_{pv}}{V_o} \tag{III.57}$$

The time derivative of Ψ can be written as:

$$\frac{d\psi}{dX} = 3\frac{\partial R_{pv}}{\partial i_L} + i_L\frac{\partial^2 R_{pv}}{\partial {i_L}^2} \tag{III.58}$$

Replacing R_{pv} by the definition of $R_{pv} = V_{pv}/I_{pv}$

$$\frac{\partial R_{pv}}{\partial i_L} = \frac{\partial\left[\frac{V_{pv}}{i_L}\right]}{\partial i_L} = \frac{1}{i_L}\left(\frac{\partial V_{pv}}{\partial i_L}\right) - \frac{V_{pv}}{{i_L}^2} \tag{III.59}$$

$$\frac{\partial^2 R_{pv}}{\partial {i_L}^2} = \frac{1}{i_L}\left(\frac{\partial^2 V_{pv}}{\partial {i_L}^2}\right) - \left(\frac{2}{{i_L}^2}\right)\left(\frac{\partial V_{pv}}{\partial i_L}\right) + 2\frac{V_{pv}}{{i_L}^3} \tag{III.60}$$

By (4), the PV voltage (V_{pv}) can be rewritten as function of PV current (I_{pv})

$$V_{pv} = \left(\frac{K_b.TA}{q}\right) ln\left(\frac{I_{ph}+I_o-I_{pv}}{I_o}\right) \tag{III.61}$$

Substituting Eq. (III.58) into Eq. (III.57), the synergetic control signal is defined as :

$$d(t) = 1\frac{\psi L}{V_o T_s\left(3\frac{\partial R_{pv}}{\partial i_L} + i_L\frac{\partial^2 R_{pv}}{\partial {i_L}^2}\right)} - \frac{V_{pv}}{V_o} \tag{III.62}$$

Asymptotic stability is obtained using the Lyapunov function candidate:

$$V_L = \frac{1}{2}\psi^2 \tag{III.63}$$

The derivate of V_L is:

$$\frac{dV_L}{dt} = \psi\left(\frac{d\psi}{dt}\right) = \psi\left[\left(-\frac{1}{T_s}\right)\psi\right] \quad \text{(III.64)}$$

Consequently we have :

$$\frac{dV_L}{dt} = \left(-\frac{1}{T_s}\right)\psi^2 \leq 0 \quad \text{(III.65)}$$

III.9.2.3. The goal of employing synergetic control:

the law of synergistic control aims to ensure overall stability in the chosen domain. This means that once the hypersurface is reached the system is not supposed to leave it, even if the parameters vary widely.

III.9.2.4 Advantages and disadvantages of synergetic control:

The Synergistic control is characterized by :

- Speed of response without significant overshoot.
- The reduction of the amplitude of the oscillations.
- Reduction of static error.
- higher precision,
- better stability,
- more simplicity and robustness.

On the other hand, there are disadvantages of the command by Synergistic control, which are:

- The system is subjected at all times to a high frequency control in order to ensure its convergence to the desired state and this is not desirable.

III.10. Conclusion:

In this chapter, we have presented different methods for operating point tracking at maximum power. We started with the classical methods (PO, IC and HC); We provided an in-depth study and present the flowcharts. we also presented the theory of fuzzy sets, its basis and its mathematical aspect exploited in automatic regulation. The GA algorithm was also presented.

As for the control by sliding and synergic mode He concluded that they both have the same objective of forcing the system to operate on the variety (S, ψ) = 0.

The sliding mode control is robust and is not based heavily on the system model unlike the synergistic control but it has the inconvenience of chattering which presents a big problem with the digital implementation [37]. The synergetic control allowed us to avoid this problem

in addition, it is less sensitive to high frequency noise and imposes a well-controlled dynamic behavior out of the manifold according to the equation (III.43). but unfortunately we see a decrease in robustness because of its sensitivity to the differences between the parameters of the model and of the physical system.

Référence :

[1] A. F. Boehinger, "Self-adaptive DC converter for solar spacecraft power supply", IEEE Transactions on Aerospace and Electronic Systems, 1968, pp. 102-111.

[2] W. Xiao, N. Ozog, and W. G. Dunford, "Topology Study of Photovoltaic Interface for Maximum Power Point Tracking", IEEE Trans. On Industrial Electronics, vol. 54, n°. 3, 2007, pp. 1696-1704

[3] C. Cabal, " Optimisation énergétique de l'étage d'adaptation électronique dédié à la conversion photovoltaïque.", Thèse Doctorat de l'Université Toulouse 3 Paul Sabatier, France, 2008.

[4] M. Boukli-Hacene Omar « conception et réalisation d'une génération photovoltaïque muni d'un convertisseur mppt pour une meilleure gestion energétique » magister en automatique productique informatique 2010/2011.

[5] d.Lee, H.Noh, D.Hyun, And I.Choy,"an improved mppt converter using current compensation method for small scaled pv-applications," IEEE applied power electronics conf. Andexposition, vol. 1, pp. 540-545, 2003

[6] R.Faranda, S.Leva, "MPPT techniques for PV systems: Energetic and cost comparison", IEEE Power and Energy Society General Meeting—Conversion and Delivery of Electrical Energy in the 21st Century, Pittsburgh, PA, 2008, pp. 1–6.

[7] Bisker Asma, Chiri Meriem, « commande d'un système photovoltaïque en mode isolé et en mode connecté au réseau », diplôme d'ingénieur d'état en électrotechnique, école nationale polytechnique, 10, av. Hassen badi, el-harrach, algérie, 2012

[8] C.Andr´Es, G.Spagnuolo, G. Petrone, M.Vitelli And J.David bastidas "a multivariable mppt algorithm for granular control of photovoltaic systems" IEEE 2010

[9] T.Kitano, M. Matsui, D. Xu "Power sensor-less MPPT control scheme utilizing power balance at DC link-system design to ensure stability and response", 27th Annual Conference of the IEEE Industrial Electronics Society IECON '01, vol. 2, 29 Nov.-2 Dec. 2001, pp.1309–1314.

[10] Subudhi, B., & Pradhan, R. (2013). A comparative study on maximum power point tracking techniques for photovoltaic power systems. Sustainable Energy, IEEE transactions on, 4(1), 89-98.

[11] L. Djellal, Y .Dib, «Etude comparative de deux commandes MPPT appliquée à un système photovoltaïque», Mémoire master, Université Abou-bekr Belkaid de Tlemcen, 2017.

[12] Norazlan Hashim , Zainal Salam , Dalina Johari , Nik Fasdi Nik Ismail " DC-DC Boost Converter Design for Fast and Accurate MPPT Algorithms in Stand-Alone Photovoltaic

System " Int J Pow Elec & Dri Syst, Vol. 9, No. 3, September 2018 : 1038 – 1050

[13] Eltawil, M. A., & Zhao, Z. (2013). MPPT techniques for photovoltaic applications. Renewable and Sustainable Energy Reviews, 25, 793-813.

[14] Bhatnagar, P., & Nema, R. K. (2013). Maximum power point tracking control techniques: State-of-the-art in photovoltaic applications. Renewable and Sustainable Energy Reviews, 23, 224-241.

[15] Ishaque, K., & Salam, Z. (2013). A review of maximum power point tracking techniques of PV system for uniform insolation and partial shading condition. Renewable and Sustainable Energy Reviews, 19, 475-488.

[16] Eltawil, M. A., & Zhao, Z. (2013). MPPT techniques for photovoltaic applications. Renewable and Sustainable Energy Reviews, 25, 793-813.

[17] H. Rezk and A. M. Eltamaly, "A comprehensive comparison of different MPPT techniques for photovoltaic systems," Solar energy, vol. 112, pp. 1-11, 2015.

[18] F. Liu, Y. Kang, Y. Zhang, and S. Duan, "Comparison of P&O and hill climbing MPPT methods for grid-connected PV converter," in Industrial Electronics and Applications, 2008. ICIEA 2008. 3rd IEEE Conference on, 2008, pp. 804-807: IEEE.

[19] K. Ishaque and Z. Salam, "A review of maximum power point tracking techniques of PV system for uniform insolation and partial shading condition," Renewable and Sustainable Energy Reviews, vol. 19, pp. 475-488, 2013.

[20] Liu, F., Kang, Y., Zhang, Y., & Duan, S. (2008, June). Comparison of P&O and hill climbing MPPT methods for grid-connected PV converter. In Industrial Electronics and Applications, 2008. ICIEA 2008. 3rd IEEE Conference on (pp. 804-807). IEEE.

[21] Kjaer, S. B. (2012). Evaluation of the hill climbing and the incremental conduc- tance maximum power point trackers for photovoltaic power systems. Energy Con- version, IEEE Transactions on, 27(4), 922-929.

[22] Hajar Bagheri "advances in electric power engineering" publisher: lulu (usa), 2015.

[23] Dalia Al Maamoury, Muhamad Bin Mansor, Ali Assim Al Obaidi ''active power control for a single-phase grid connected pv system " , international journal of scientific & technology research vol 2, issue 3, 2013.

[24] B. Das, A. Jamatia, A. Chakraborti, P. R. Kasari, et M. Bhowmik, « New Perturb and Observe MPPT algorithm and its validation using data From PV module », Int. J. Adv. Eng. Technol., vol. 4, n° 1, p. 579‑591, 2012.

[25] T. C. C. Saibabu et J. S. Kumari, « Modeling and Simulation of PV Array and its Performance Enhancement Using MPPT (P&O) Technique », Int. J. Comput. Sci.

Commun. Netw., vol. 1, n° 1, p. 9‑16, oct. 2011.

[26] H.Slimane " Optimisation de la conversion énergétique pour les systèmes à énergie Photovoltaïque " Thèse Doctorat en Sciences Université Ferhat Abbas Sétif 1 Faculté de Technologie 10 octobre 2018

[27] A.Neda, M.Mohammad , M.Amran ,M.Radzi , N.Azis, S.Shafie and M.Ammirrul, M.Zainuri .Article "An Enhanced Adaptive Perturb and Observe Technique for Efficient Maximum Power Point Tracking Under Partial Shading Conditions" Published: 5 June 2020.Appl. Sci. 2020, 10, 3912; doi:10.3390/app10113912.

[28] J.H.Lee, H.B.Bo, H.Cho, "Advanced incremental conductance MPPT algorithm with a variable step size", Power Electronics and Motion Control Conference, 2006, EPE-PEMC 2006. 12th International, pp. 603-607, Aug. 2006.

[29] T.Y.Kim, H.G.Ahn, S.K. Park, Y.K.Le, "A novel maximum power point tracking control for photovoltaic power system under rapidly changing solar radiation", IEEE International Symposium on, Vol. 2, pp. 1011-1014, Jun. 2001.

[30] Dr. B.LALOUNI Sofia " Cours Energie Solaire Photovoltaïque " Université A.MIRA de BEJAIA Faculté de Technologie 2014/2015 .

[31] A.Mohamed" Contribution à l'optimisation d'une chaine de conversion d'énergie photovoltaïque " Thèse Doctorat en Sciences en electrotechnique universite constantine 1 Faculté de Technologie de la technologie .02 / 03 / 2014 .

[32] Eltamaly, A. M., Abdelaziz, A. Y. (2020). Modern Maximum Power Point Tracking Techniques for Photovoltaic Energy Systems. Suisse : Springer. https://doi.org/10.1007/978-3-030-05578-3

[33] Bendiba, B., Krimb, F., Belmilia, H., Almia, M. F., Bouloumaa, S., (2014). Advanced fuzzy MPPT controller for a stand-alone PV system. Elsevier Energy Proc. Vol. 50, pp. 383–392.

[34] Abubakkar Siddik, A., Shangeetha, M. (2012). Implementation of Fuzzy logic controller in photovoltaic power generation using boost converter and boost inverter. Int. J. Power Electron. Drive Syst. Vol. 2, pp. 249–256.

[35] Praful, R. M., Joshua, A. M. (2017). Design, Implementation and Performance Analysis of a LabVIEW based Fuzzy Logic MPPT Controller for Stand-Alone PV Systems. IEEE International Conference on Power, Control, Signals and Instrumentation Engineering.

[36] B.YASSINE " Commande MPPT à base de la logique floue appliquée à un Système Photovoltaïque " MEMOIRE de master .Commandes Electriques .Université Aboubakr Belkaïd – Tlemcen – Faculté de TECHNOLOGIE .29 / 09 / 2020

[37] Mechernene, A. (2018). Concepts de la logique floue. [Cours, université abou bekr belkaid, Tlemcen]

[38] Martaj, N. Mokhtari, M. (2010). Contrôle par logique floue. MATLAB R2009, SIMULINK et STATEFLOW pour Ingénieurs, Chercheurs et Etudiants. Springer-Verlag Berlin Heidelberg. DOI 10.1007/978-3-642-11764-0_16

[39] Alajmi, B. N., Ahmed, K. H., Finney, S. J. (2011). Fuzzy-logic control approach of a modified hill climbing method for maximum power point in microgrid standalone photoviltaic system. IEEE Trans. Power Electron. Vol. 26, pp. 1022–1030.

[40] Panigrahi, A., Bhuyan, K. C. (2017). Fuzzy Logic Based Maximum Power Point Tracking Algorithm for Photovoltaic Power Generation System. Journal of Green Engineering. Vol. 6, N. 4, pp. 403–426. doi: 10.13052/jge1904-4720.644

[41] Shaiek Y, SmidaMB, Sakly A,Mimouni MF (2013) Comparison between conventional methods and GA approach for maximum power point tracking of shaded solar PV generators. Sol Energy 90:107–122. https://doi.org/10.1016/j.solener.2013.01.005

[42] D.E. Goldeberg, "Genetic Algorithms in search, Optimization and Machine learing", Addison-Wesley, 1989.

[43] D. E. Goldberg, Genetic Algorithms in Search, Optimization and Machine Learning, 1st éd. Boston, MA, USA: Addison-Wesley Longman Publishing Co., Inc., 1989.

[44] H.Slimane " Optimisation de la conversion énergétique pour les systèmes à énergie Photovoltaïque" Thèse Doctorat en Sciences Université Ferhat Abbas Sétif 1 Faculté de Technologie departement d'electronique 10 octobre 2018.

[45] H. Dawid, Adaptive Learning by Genetic Algorithms: Analytical Results and Applications to Economic Models, 2e éd. Berlin Heidelberg: Springer-Verlag, 1999.

[46] A. HIJAZI, "Modélisation électrothermique, commande et dimensionnement d'un système de stockage d'énergie par supercondensateurs avec prise en compte de son vieillissement : application à la récupération de l'énergie de freinage d'un trolleybus", Thèse de Doctorat de l'université de Lyon (France), 13 décembre 2010.

[47] J.J.SLOTINE, « Sliding controller design for non linear systems », *IJC*, vol. 2, 1984, pp 421- 434.

[48] V.I. Utkin "*Sliding modes in control and optimization*", vol. 2, Springer Verlag Berlin, 1992.

[49] H. Komurcugil, "Adaptive terminal sliding-mode control strategy for DC–DC buck converters", *ISA Transactions* vol.51, 2012, pp.673-681.

[50] R. Husson, «*Méthodes de commande des machines électriques*», Lavoisier, Paris, France, 2003

[51] Wang, Q., J. Feng, and T. Li, ―Analysis of the synergetic control based on variable structure and application of power electronics, ‖ International Conference on Information Engineering and Computer Science, Wuhan, China, pp. 9–12, 2009.

[52] E. Santi, A. Monti, D. Li; K. Proddutur, R. A. Dougal, "Synergetic control for DC-DC boost converter: implementation options", IEEE Transactions on Industry Applications, vol. 39, no. 6, pp. 1803-1813, Nov. 2003.

[53] E. Santi, R. Dougal, D. Li, A. Monti, K. Prodduttur, ―Synergetic control for power electronics applications: a comparison with the sliding mode approach, ‖ WSP Journal of Circuits, Systems and Computers, Vol. 13, No. 4, pp. 737-760, August 2004.

[54] I. Kondratiev, E. Santi, R. Dougal, G. Veselov, Synergetic control for m-parallel connected DC–DC buck converters, PESC, in: 30th Annual IEEE, vol. 1, pp. 182–188 , 2004.

[55] D. Li, K. Proddutur, E. Santi, and A. Monti, ―Synergetic control of a boost converter: Theory and experimental verification,‖ in Proc. IEEE Southeast Conf., Apr. 2002, pp. 197–200.

[56] D. Li, K. Proddutur, E. Santi, A. Monti, in Proc. IEEE Southeast Conf., p. 197, Apr. 2002

[57] H. ATTOUI, F. KHABER, M. MELHAOUI, K. KASSMI, N. ESSOUNBOULI "Development and experimentation of a new MPPT synergetic control for photovoltaic systems"QUERE Laboratory, Faculty of technology, University of Setif 1, 19000 Setif, Algeria. LETAS Laboratory, Faculty of Science, University Mohamed the First, Oujda 60000, Morocco.CReSTIC Laboratory, University of Reims Champagne Ardennes. IUT de Troyes, 9 rue de Quebec B.P. 396, 10026 Troyes, France

Chapter IV

MPPT Methods Implementation

IV.1. Introduction:

Simulation is a tool for evaluating the theoretical performance of a system. Indeed this part will allow us to perform simulations of a photovoltaic generator followed by a DC / DC converter and to test the MPPT methods. This allows us to easily modify the system parameters such as the metrological conditions, and to visualize the contribution of the order on the photovoltaic generator.

MATLAB software and its associated graphics extension SIMULINK are part of a set of integrated signal processing tools that provide the ability to simulate systems in their continuous and discrete states, so it is well suited for testing digital MPPT methods.

As a continuation of this project, some of the most used MPPT methods are implemented.

This chapter is devoted to the simulation and the comparative study between the control methods in order to obtain better results.

IV.2. Simulation of the photovoltaic system:

The system is made up of three distinct elements, the PV panel, the step-up chopper converter (power part) with its control (control part) which represent the MPPT regulator. For each part, a model was chosen for the simulation. This allows us to better understand the influence of system parameters and to draw interesting conclusions.

Figure IV.1. MPPT system using 1Soltech 1STH-215-P PV Panel

IV.2.1 Simulation of the photovoltaic panel(1Soltech 1STH-215-P):

a) Description:

The PV Array block implements an array of photovoltaic (PV) modules. The array is built of strings of modules connected in parallel, each string consisting of modules connected in series. This block allows you to model preset PV modules from the National Renewable Energy Laboratory (NREL) System Advisor Model (2018) as well as PV modules that you define.

The PV Array block is a five-parameter model using a light-generated current source (IL), diode, series resistance (Rs), and shunt resistance (Rsh) to represent the irradiance- and temperature-dependent I-V characteristics of the modules.

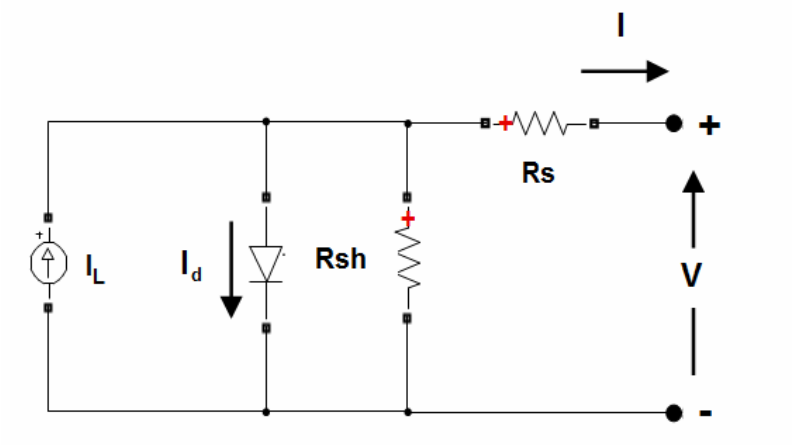

Figure IV.2.Equivalent circuit of the 5 parameter model

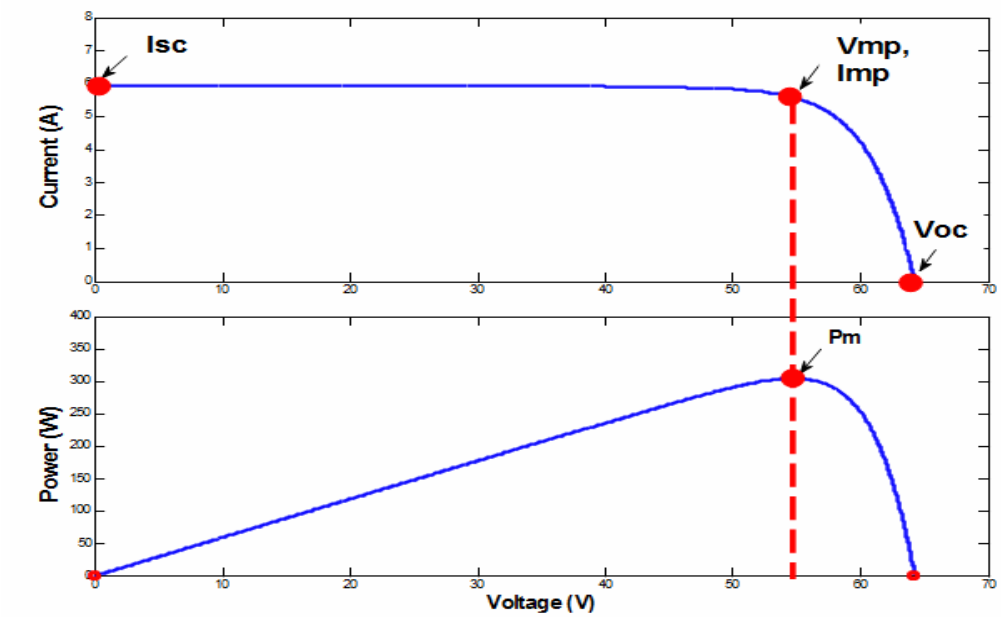

Figure IV.3.Characteristic I (V) and P(w) of a photovoltaic cell.

The diode I-V characteristics for a single module are defined by the equations

$$Id = Io\left[\exp\left(\frac{Vd}{VT}\right) - 1\right] \quad \text{(IV.1)}$$

$$\mathrm{VT} = \frac{\mathrm{K.Y}}{\mathrm{q}}.\,\mathrm{nl}.\,\mathrm{ncell} \quad \text{(IV.2)}$$

PV model	1STH-215-P
Short circuit current (Isc)	7.84 A
Open circuit voltage (Voc)	36.3 V
Maximum Voltage (Vmpp)	29 V

Maximum current (Impp)	7.35 A
Maximum power (Pmpp)	213.15 W
Number of cells in series (Ns)	60
Temperature coefficient of Isc	-0.36099%/°C
Temperature coefficient Voc	0.102%/°C
Diode ideality factor (A)	0.98117
Series resistance (Rs)	0.39383Ω
Shunt resistance (Rsh)	313.3991Ω

Table IV.1. Soltech 1STH-215-P PV Panel specifications

IV.2.2 Test a DC / DC converter:

Boost converter is utilized as source and load impedance matching. In this paper it is designed to step up the DC voltage when the duty cycle is approaching one. The duty cycle is used to control the power flow by varying the ON/OFF duty cycle of the switching. The output voltage of the PV system is the input of the DC/DC converter (Voltage source) that generates a constant voltage output value . This incomparable is obtained by accumulating energy in an inductor and discharge it to the load at higher voltage. In this design the ripple current is selected to be 20% of the output current and the voltage ripple to be 1.5% respectively. The average output and input voltages are determined by the equation (6).

$$\frac{V_{out}}{V_{in}} = \frac{1}{(1-D)} \tag{6}$$

Where Vin and Vout are the respective input and output voltages of the boost converter and D is the duty cycle of switching. The suitable values of the inductors and capacitors were calculated to suit the design using the equation (7) and (8) [20].

$$C = \frac{D}{R\left(\frac{\Delta Vo}{Vo}\right)f} \tag{7}$$

$$L = \frac{D(1-D)^2 R}{2f} \tag{8}$$

Figure IV.1 gives the block diagram of a BOOST tested under MATLAB / SIMULINK, connected to a resistive load with an input voltage:

Ve = 28V.

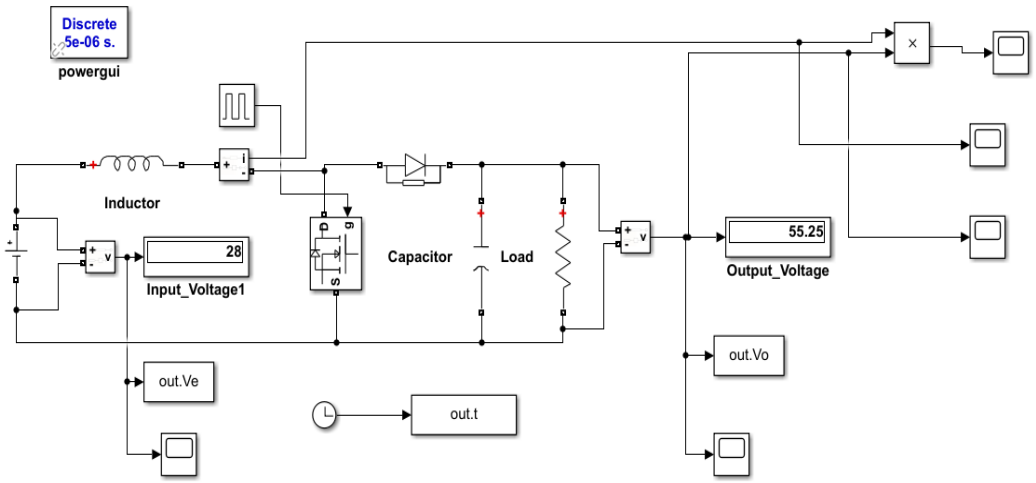

Figure IV.4. Diagram of a BOOST under MATLAB / SIMULINK.

C1	C2	L	R
100.10^{-6}(F)	100.10^{-6}(F)	4.10^{-3}(H)	20(ohm)

Table IV.2. Boost DC/DC converter specification

The simulation results for a frequency f = 10 kHz, are illustrated in the figure above.

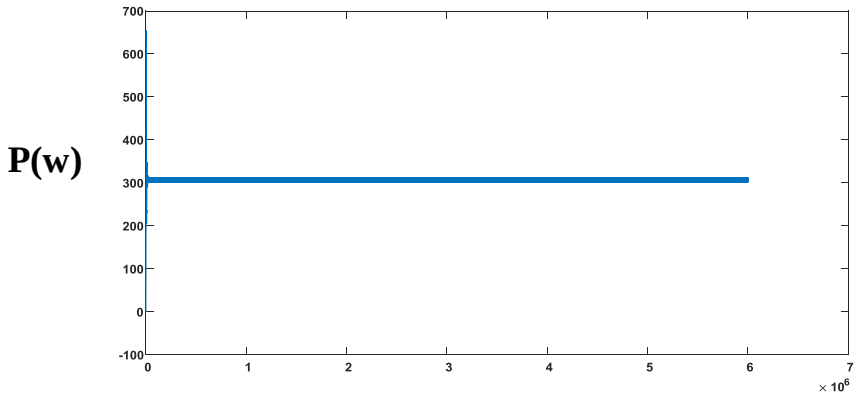

Figure IV.5. Curve of the POWER of a BOOST.

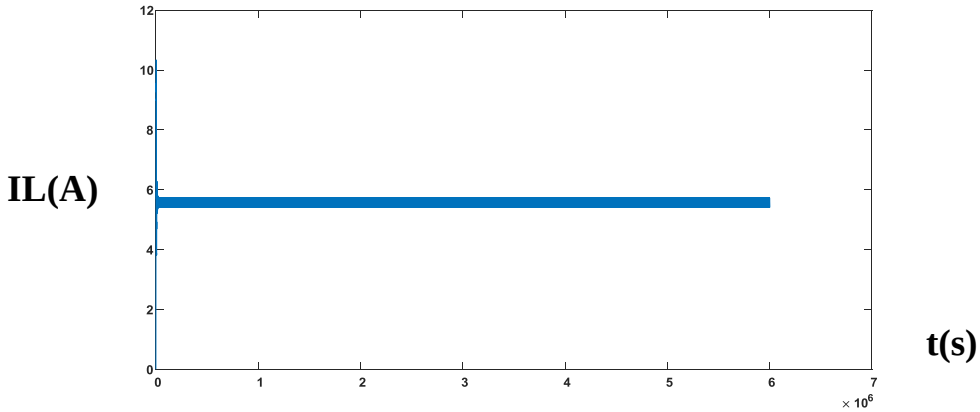

Figure IV.6. Curve of the IL(A) of a BOOST.

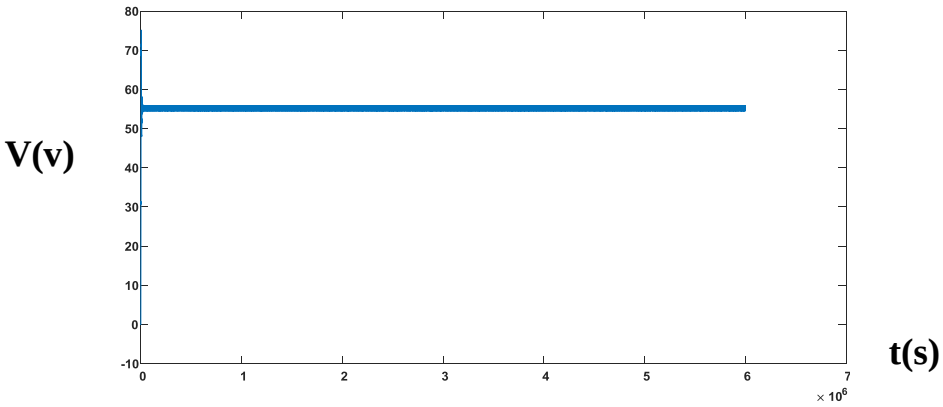

Figure IV.7. Curve of the output voltage of a BOOST.

IV.3. MPPT methods Implementation:

Figure IV.8 shows the HC,P&O,INC and FLC MPPT methods are used as MPPT controller. The four techniques are independently connected to a Boost converter controlled by duty cycle D. The solar irradiance (G) and temperature (T) are the input of the PV system respectively. The PWM generator was utilized at the frequency of 10kHz. The simulation time of all the case studies is t=6 seconds.

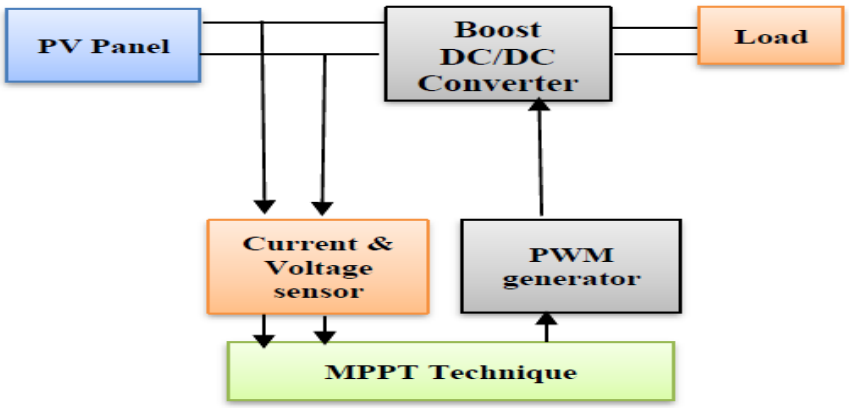

Figure IV.8. PV system block diagram

The simulation model of PV system with HC,P&O and INC MPPT algorithm is carried out in MATLAB/Simulink (2020a) environment as in Figure IV.10,12,14. The electrical parameters at standard test conditions of PV solar module are taken from Soltech 1STH-215-P model as tabulated in Table IV.1 .The simulation is carried out for 6 seconds using the solver of ode3 with variable time step and relative tolerance of 5e-6. sudden decrease in the irradiance is simulated from 1000W/m2 to 250W/m2. Meanwhile, sudden increase is simulated from 250W/m2 to 1000W/m2 and at 25 C temperature.

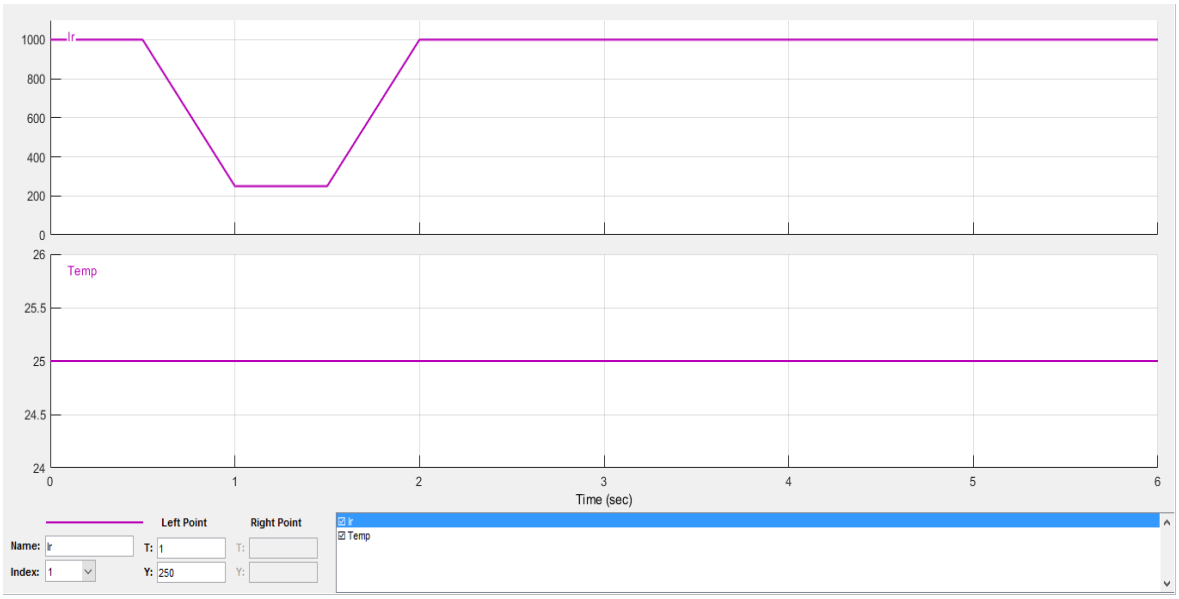

Figure IV.9. Curve showing turbulence in radiation

IV.3.1 Hill Climbing (HC) Algorithm:

Figure IV.10 represents a model of a Soltech 1STH-215-P solar PV module coupled to the load through a constant power converter (DC / DC-Boost) where we make changes in the ratio of radiation applied to the solar module and observe the effectiveness of the hill climbing algorithm in finding the maximum power point Through the curves of the figure IV.11

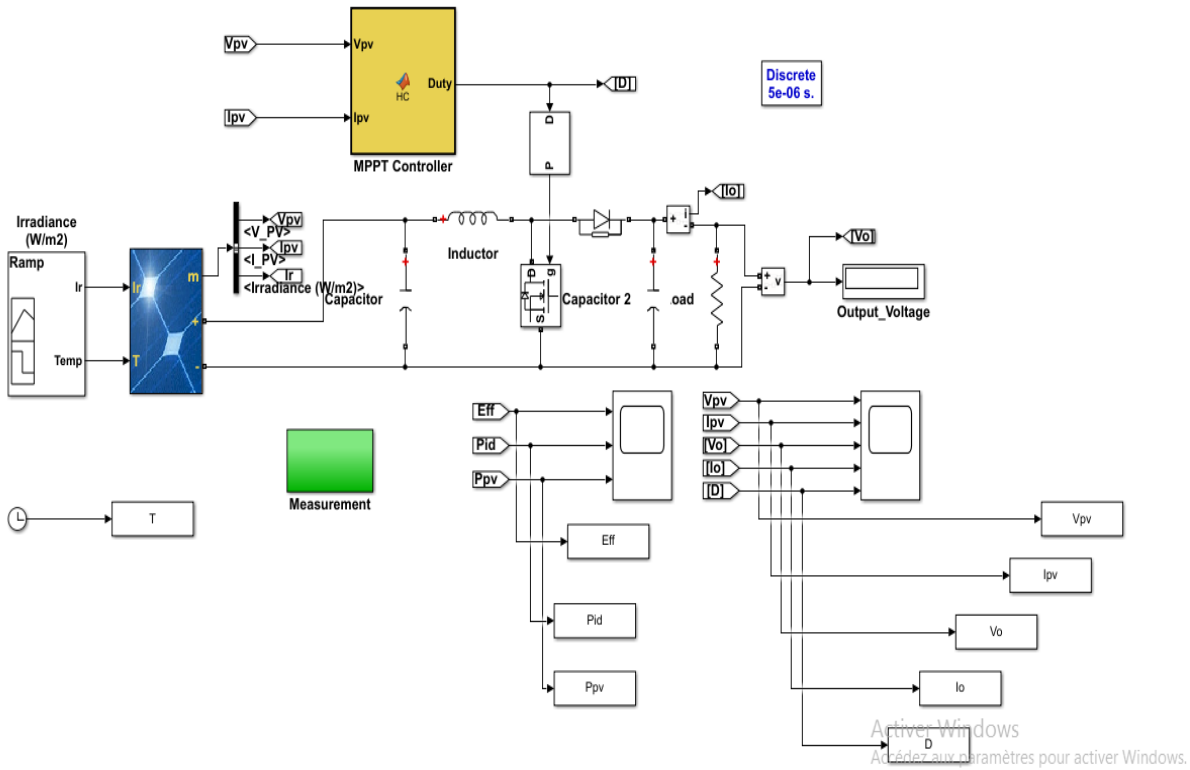

Figure IV.10. System Model in MATLAB

IV.3.1.1 function of HC Algorithm:

Here we will show part of the hill climbing algorithm :

```
function Duty = HC(Vpv, Ipv)

Delta = 125e-6;
duty_init = 0.45;
duty_min=0;
duty_max=0.85;

persistent Pold Dold;

if isempty(Pold)
    Pold=0;
    Dold=duty_init;
end

P= Vpv*Ipv;
dP= P - Pold;
```

IV.3.1.2 Simulation results:

Figures IV.11 shows the tracking of duty cycle, voltage(Vpv,Vo) , current(Ipv,Io) , and power of the PV array and effiency of systeme using the conventional HC algorithm for a sudden decrease in the irradiance. Initially, the PV array is simulated at irradiance of 1000W/m2. Hence, HC algorithm start the exploration process to search the MPP at point t=1.222 s (D=0.5, Vpv=59.74V, Ipv= 11.46A, Ppv= 771.7W).

After t=1.299 s instant, the irradiance is gradually decreased from 1000W/m2 to 250 W/m2. Therefore, HC starts exploring the new MPP by reducing the duty cycle from 0.5 (MPP (new)) to 0.47 to 0.44 and to until reaching 0.060 MPP (old). As the duty cycle decreases, the PV power will decreases from 771.7 W to 717.3 W to 5050.5W and to 206.9 W. Once it enters the zone of MPP (new), the exploitation process is used to reach MPP which is 206.9W. During the time period between 1.122s - 1.998 s As seen, both voltage(Vpv,Vo) , current(Ipv,Io) and power(Ppv) are decreased due to the decrease in irradiance before rising exponentially and stabilizes at : Ppv = 852.9 , Vpv = 59.9v , Vo=132.5 v , Ipv=15.2 A , Io=6.62 A Once it enters the zone of MPP (new) , the exploitation process is used to reach true MPP which is 852.9 W at t=4.09s . The system proves an efficacy of 98% after t=1.257 s

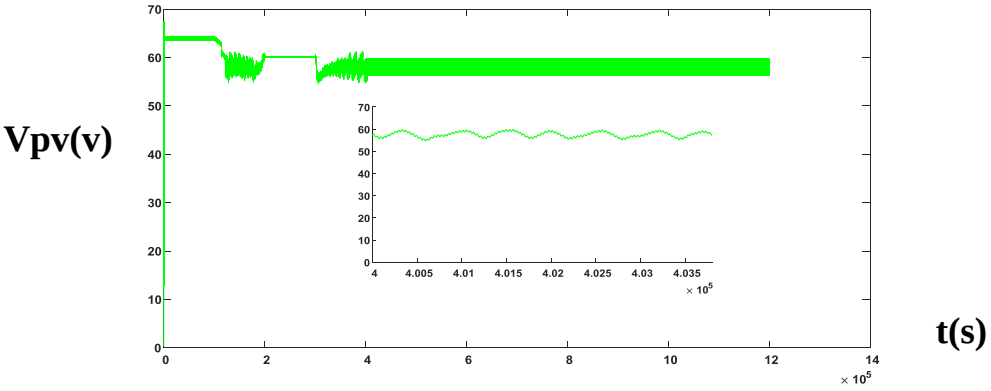

a) Curve of the input voltage Vpv.

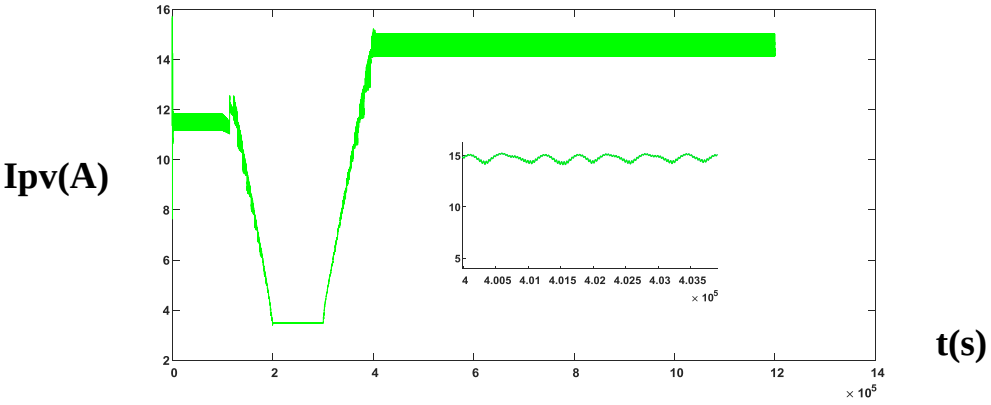

b) Curve of the input current Ipv

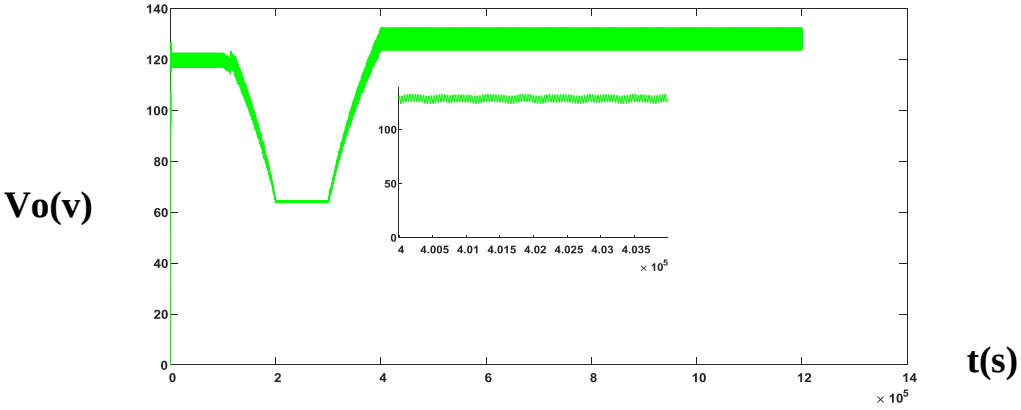

c) Curve of the output voltage Vo.

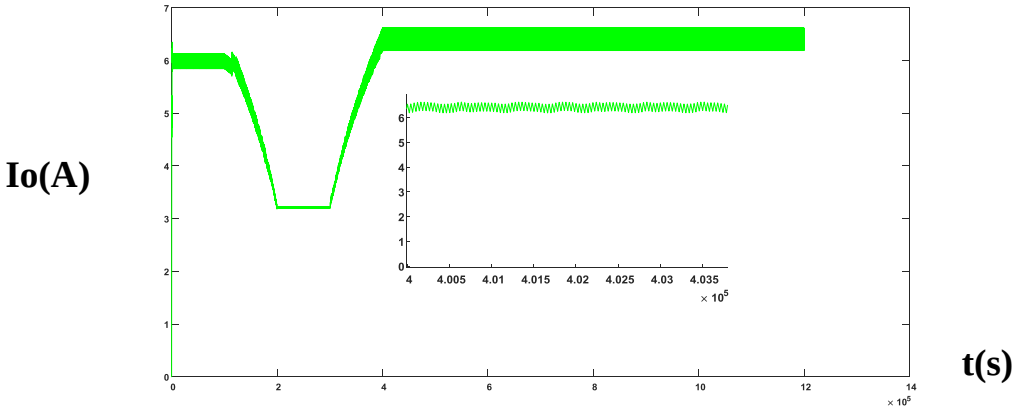

d) Curve of the output current Io.

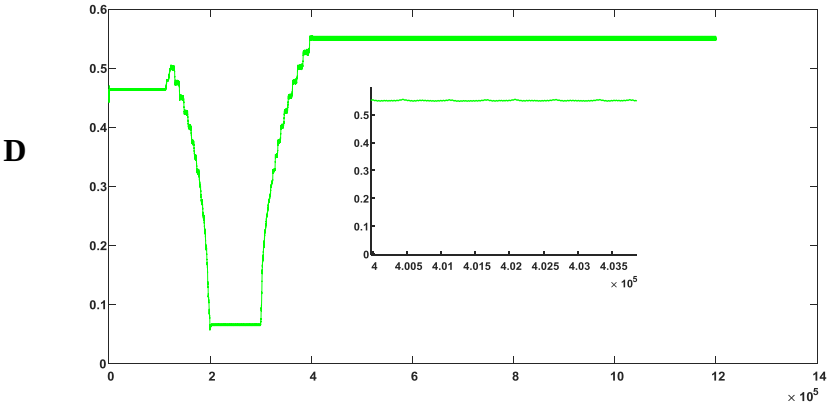

e) Curve of the duty cycle.

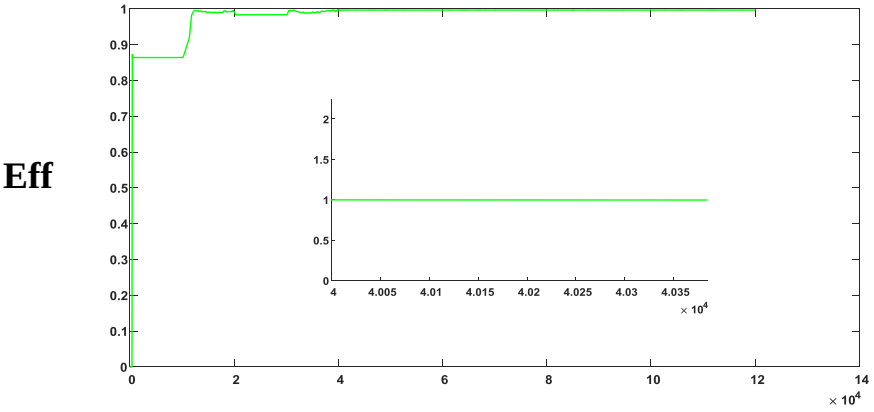

f) Curve of the effiency.

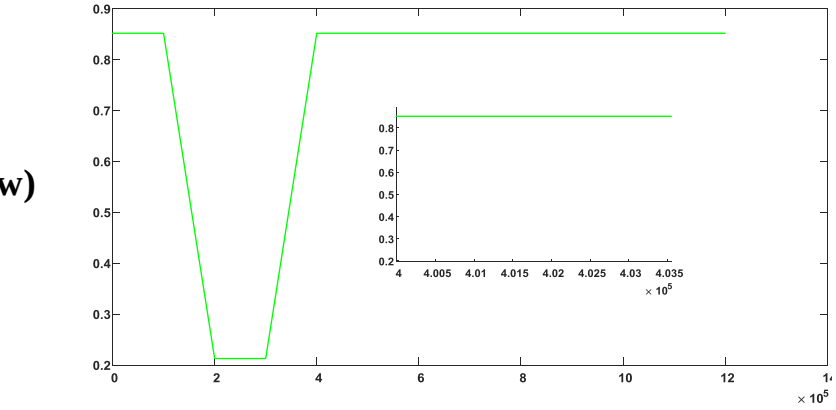

i) Curve of the power ideal.

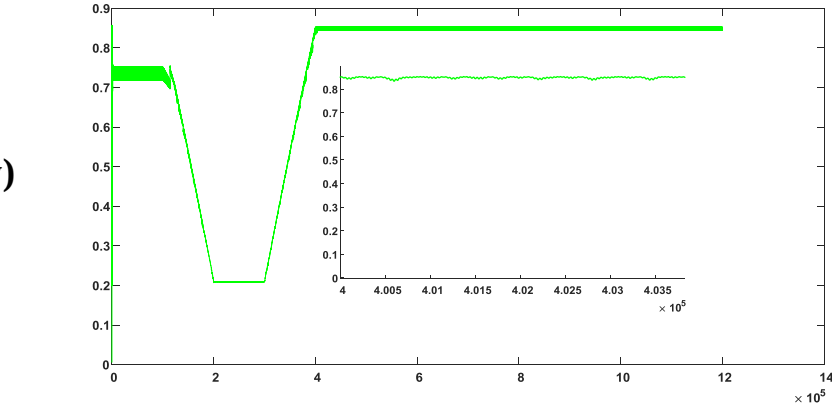

j) Curve of the power Ppv

Figure IV.11. Simulation results

IV.3.2 Perturb and Observe Algorithm:

Figure IV.12 represents a model of a Soltech 1STH-215-P solar PV module coupled to the load through a constant power converter (DC / DC-Boost) where we make changes in the ratio of radiation applied to the solar module and observe the effectiveness of the perturb and observe algorithm in finding the maximum power point Through the curves of the figure IV.13

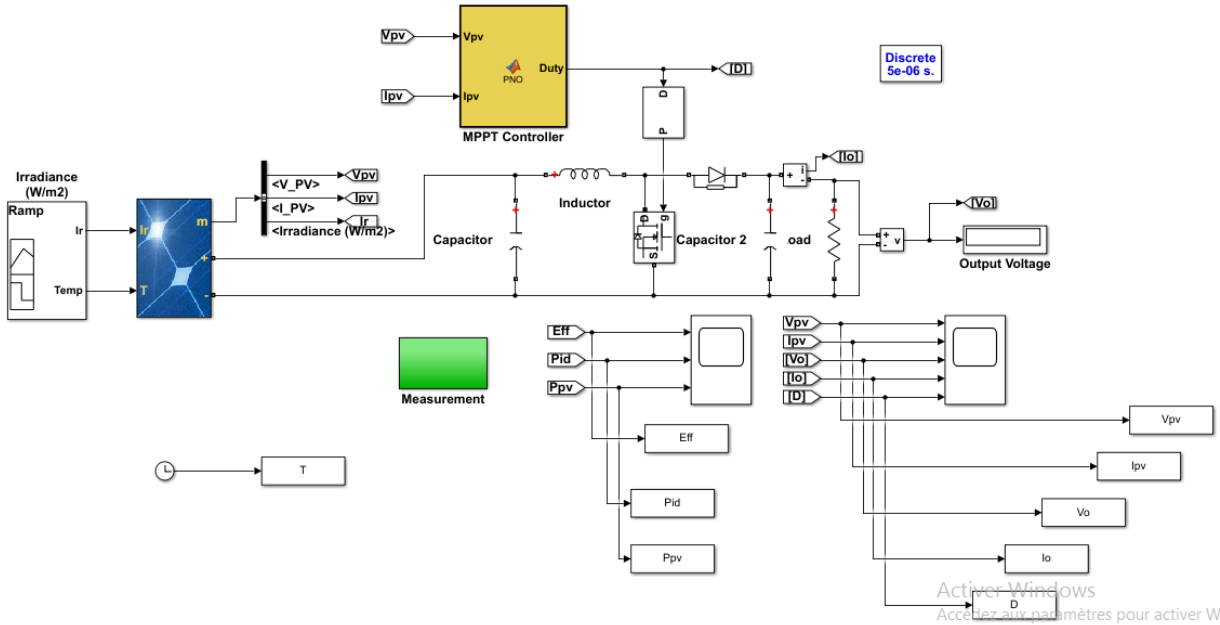

FigureIV.12. System Model in MATLAB

IV.3.2.1 function of P&O Algorithm:

Here we will show part of the perturb and observe algorithm :

```
function Duty = PNO(Vpv, Ipv)

Delta = 125e-6;
duty_init = 0.45;
duty_min=0;
duty_max=0.85;

persistent Vold Pold duty_old;

if isempty(Vold)
    Vold=0;
    Pold=0;
    duty_old=duty_init;
end

P= Vpv*Ipv;
dV= Vpv - Vold;
```

IV.3.2.2 Simulation results:

Figures IV.13 shows the tracking of duty cycle, voltage(Vpv,Vo) , current(Ipv,Io) , and power of the PV array and effiency of systeme using the conventional P&O algorithm for a sudden decrease in the irradiance. Initially, the PV array is simulated at irradiance of 1000W/m2. Hence, P&O algorithm start the exploration process to search the MPP at point t=0.987 s (D=0.55, Vpv=59.68V, Ipv= 15.19A, Ppv= 852.4 W).

After t=0.987 s instant, the irradiance is gradually decreased from 1000W/m2 to 250 W/m2. Therefore, P&O starts exploring the new MPP by reducing the duty cycle from 0.55 MPP (old) to 0.51 to 0.48 and to until reaching 0.085 (MPP B). As the duty cycle decreases, the PV power will decreases from 852.4 W to 731 W to 663W and to 206.9 W. Once it enters the zone of MPP (new), the exploitation process is used to reach MPP which is 207W.

During the time period between 0.987s - 2.09 s As seen, both voltage(Vpv,Vo) , current(Ipv,Io) and power(Ppv) are decreased due to the decrease in irradiance before rising exponentially and stabilizes at : Ppv = 852.9 , Vpv = 59.9v , Vo=132.4 v , Ipv=15.18 A , Io=6.60 A Once it enters the zone of MPP(new) , the exploitation process is used to reach true MPP which is 852.9 W at t=4.09s . The system proves an efficacy of 99.57 % after t=0.04 s

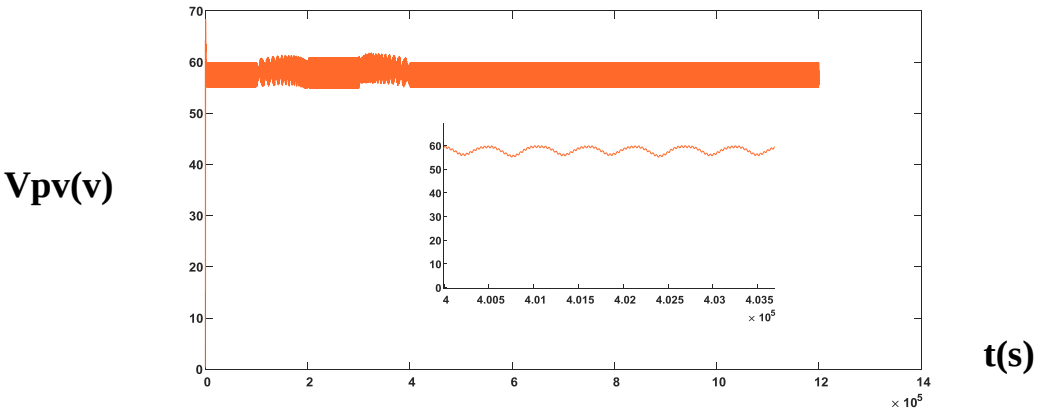

a) Curve of the input voltage Vpv.

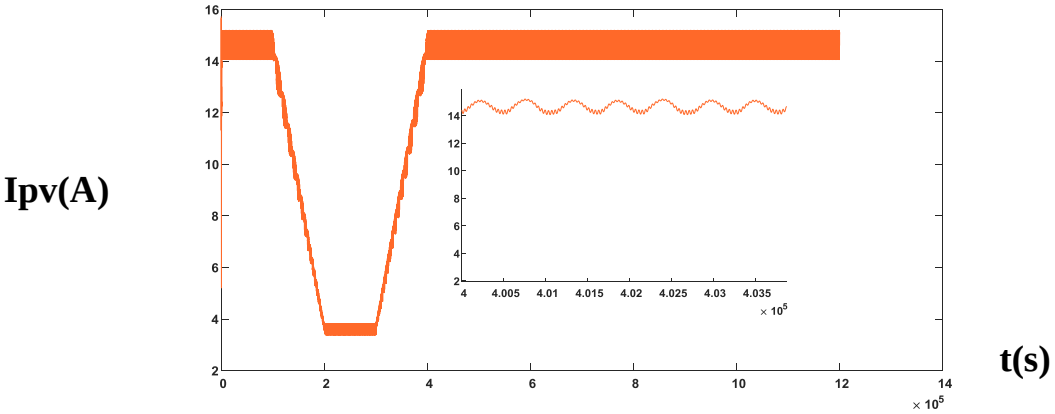

b) Curve of the input current Ipv

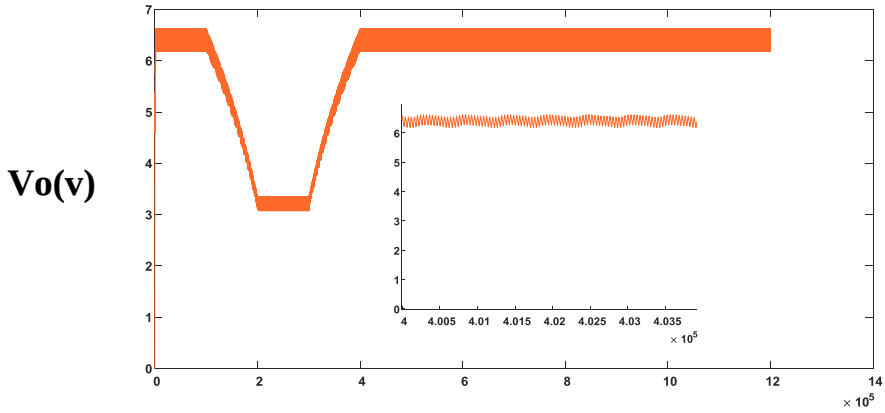

c) Curve of the output voltage Vo.

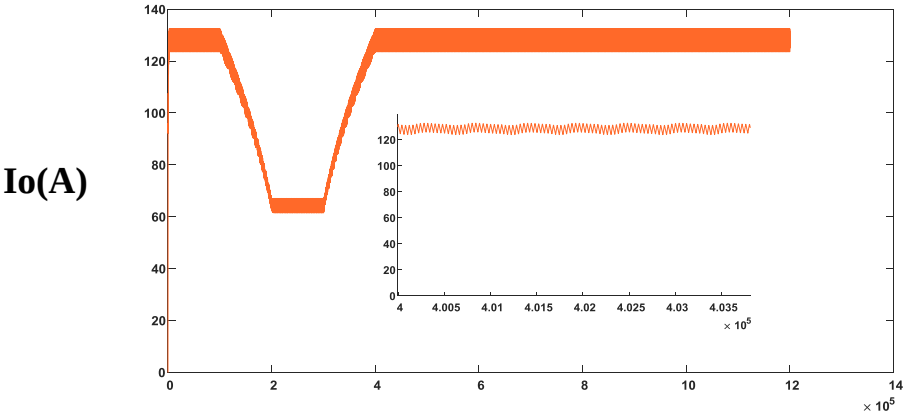

d) Curve of the output current Io.

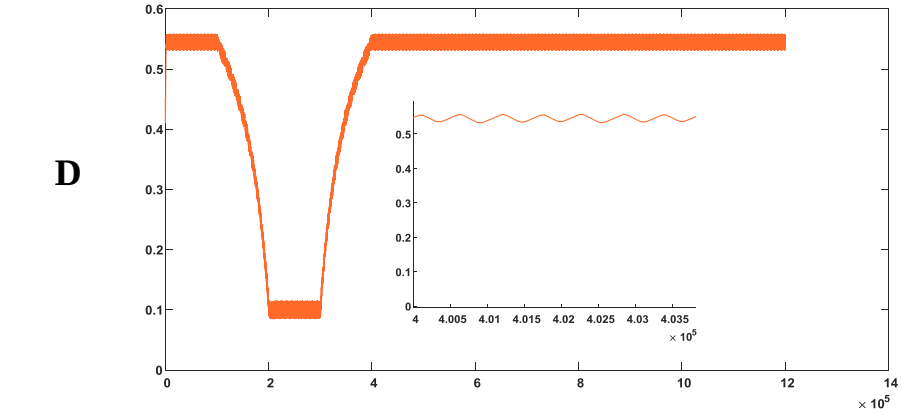

e) Curve of the duty cycle.

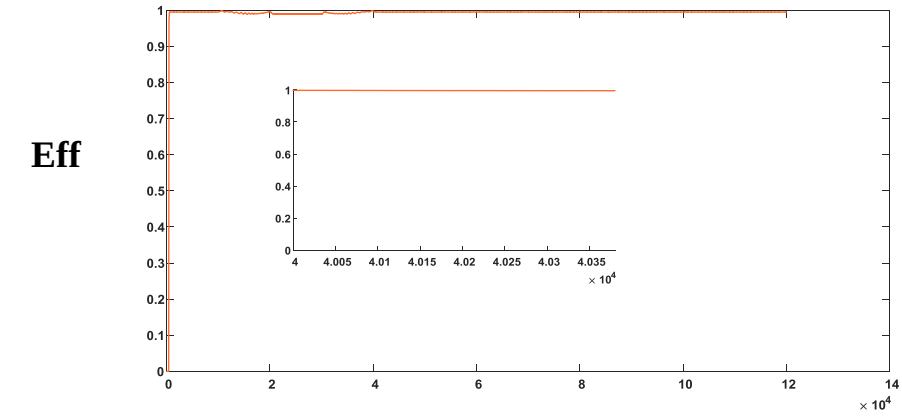

f) Curve of the effiency.

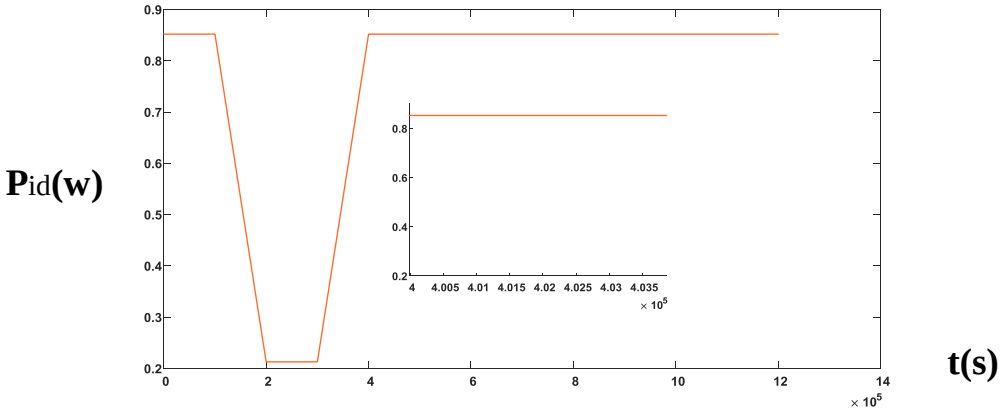

i) Curve of the power ideal.

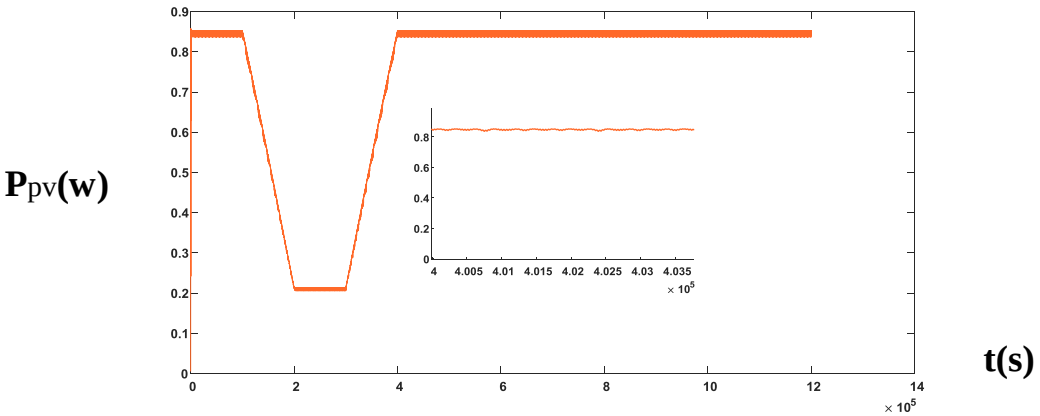

j)Curve of the power Ppv

Figure IV.13. Simulation results

IV.3.3 Incremental Conductance Algorithm:

Figure IV.14 represents a model of a Soltech 1STH-215-P solar PV module coupled to the load through a constant power converter (DC / DC-Boost) where we make changes in the ratio of radiation applied to the solar module and observe the effectiveness of the INC algorithm in finding the maximum power point Through the curves of the figure IV.11

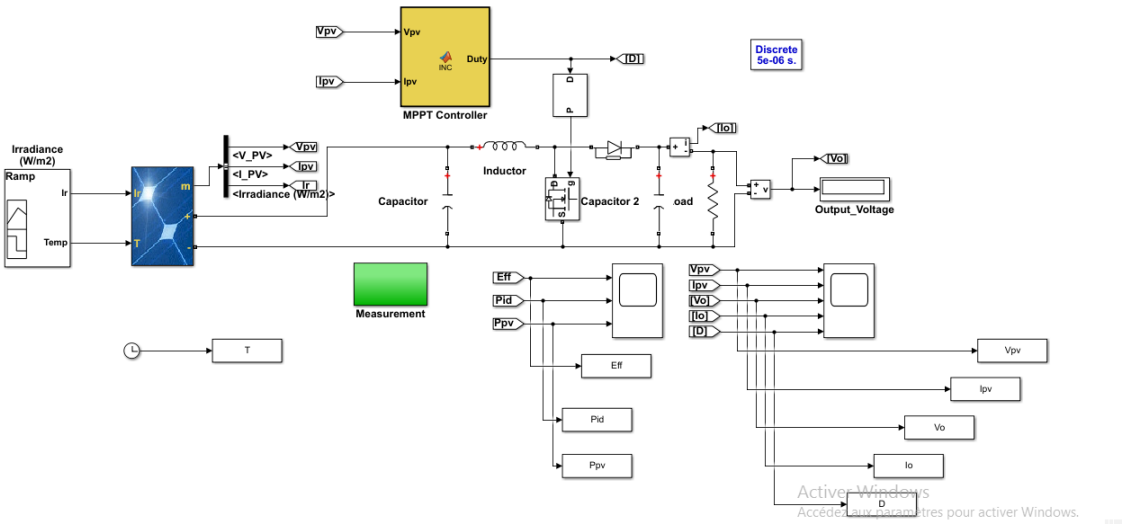

Figure IV.14.System Model in MATLAB

IV.3.3.1 function of INC Algorithm:

Here we will show part of the Incremental Conductance algorithm :

```
function Duty = INC(Vpv,Ipv)

Delta = 125e-6;
duty_init = 0.45;
duty_min=0;
duty_max=0.85;

persistent Vold duty_old Iold;

if isempty(Vold)
    Vold=0;
    Iold=0;
    duty_old=duty_init;
end

dV= Vpv - Vold;
dI= Ipv - Iold;
```

IV.3.3.2 Simulation results:

Figure IV.15 shows the tracking of duty cycle, voltage (Vpv,Vo) , current (Ipv,Io) , and power of the PV array and effiency of systeme using the conventional INC algorithm for a sudden decrease in the irradiance. Initially, the PV array is simulated at irradiance of 1000W/m2. Hence, INC algorithm start the exploration process to search the MPP at point t=0.97 s (D=0.57, Vpv=60.2V, Ipv= 15.2A, Ppv= 852.8 W).

After t=0.987 s instant, the irradiance is gradually decreased from 1000W/m2 to 250 W/m2. Therefore, INC starts exploring the new MPP by reducing the duty cycle from 0.57 MPP (old) to 0.54 to 0.51 and to until reaching 0.085 MPP B. As the duty cycle decreases, the PV voltage(Vpv) will increases from 60.2v to 60.80 to 61 and to 61.75 v. Once it enters the zone of MPP (new), the exploitation process is used to reach MPP which is 61.75 v and decreases the PV current(Ipv) from 15.2 A to 14.4 A to 11.4 A and to 3.405 A . Once it enters the zone of MPP (B), the exploitation process is used to reach MPP which is 3.405 v .

During the time period between 0.97s - 2.04 s As seen, both voltage(Vpv,Vo) , current(Ipv,Io) and power(Ppv) are decreased due to the decrease in irradiance before rising exponentially and stabilizes at : Ppv = 852.9 , Vpv = 59.91v , Vo=132.6 v , Ipv=15.19 A , Io=6.62 A Once it enters the zone of MPP(new) , the exploitation process is used to reach true MPP which is (Vpv=59.91,Ipv=15.19) at t=4.09s . The system proves an efficacy of 92 % after t=0.04 s.

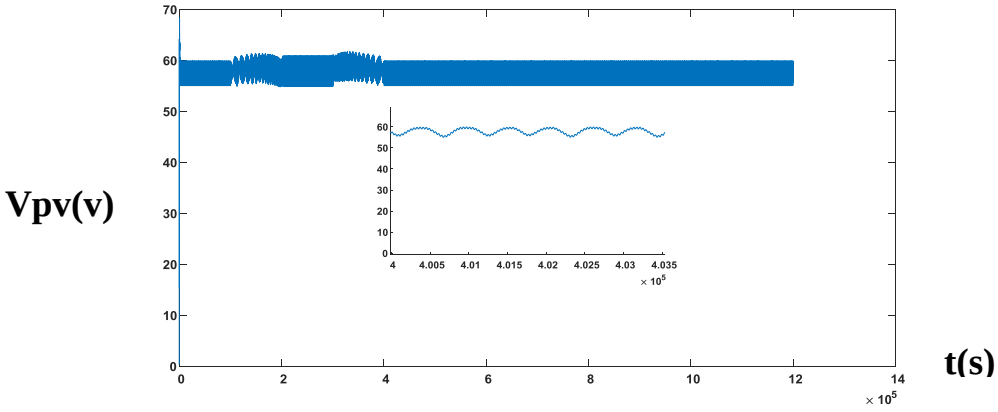

a) Curve of the input voltage Vpv.

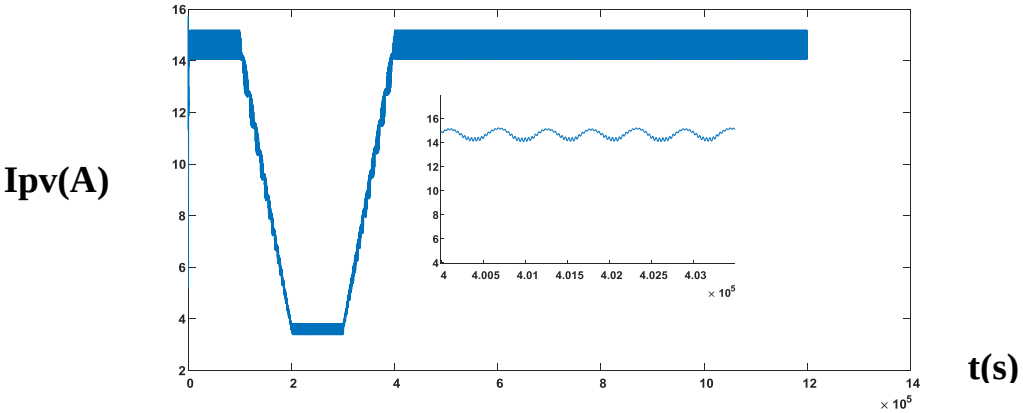

b) Curve of the input current Ipv

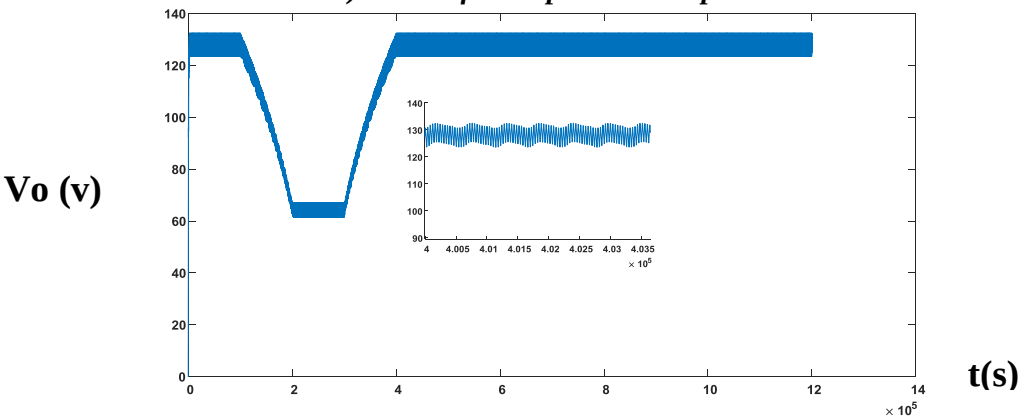

c) Curve of the output voltage Vo.

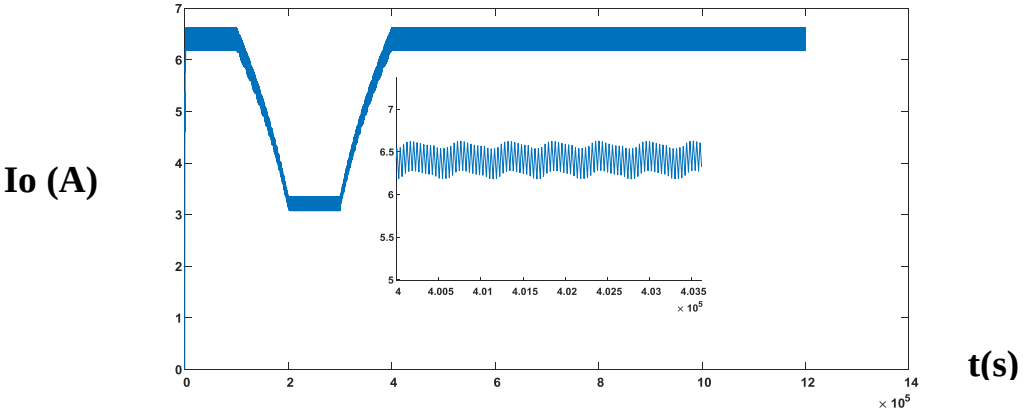

d) Curve of the output current Io.

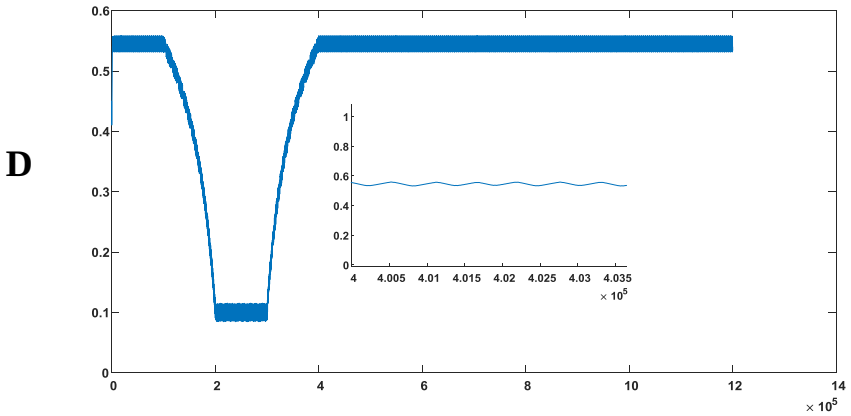

e) Curve of the duty cycle.

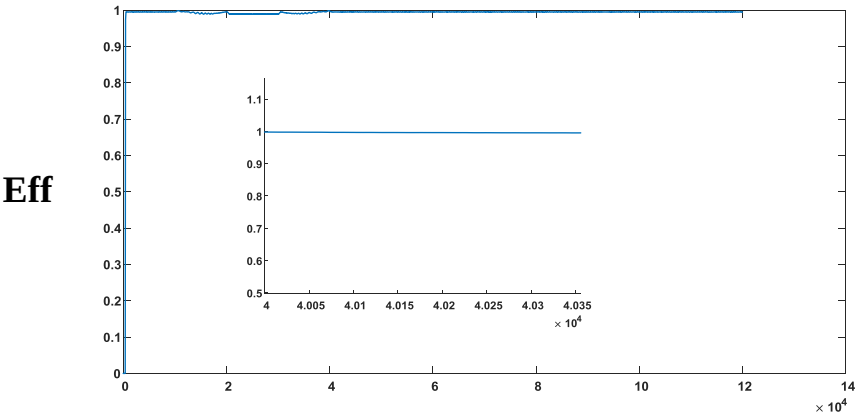

f) Curve of the effiency.

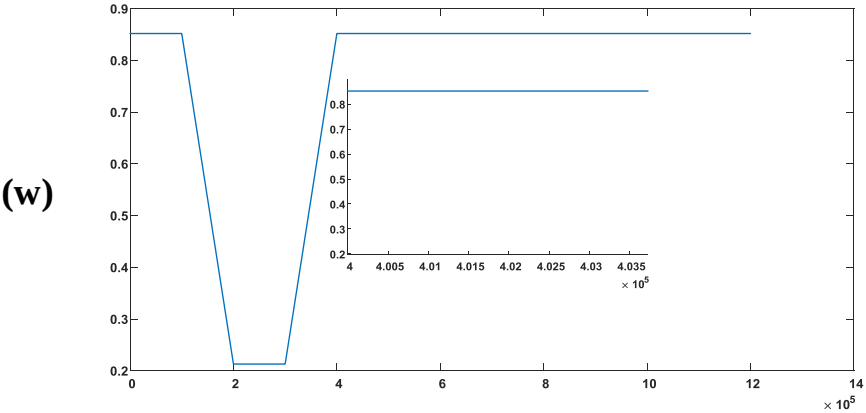

i) Curve of the power ideal.

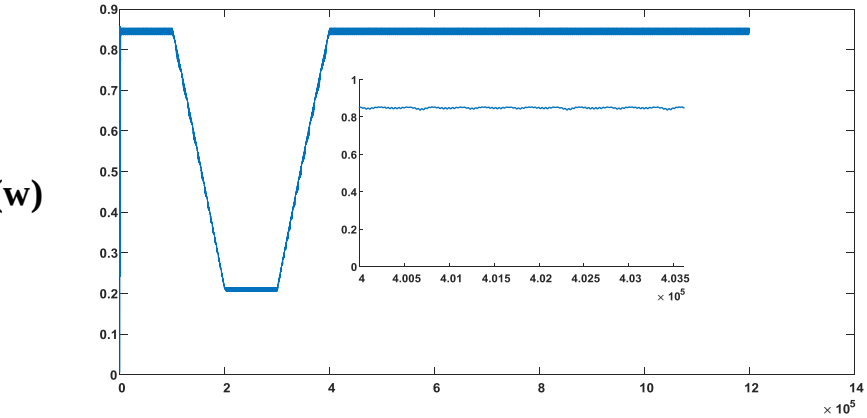

j) Curve of the power Ppv

Figure IV.15. Simulation results

IV.4. Comparison of HC,P&O and INC Methods:

IV.4.1.Comparison of HC and P&O Methods:

Although in the classi cation, the algorithm P&O and Hill Climbing, appear as two independent methods, in some texts are considered as di erent applications of the same basic concept, that of disturbing a magnitude, and analyzing the result for the direction of next disturbance.

The only di erence is the variable which is a ected by the perturbation. In P&O method, it will be the voltage, while in HC method, it will be the duty ratio of the DC/DC converter.

IV.4.2.Comparison of INC and P&O Methods:

- Concerning power efficiency, theoretically, INC method couldprovide a better tracking of MPP than P&O algorithm
- Due to the noise and error measurements it is difficult to satisfy some of the equations
- It produces oscillations around the MPP and power loss
- Complex to implement when compared to P&O
- When tracking step value is chosen correctly, P&O can have an energy efficiency equivalent to that obtained with INC

From the foregoing, we conclude that the best MPPT Algorithms is P&O

IV.5. Adaptive P&O–FLC :

Zainuri et al. designed an Adaptive P&O–FLC with 25 fuzzy rules that can operate only with a boost converter, to eliminate oscillations around the MPP and increase the PV system efficiency.

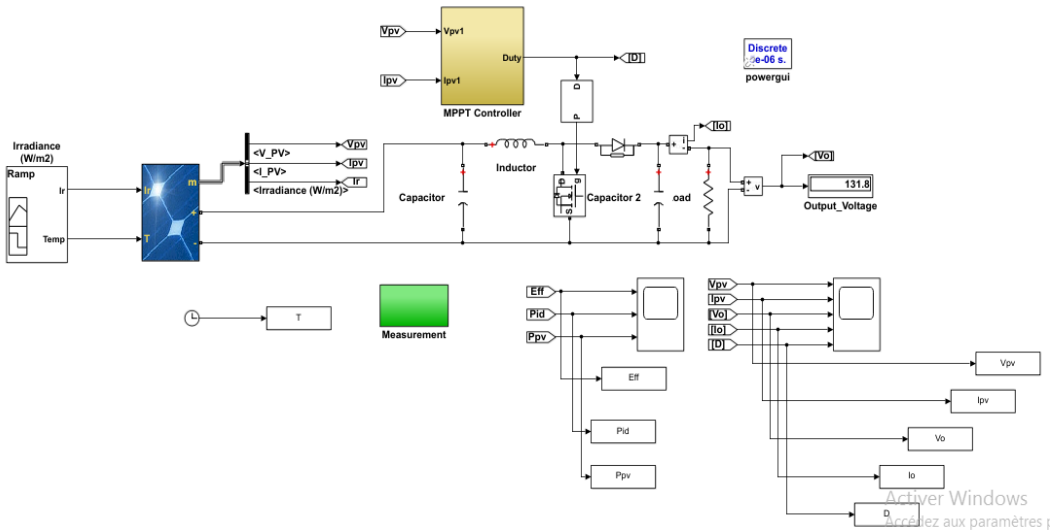

Figure IV.16.System Model in MATLAB

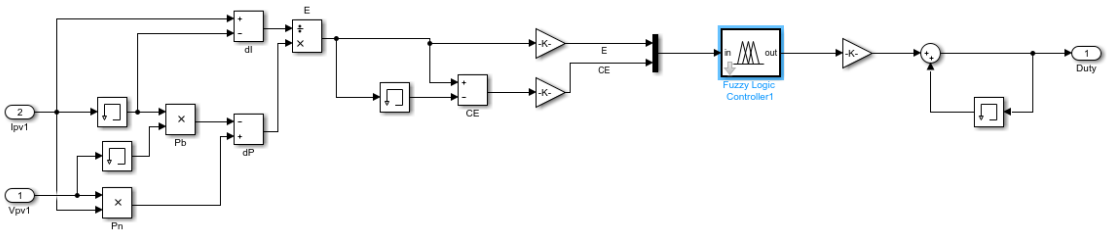

Figure IV.17.P&O-FLC Algorithm Model

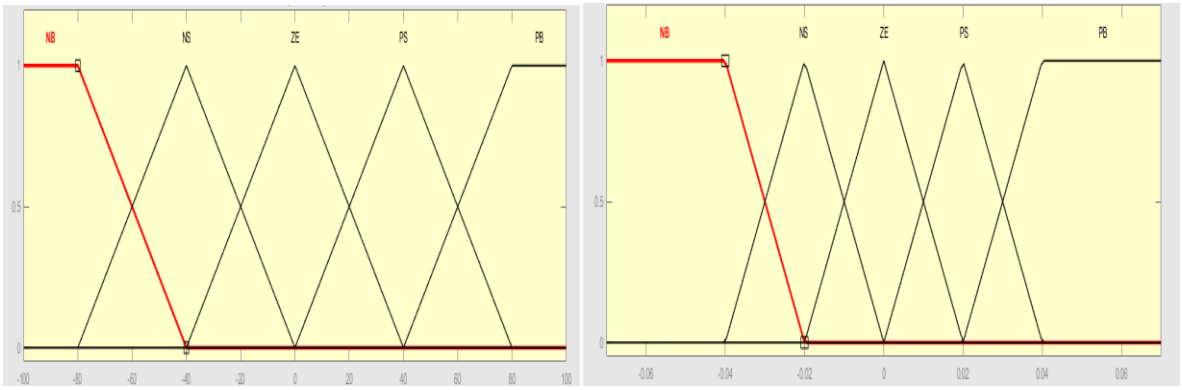

Figure IV.18.a inputs ΔPpv, and ΔVpv

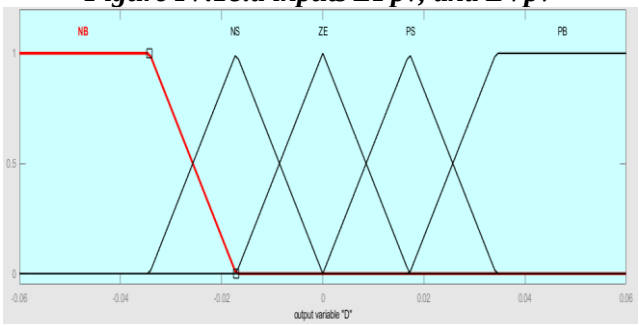

Figure IV.18.b the output ΔD

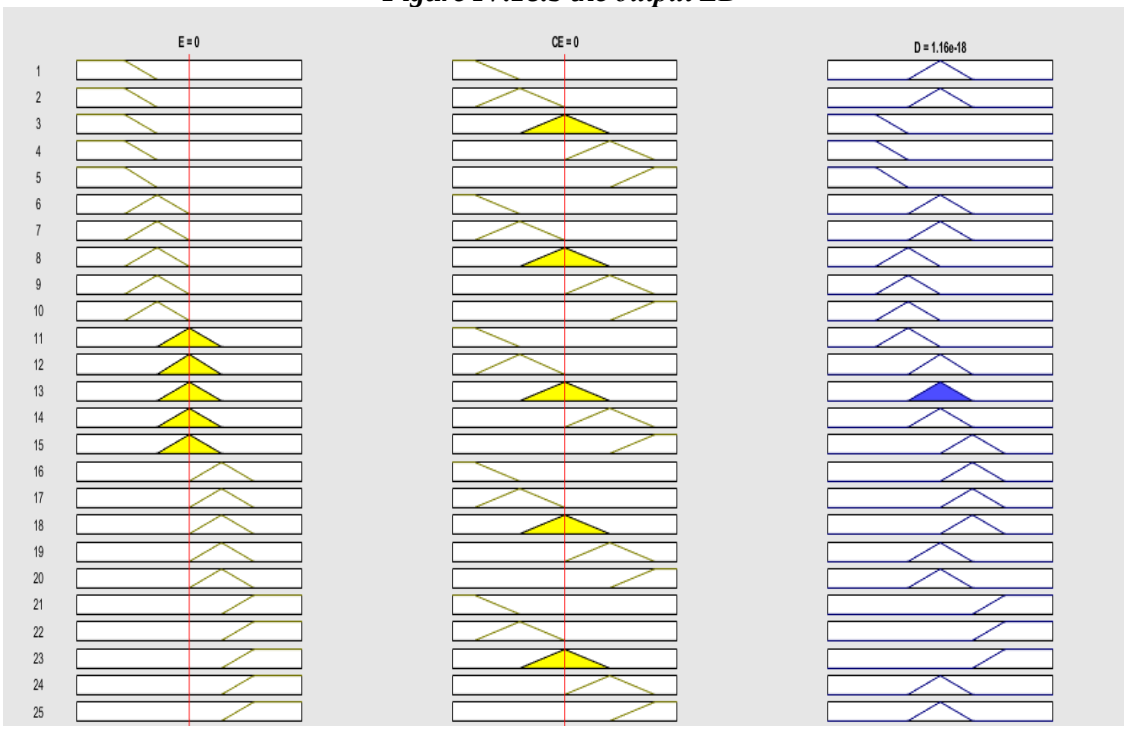

Figure IV.19.Fuzzy rules of adaptive P&O–FLC

IV.5.1 Simulation Results and Comparison:

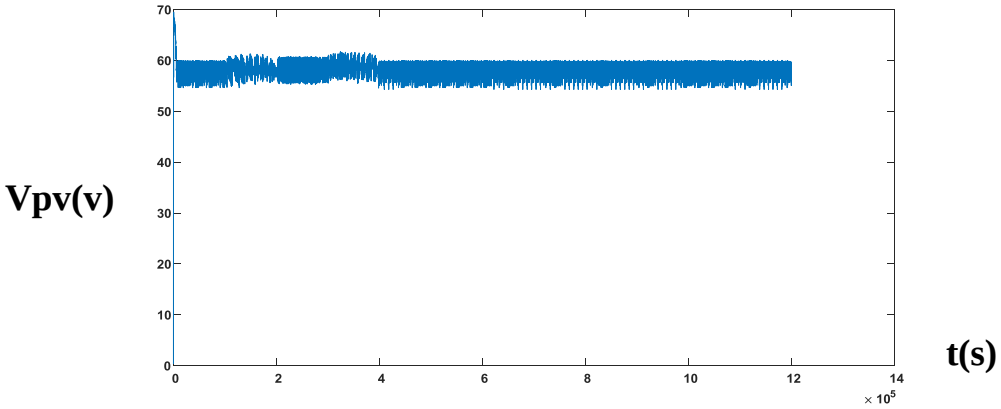

a) Curve of the input voltage Vpv.

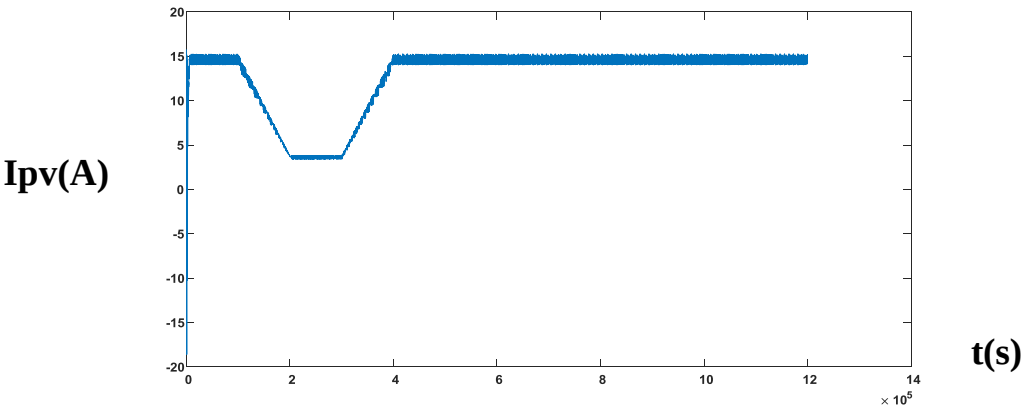

b) Curve of the input current Ipv

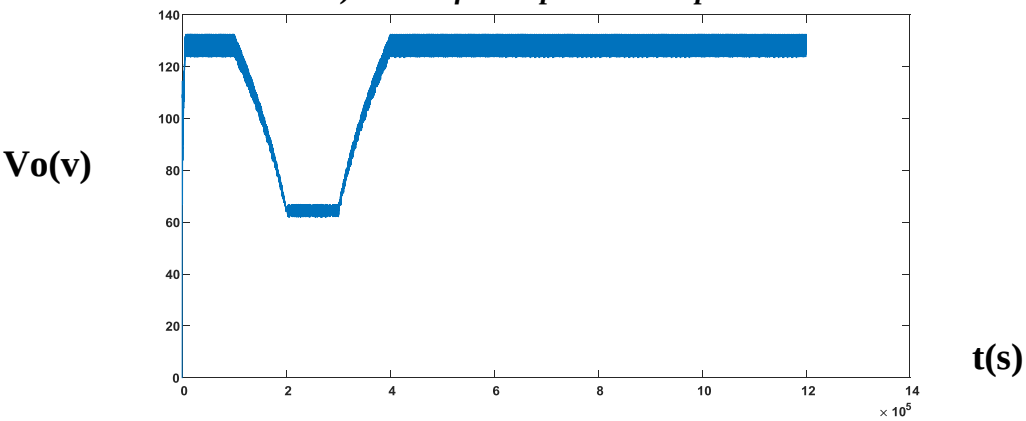

c) Curve of the output voltage Vo.

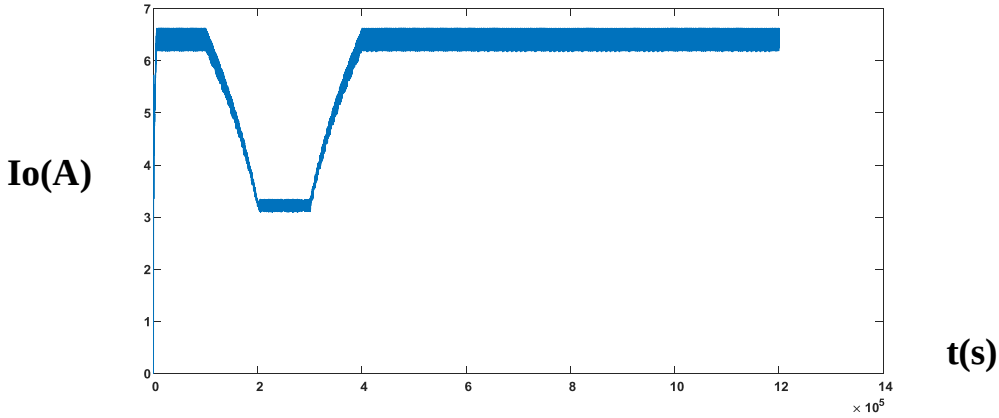

d) Curve of the output current Io.

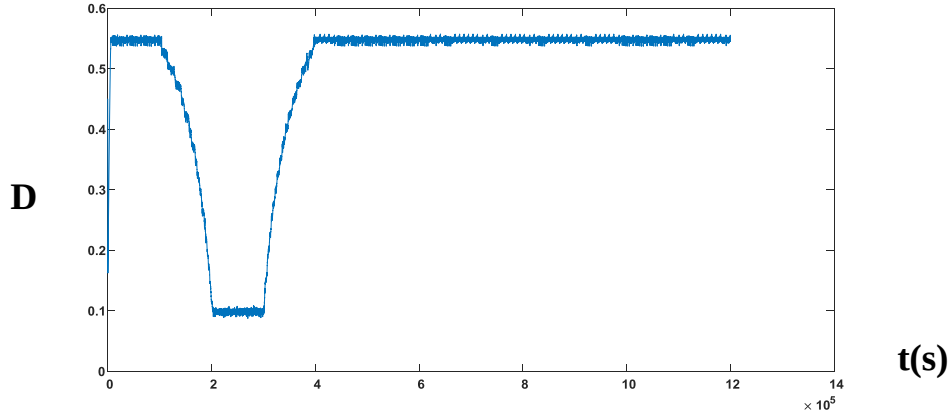

e) Curve of the duty cycle.

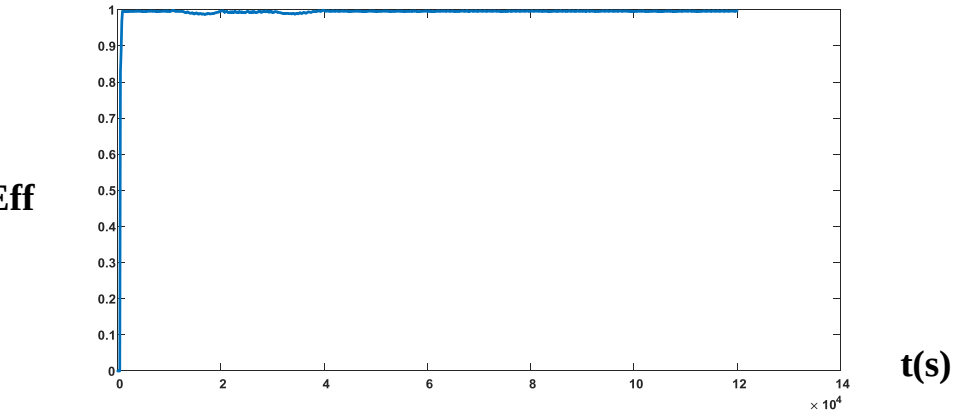

f) Curve of the effiency.

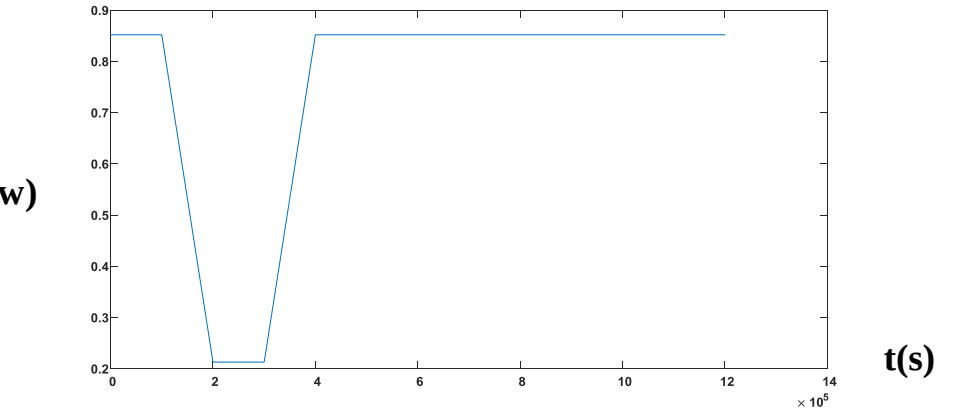

i) Curve of the power ideal.

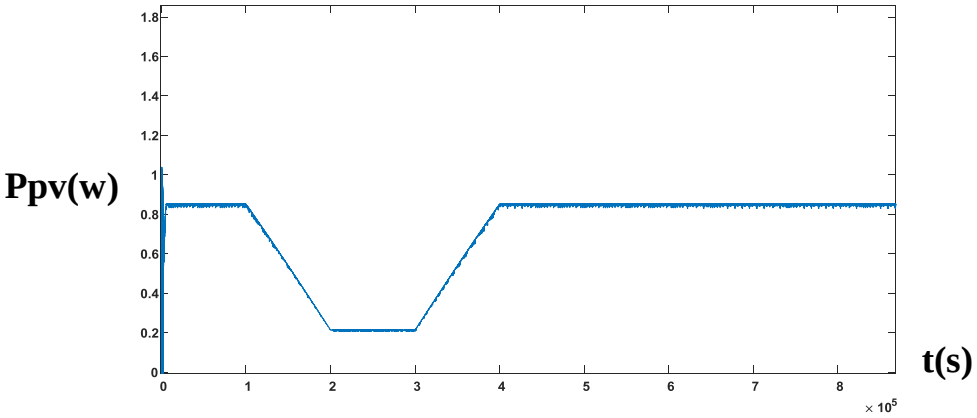

j) Curve of the power Ppv

Figure IV.20. Simulation results under fast variations of irradiation

Evaluated indices	Conventional P&O	Adaptive P&O–FLC
Response time	Slow	Fast
Static error	17 W	2 W (Negligible)
Tracking technique	P&O	FLC–25 rules
Tracking efficiency	99.57%	99.87%
Complexity level	Low	Medium
Control variable	Duty cycle	Duty cycle
Dependence on the PVG parameters	No	No
Initial parameter settings	3 parameters	3 parameters (3 scaling factors of the FLC inputs and output)

Table IV.3. Comparison of adaptive P&O–FLC and Conventional P&O

The results obtained, Figure IV.13 and Figure IV.20 , show that the control based on P&O–FLC MPPT responds correctly to the characteristics of the panel. The electrical power generated by the solar panel and always maintained at its maximum power, whatever the atmospheric conditions.

Finally we conclude the Fuzzy logic control is a step towards precise mathematical reconciliation based on human decision-making, or expertise. Algorithm based on fuzzy logic is a robust and efficient technique that works, in the case of MPPT, at the optimal point. However, the implementation of this type of command is more complex than classical algorithms. The main difficulty consists in choosing the parameters of the fuzzy command (the choice of membership functions and inference rules). This is why we will opt to optimize this controller, in the case of partial shading, with an evolutionary approach.

IV.6. Conclusion :

This chapter presents the results obtained by three methods of controlling MPPT applied to a PV generator. The work was carried out under the MATLAB / SIMULINK environment. We count two scenarios: ideal atmospheric conditions (25 ° and 1000 w / m2) and partial shade. We performed a comparative study between three MPPT methods, the first is the HC method, the second is the P&O method and the third is the INC . Under standard atmospheric conditions, all three methods give fairly good results. However, from the results obtained, in partial shading, the P&O presents very competitive results compared to the other two methods, but does not lead to the maximum extraction of the power. We then opted for the optimization of the latter by the P&O–FLC which was used to find the good membership functions for the fuzzy variables. The results then obtained by the use of fuzzy logic are much more promising and give better performance with convergence at PPM .

General conclusion

General conclusion:

This work is a Master 2 thesis in electrical control carried out at abbes laghrour khenchela university It can be considered as a Study of the different MPPT techniques for the Photovoltaic system, which are looking for a maximum power point when the GPV is coupled to the load through an energy static converter. The main objective is to clarify the method that result an extraction of the maximum power from the PV panel.
We have started this work with a theoretical study of the photovoltaic system. We have reviewed the different types of DC/DC converters and inverters DC/AC, then described how they work.

Then a comprehensive study of the most popular methods is presented. First of all, we explained the traditional methods such as Perturb and Observe (P&O), Hill Climbing (HC) and INC. Despite the simplicity of these methods, and what is useful in the very imprecised applications, though they present problems associated with large oscillations, long response time, or measurements powerlessness.

In addition, more advanced methods are also included.Such as Fuzzy Logic Control (FLC) method that offers fast solutions for the imprecised models, while an method based on genetic (AG) provide very precised results. Moreover, other methods based on oscillations controll caused by the converter, tables or mixed methods based on some intermediate parameters such as synergetic and sliding mod control.

Therefore, in the last chapter of this work, we focused on the implementation of the most simple methods, such as HC, P&O and INC method.

As a conclusion, the results obtained show a very similar performance for conventional methods ;HC, P&O and INC algorithm. However, in partial shading, the P&O presents very competitive results compared to the other two methods, but it does not lead to a maximum extraction of the power. We then opted the optimization of the latter by the P&O–FLC which was used to find the good membership functions for the Fuzzy variables.The results obtained by the use of Fuzzy Logic are much more promising and giving better performance with convergence at PPM with significantly reduced oscillations.

Even though, there are no great differences can be found since the ideal method has not been found yet, which get maximum power at every time, with much higher effciency acting with a low time response and an acceptable complexity . Many MPPT methods continue to develop ,some other methods are named in this work, and many others can be found.

Abstract:

The demand for electrical energy has continued to increase in recent years, as well as the constraints linked to its production, such as the effect of pollution and global warming, are driving research towards the development of renewable energy sources.

In this context, photovoltaic (PV) systems offer a very competitive solution. To overcome the efficiency problem of solar panels and achieve maximum efficiency, it is necessary to optimize the design of all parts of the PV system. In addition, it is necessary to optimize the Static converters employed as the interface between the PV generator and the load in order to extract the maximum power and thus operate the GPV generator at its maximum power point (MPP) using an MPPT controller (maximum power point tracking), consequently, obtain a maximum electric current under the variation of the load and the atmospheric conditions (brightness and temperature).

In this work, we briefly describe the most used solar cells and their operating principles, as well as the modeling of a photovoltaic cell (CPV), the influence of different metrological parameters (temperature and illumination). and we review the types of static converters DC / AC converters and DC / DC converters (buck, boost and buck boost), then we Study of different MPPT methods, and it is which searches for the maximum power point when the GPV is coupled to a load through a static converter after that, a simplified model of PV system is implement, and it is tested to work. Then, different methods are implemented. after all methods operate correctly, main features are analyzed and compared to other methods, and all results and conclusions are obtained.

الملخص :

استمر الطلب على الطاقة الكهربائية في الزيادة في السنوات الأخيرة ، فضلاً عن القيود المرتبطة بإنتاجها ، مثل تأثير التلوث والاحتباس الحراري، مما يدفع البحث نحو تطوير مصادر الطاقة المتجددة.

في هذا السياق ، تقدم الأنظمة الكهروضوئية حلاً تنافسيًا للغاية. للتغلب على مشكلة كفاءة الألواح الشمسية وتحقيق أقصى قدر من الكفاء ، من الضروري تحسين تصميم جميع أجزاء النظام الكهروضوئي. بالإضافة إلى ذلك، من الضروري تحسين المحولات الثابتة المستخدمة كواجهة بين المولد الكهروضوئي والحمل من أجل استخراج الطاقة القصوى وبالتالي تشغيل مولد الطاقة الشمسية عند أقصى نقطة للطاقة باستخدام وحدة تحكم تتبع اقصى نقطة للطاقة ، وبالتالي الحصول على أقصى تيار كهربائي في ظل تغير الحمل والظروف الجوية (السطوع ودرجة الحرارة).

في هذا العمل ، نصف بإيجاز الخلايا الشمسية الأكثر استخدامًا ومبادئ تشغيلها ، بالإضافة إلى نمذجة الخلية الكهروضوئية ، وتأثير المعلمات المترولوجية المختلفة (درجة الحرارة والإضاءة). ونراجع أنواع المحولات الثابتة محولات التيار المستمر / التيار المتردد ومحولات التيار المستمر / التيار المستمر ، ثم ندرس طرق التتبع المختلفة ، وهي التي تبحث عن أقصى نقطة طاقة عندما يقترن مولد الطاقة الشمسية بالحمل من خلال محول ثابت بعد ذلك ، يتم تنفيذ نموذج مبسط للنظام الكهروضوئي ، ويتم اختباره للعمل. ثم يتم تنفيذ طرق مختلفة. بعد أن تعمل جميع الطرق بشكل صحيح ، يتم تحليل السمات الرئيسية ومقارنتها بالطرق الأخرى ، ويتم الحصول على جميع النتائج والاستنتاجات.